HHS Public Access

Author manuscript

Compr Physiol. Author manuscript; available in PMC 2020 March 20.

Published in final edited form as:

Compr Physiol. ; 9(2): 715–766. doi:10.1002/cphy.c180012.

Evolution and Functional Differentiation of the Diaphragm Muscle of Mammals

Matthew J. Fogarty, **Gary C. Sieck**

Department of Physiology & Biomedical Engineering, Mayo Clinic, Rochester, Minnesota

Abstract

Symmorphosis is a concept of economy of biological design, whereby structural properties are matched to functional demands. According to symmorphosis, biological structures are never over designed to exceed functional demands. Based on this concept, the evolution of the diaphragm muscle (DIAm) in mammals is a tale of two structures, a membrane that separates and partitions the primitive coelomic cavity into separate abdominal and thoracic cavities and a muscle that serves as a pump to generate intra-abdominal (P_{ab}) and intra-thoracic (P_{th}) pressures. The DIAm partition evolved in reptiles from folds of the pleural and peritoneal membranes that was driven by the biological advantage of separating organs in the larger coelomic cavity into separate thoracic and abdominal cavities, especially with the evolution of aspiration breathing. The DIAm pump evolved from the advantage afforded by more effectively generation of both a negative P_{th} for ventilation of the lungs and a positive P_{ab} for venous return of blood to the heart and expulsive behaviors such as airway clearance, defecation, micturition, and child birth.

Didactic Synopsis

The DIAm separates abdominal and thoracic cavities; thus, it is a partition, and its evolution reflects that important role in isolating organs into separate thoracic and abdominal cavities. However, the DIAm is also a muscle, and is most often described as the principal pump muscle of inspiration. However, the DIAm also serves as a pump for generating both negative P_{th} and positive P_{ab} in other motor behaviors. Accordingly, the evolution of the DIAm is more complex and should be considered in the context of its dual physiological roles as a partition and muscular pump. In considering DIAm evolution, we adopt the guiding concept of symmorphosis or economy of design, where biological structures are not over designed for their functional roles. Thus, this is a tale of the evolution of two diaphragms, a partition and a muscular pump that separates thoracic and abdominal cavities but also affects generation of P_{th} and P_{ab}.

Introduction

When we think of the striking diversity of mammalian systems and observe the myriad of forms and ecological niches these species inhabit, child-like wonder stokes an instinct to imagine a plethora of unique adaptations in order to solve different challenges each species has for life on earth. Instinct could not be more wrong, as Kerr (1808–1890) entreats, "*plus ça change, plus c'est la même chose"* ("the more things change, the more they stay the same"). Immutable principles of comparative biology whittle away the superficial differences and we are left with the core constraints dictated by function. Symmorphosis is a

concept introduced by Ewald Weibel and Charles Richard Taylor in 1981 [652] that codifies a biological design principle based on an economy of design, whereby the structure and function of integrative systems are linked, and no one component has excessive performance capacities above that which is necessary for the preservation of life. If a system has excess capacity, then it is likely to be involved in two distinct physiological processes [652, 653, 689, 690].

The DIAm is unique to mammals, and physiologists generally ascribe the main function of the DIAm as generating a negative P_{th} to drive airflow and fill the lungs during breathing (i.e., the principal muscle of inspiration). Accordingly, based on the symmorphosis concept, the DIAm should be primarily designed to accomplish ventilatory behaviors that have a high duty cycle (time active versus inactive) and are highly repetitive day in and day out. However, in most if not all mammals, the forces or transdiaphragmatic pressures (P_{di}) generated by the DIAm during ventilation represent less than half of the total force generating capacity of the DIAm. In addition, when fully activated the DIAm is susceptible to fatigue – not a good feature for a muscle primarily designed to accomplish ventilation. So this raises the question; is the DIAm over-designed just for ventilation or is it optimally designed to contribute to other physiological processes not just ventilation? In exploring the evolution of the DIAm across mammalian species, most investigators have considered only ventilatory demands. In this comprehensive review, we will consider not only the range of ventilatory behaviors across mammals but also differences in non-ventilatory behaviors of the DIAm as a partition and muscular pump to generate P_{ab}.

Symmorphosis: Linking Biological Structure with Functional Demands

Biological evolution is often considered in the context of structural and functional changes that afford some survival advantage. Structural biology spans from molecular, cellular, tissue, organ and whole organism levels. Similarly, physiology or function spans the full scale of structure. Symmorphosis is a theory of biology where structural design features (e.g., morphological properties) are matched to functional demands (i.e., range of physiological requirements) within an integrated system [652, 653, 689, 690]. The theory of symmorphosis was originally tested in the pulmonary system where diffusing capacity of the lungs (alveolar surface area) was compared to the maximum rate of O_2 consumption. As an integrated system, the theory also included the capacity for capillary diffusion and muscle O_2 consumption (mitochondrial density). In this regard, the DIAm, with its high duty cycle, is a major consumer of O_2 and this is reflected by the high mitochondrial density and oxidative capacity of at least some DIAm fibers [49–52, 163, 329, 606, 607, 625]. Though this concept has a proven utility in many biological systems, particularly when observing broad trends, there are a variety of limitations and exceptions to these trends both within and across species, a flaw readily acknowledged by the originators of the hypothesis [689]. For example, when linking structure and functional requirements in trained athletes and in the thoroughbred horse, lung structures remain unchanged, despite remarkable efficiency gains within the circulation (hematocrit, blood flow) and increased mitochondrial density in muscle [675], and obvious mismatch in the structure function relationship. Indeed, in horses, the structure function mismatch is so great that phenomenal gains in maximal VO_2 levels (~160 ml kg^{-1} min^{-1}), peak cardiac output (0.8 L kg^{-1} min^{-1}), splenic augmentation of

blood volume and hematocrit (30% increases), values ~2–3 times higher than fit humans, are coupled with arterial hypoxemia, pulmonary hypertension, hypercapnia and pulmonary hemorrhage [675], a striking outlier from symmorphic principles and more resembling 'dysmorphosis', a term coined by Peter D. Wagner to describe serious mismatches between structure and function in some cases [674]. Sadly, the concept of dysmorphosis has never been fully developed or defined. The definition of *dys* – from the original Greek, meaning bad or difficult has implications for pathology or disease, and fails to capture the full gamut of the examples of 'failed' symmorphosis. Indeed, many examples of failed symmorphosis may be due to one system having multiple functions (e.g., the DIAm, as elaborated upon in this review), a function related to sexual selection (e.g., secondary sex characteristics such as the mane of a lion, the antlers of cervidae, peacock feathers and narwhal tusks) or merely an over-production. Perhaps the greatest example of failed symmorphosis is the venom of the taipan snake, which typically releases ~20 mg of venom per bite [696], with an intravenous LD_{50} of ~0.01 μg g^{-1} [646] and a subcutaneous LD_{50} (analogous to the action of a bite) of ~0.1 μg g^{-1} [457, 696]. Thus, with a single bite, enough venom is delivered to kill ~8000 mice, an egregious over-production!

In a more general presentation of the symmorphosis hypothesis, biological systems adhere to an "economy of design" such that no single parameter in the system has unnecessary excess capacity, beyond that which fulfills the range of physiological demands. Quantitative differences in design features and/or functional effects add to biological diversity and drive evolution. In this respect, symmorphosis postulates that the evolution of structural design and function are linked to the guiding principal of "enough but not too much" [652, 653, 689, 690]. Such an economy of design should also be present in the evolution of the DIAm, especially since this muscle is unique to and thereby distinguishes mammals. Indeed, this begs the questions: did the DIAm emerge through evolution to efficiently support only lung ventilatory requirements? Is the full capacity of the DIAm or any of its structural features overdesigned to achieve adequate ventilation? Is the DIAm also designed to efficiently generate P_{ab}? Hopefully, these questions will be at least partially addressed in this review.

Compared to humans, smaller mammals consume approximately six times more energy even when normalized for differences in body mass. Some outliers exist, with the Etruscan shrew having a submaximal O_2 consumption rate of 1000 ml kg min^{-1}, a rate ~30 times that of man [333], with rats ~8 times [144]. This basic observation has intrigued physiologists for more than 100 years. Part of this difference in energy consumption may relate to basal requirements for thermoregulation. It is well known that metabolic rate depends on body mass such that the surface-to-volume ratio of the body is ~2/3 [551]. However, in 1932, Kleiber reported that an animal's O_2 consumption at rest scales to body mass with an ~3/4 ratio [353, 354]. While the absolute value of this scaling remains controversial, it is clear that in animals there is scaling between structural and functional properties that follows some power relationship to body mass (i.e., allometric scaling) and that this may represent a fundamental principle in biology.

In 1999, West and colleagues [693] introduced a fractal network model for the supply of O_2 to tissues via capillaries. Based on this fractal model, these investigators derived an allometric exponent for basal metabolic rate of 3/4 body mass. However, the 3/4 exponent

describes a relationship for basal metabolic rate rather than a limitation on the O_2 supply. Taylor et al. [651] found that the maximal metabolic rate (MMR) during exercise scales with body mass with a higher ratio of 0.86 compared to the 0.75 predicted by the fractal model proposed by West and colleagues. Regardless of the absolute power relationships, the basic concept of such scaling relationships has intrigued physiologists for years [687], and there are a number of original and review articles on related subjects [124, 133, 134, 217, 297–299, 573, 574].

Various cell functions require energy (ATP largely supplied by mitochondria) including protein synthesis, active membrane ion transport, muscle work by contractile proteins (Figure 1). Clearly, during exercise the relative consumption of energy across cell functions shifts to a larger proportion by muscle work. At rest, muscle ATP consumption is minimal, while during peak power output of exercise, muscle ATP consumption markedly increases, while other the metabolic demands of other body functions may decrease. Thus, basal metabolic rate reflects the energy demands for maintaining processes such as thermoregulation in mammals. Blood flow to tissues is distributed based on need for energy substrates, ranging from basal requirements to maximum exercise. Thus, muscle energy demands range widely (an ~10–50-fold range depending on species) while muscles also account for a substantial proportion of total body mass. Since O_2 cannot be stored indefinitely for later use, the supply of O_2 from lung ventilation to arterial/capillary transport to cellular mitochondria must be able to match this range of muscle demand. Thus, the allometric scaling exponent for maximum metabolic rate varies across species depending on the relative metabolic requirements of muscle during exercise. In mitochondria, the maximum rate of ATP synthesis via oxidative phosphorylation does not vary with body mass when normalized for the surface area of the mitochondrial membrane [296]. Thus, at the mitochondrial level, the most athletic mammal on earth (the Rocky Mountain pronghorn antelope) consumes O_2 at similar rates to the mouse at maximum metabolic rate [402], though measurements of maximal consumption are confounded by different exercise types, muscles assessed and durations [535].

Scaling of Lung Volumes Across Mammalian Species

The concept of symmorphosis was first established to compare the pathway for O_2 from the lung to the mitochondria in muscle [652], with critical assessments performed in showing the cellular aspects (capilliaries, blood and mitochondria) to be highly matched to demand, whereas lung structures had increased excess O_2 diffusion capacity, indicative of its limited plasticity in relation to exposure to external environments [689, 690]. Various experimental structural and functional characteristics of the lung have also been assessed in this regard [217, 433, 649, 651, 652]. In the mammalian lung, capillary blood is exposed to an extensive surface area for gas exchange. This large surface area for gas exchange is achieved through consecutive subdivision of airways into smaller and smaller airways ending in terminal units for gas exchange called alveoli. For comparison, a single sphere of 1 cm^3 volume has a surface area of 4.8 cm^2, whereas a 1 cm^3 volume of the lung has an alveolar surface area of 2,100 cm^2 due to the extensive subdivision into smaller alveoli [218]. Thus, the branching strategy of the mammalian lung can increase the surface area for gas exchange by ~430 fold. With ~250 million alveoli in the human lung, the gas exchange surface area is ~100 times

greater than that of the body surface area, [686, 688]. Assuming an ~5 L lung volume in humans, with an average alveolar diameter of 250 μm, the lung alveoli have a gas exchange surface area of ~150 m^2 that is interfacing with ~213 cm^3 of blood contained in lung capillaries [216].

Although by internal subdivision, the mammalian lung is very efficient in accomplishing gas exchange, the extent of subdivision of the lung is limited with respect to this as a strategy for increasing the respiratory surface area before structural integrity is compromised [412]. Importantly, the volume within the lung comprising large airways and vasculature remains steady across species [216, 225, 411, 523, 658], with parenchyma contributing ~84% of the total anatomical volume of the lung [658]. Subdivision of the lung results in a large number of small gas exchange units in a limited volume. These smaller gas exchange units with higher surface tension are susceptible to collapse at the air-tissue interface and require more work (energy) to inflate. Based on the Young-Laplace Law, the pressure required to inflate an alveolus is directly dependent on its surface tension and inversely related to its radius. Amongst mammals, the lungs of bats have the smallest diameter alveoli (~30 μm), whereas dugongs and manatees have the largest diameter alveoli (~1300 μm) [656]. The bat is astonishing in the sense that airborne locomotion is energetically taxing, requiring high levels of gas exchange in the lungs, a feat that is achieved through very small alveoli that are packed into large lungs (for its body weight) and a high hematocrit and high blood O_2 affinity [334, 412, 413]. In general, the diameter of alveoli is negatively correlated with metabolic O_2 consumption per unit of body weight, VO_2 [656]. The respiratory surface density, the surface area available for gas exchange divided by the lung parenchymal volume plotted against body weight shows a steady conservation in the amount of subdivision in the lung across mammalian species. Consequently, resting metabolic rate also correlates to total body weight in mammals [105, 159, 229, 258, 451, 463, 568, 643, 695] (Figure 1).

The initial proposal of symmorphosis dealt with gas exchange not only in the lung, but also at the tissue level where O_2 is utilized for energy production within mitochondria. In this respect, the gas exchange capacity within the lungs of mammalian species has an ~2 fold excess [689], with only the smallest mammals using their entire capacity during hypoxic conditions [648–650]. An important caveat for these assessments is that many of these measures are predicated on assumptions and estimations derived from anaesthetized preparations. Thus, the apparent ‘excess’ capacity of the lung gas exchange may actually reflect the short-term requirements for highly athletic behaviors in the wild. Overall, the apparent mismatch between structural and functional requirements may be interpreted to mean two things: 1) that in many cases considerable reserve capacity exists to tailor gas exchange requirements to increased energetic demands, be they developmental, aging, illness- or ecology-related and interspecies-related; or 2) that lung design is not fully determined by requirements for gas exchange, and that other factors such as biomechanical advantage and endocrine activities also drive lung design [412, 414, 415, 689, 690]. Indeed, dual roles are exactly the reason that the DIAm, at first glance, violates the principles of symmorphosis.

Symmorphosis: Evolution of the Diaphragm

The DIAm functions both as a partition, separating the thoracic and abdominal cavities, and also as a muscular pump generating negative P_{th} and positive P_{ab}. It is this dual functional role that should be accounted for in considering the evolution of the structural design features of the DIAm, and how these are matched to functional demands (i.e., the range of physiological roles in which the DIAm participates). Symmorphosis postulates that there should be no unnecessary, excess capacity in design features, so the evolution of the DIAm should be explored by considering how its structural design meets physiological demands. In this respect, we will first consider the partitioning role of the DIAm in forming separate abdominal and thoracic cavities. This partition prevents movement of abdominal organs into the thoracic space, especially during aspiration breathing. In addition, by reducing compartment volume, this partitioning improves the efficacy of P_{th} and P_{ab} generation.

We will also consider the role of the DIAm as a muscular pump for generating P_{th} and P_{ab}. In this context, the involvement of the DIAm in different motor behaviors requiring pressure generation must be considered. Certainly, it is well recognized that the DIAm is the major inspiratory muscle for lung ventilation. Since these respiratory efforts have a high duty cycle (i.e., time active versus inactive), the DIAm must be designed to avoid fatigue during inspiratory efforts. However, the DIAm is also involved in higher force, low duty cycle efforts associated with increased abdominal pressure generation. Thus, we suggest that the DIAm should be considered as two pumps, one used persistently for generating negative P_{th} for lung ventilation and the second used more infrequently for generating higher P_{ab} to promote venous return and for expulsive behaviors. Throughout this review, we refer to measurements obtained in a variety of species. We have endeavored to capture the entire breadth of available knowledge on the DIAm and many of the observations cited herein are not necessarily exemplars, but constitute the only available data.

Diaphragm as a Partition Between Abdominal and Thoracic Cavities

Formation of an internal body cavity is a major distinguishing feature in zoology and evolution, with vertebrates exhibiting a range of configurations (Figure 2). There was an important evolutionary sequence from acoelomate animals without internal body cavities to pseudocoelomate and finally to coelomate animals that have a true internal fluid filled body cavity lined with epithelial cells forming a double-layered (parietal and visceral) peritoneum, pleura or pericardium depending on location [446]. In fish, these cavities consist of a pericardial (containing the heart) and peritoneal (containing the visceral and urogenital organs) cavity [351, 366]. In amphibians and most reptiles, the body contains the pericardial cavity and the pleuroperitoneal cavity (comprising the lungs, visceral and urogenital organs) [351]. In some reptiles and all mammals, the pleural cavity (containing the lungs) and pericardial cavity are consolidated into the thoracic cavity [351]. Furthermore, in some mammalian species, there is a separation of the left and right lungs by the presence of a partition (the mediastinum) separating left and right pleural cavities [679]. The peritoneal cavity, also termed the abdominal cavity in mammals is completely partitioned from the rostral pleural cavities by the DIAm.

Formation of a fluid filled coelomic cavity provided spatial and physiological independence of organs. The posterior portion of the coelomic cavity is lined by the peritoneum comprising a squamous epithelial cell layer on top of a mesenchymal layer with an intervening serous fluid-filled space that hosts blood vessels, lymphatics and nerves both on the outside wall (parietal peritoneum) and on the intestine (visceral peritoneum). In the anterior portion of the coelomic cavity, the pleura and the pericardium reflect an equivalent double layered epithelial lining that envelops not only the thoracic wall but also the lungs and heart, respectively.

The serous fluid-filled space between peritoneal layers allows movement of the viscera, especially the gastrointestinal tract, while providing support for the organs within the posterior coelomic cavity. Some organs such as the kidneys and portions of the gastrointestinal tract are positioned behind the peritoneum between the peritoneum and posterior coelomic cavity wall, and thus, they are classified as being retroperitoneal. Parts of the parietal and visceral peritoneum come together to form large folds that bind the internal organs together and to the walls of the posterior coelomic cavity. Examples include the mesenteric, omental and falciform ligaments. These peritoneal folds also form compartments within the coelomic cavity. The embryological development of the pericardial, pleural and peritoneal cavities clearly shows the relationship between the compartments of the body cavity and their partitions [496] (Figure 3). Thus, compartmentalization is a major evolutionary trait matching structure and function.

The structure of the pleural and pericardial lining comprises two layers that form a serous fluid-filled space, which facilitates movement of the lungs and heart while providing structural support and partitioning [446]. Similar to the peritoneum, the merging of parietal and visceral pleura and pericardial membrane forms folds that delineate partitions within and across cavities. Importantly for the DIAm, the pleuroperitoneal fold contains the phrenic nerves emerging from the cervical spinal cord [107, 444, 503] (Figure 3). Myocytes that will fuse and form the DIAm also migrate along the pleuroperitoneal fold [107, 444, 503].

The parietal lining of the coelomic cavity forms a tight seal for pressure development by muscular contraction to enhance critical body functions. These functions included voiding of metabolic waste products (e.g., defecation and micturition), egg laying (procreation), pressure gradients for blood and lymph circulation and venous return of blood to the heart. There were distinct evolutionary advantages to develop mechanisms for increasing pressure generation within the coelomic cavity. For example, with the evolution of calcified (hard shelled) eggs in reptiles, extrusion required increased coelomic cavity pressure development [629]. Similarly, as animals grew in size, the requirements for voiding increased, again requiring increased coelomic cavity pressure generation. With increased energy demands and upright posture in some reptiles, coelomic cavity pressure was essential for venous return of blood to the heart [327]. The symmorphosis concept applied to DIAm evolution cannot exclude the evolutionary advantage gained by the impact of DIAm contraction on more efficient generation of P_{ab}. Thus, there is an evolutionary advantage afforded by the more efficient generation of positive P_{ab} and muscularization of the DIAm partition provided an evolutionary advantage in this respect.

The DIAm evolved from a membranous physical partition that separated a single coelomic cavity into separate abdominal and thoracic cavities [503]. As mentioned above, formation of peritoneal folds was a common feature for partitioning compartments within the coelomic cavity (Figure 2). In lower vertebrates, the hindgut of the digestive tract is contained within a single coelomic (abdominal) cavity but suspended by peritoneal folds. In air breathing vertebrates (e.g., amphibians), comingling of the lungs and digestive tract was fine when breathing was accomplished by buccal or positive pressure breathing (Figure 4). However, in reptiles, aspiration breathing evolved to facilitate the external circulation of air into the lungs for gas exchange [69, 503]. The strategy of aspiration breathing in reptiles was critical for more efficient external circulation of air into the lungs. However, the negative intra-coelomic pressure generated by rib cage muscles caused rostral movement of the digestive organs (stomach, liver, gut) into the thorax, which impeded expansion of the lungs. This led to the evolution of a physical partition of the abdominal and thoracic cavities in order to prevent movement of visceral organs so that they would not impinge on lung inflation during aspiration breathing (Figure 4).

The septum transversum is related to the formation of the pericardial sac, cardiac tube and liver [351] (Figure 3). It serves as a partition to separate the heart and pericardium from the peritoneal cavity, containing the visceral and urogenital organs in lower vertebrates, including fish [343] (Figure 2). In animals with lungs, such as amphibians and reptiles, the septum transversum partitions the pericardial cavity and the pleuropertioneal cavity, containing the lungs, visceral and urogenital organs [351]. In fish, the septum transversum partition facilitates generation of a positive intra-coelomic pressure gradient when muscles of the coelomic cavity wall contract. This positive pressure is important in enhancing venous return of blood to the heart [343]. A positive intra-coelomic cavity pressure is also important for other body functions such as defecation, urination, egg laying and, in some cases, vomiting/regurgitation. In amphibians, contraction of coelomic wall muscles contributes to positive intra-coelomic cavity pressure generation [343]. Thus, muscular contraction in amphibians facilitates venous return of blood to the heart as well as other bodily functions that require a pressure gradient.

The first physical partition of the abdominal and thoracic cavities appeared in reptiles by the fusion of the septum transversum with the peritoneal folds of the post-hepatic septum and post-pulmonary septum [503] (Figure 2). In reptiles, the development of positive intra-coelomic cavity pressure is still important to enhance venous return of blood and to drive other bodily functions. Importantly, in most reptiles the lungs are comingling with visceral and urogenital organs within the pleuroperitoneal cavity [351]. By partitioning separate abdominal and thoracic cavities, smaller relative abdominal and thoracic spaces are created, which improves the efficiency of P_{ab} and P_{th} generation (Figure 2). However, in most extant reptiles, there is no separation of abdominal and thoracic cavities, but there is extensive development of the ribcage [343]. In these animals, intercostal muscle activation expands the coelomic cavity thereby developing a negative intra-coelomic pressure for lung inflation (aspiration breathing). This certainly is counterproductive for bodily functions that require a positive intra-coelomic pressure and thus, there was a need for conflict resolution through evolution.

In reptiles such as lizards with higher energetic demands due to their active predation lifestyle (e.g., tegu lizards), a separation of the lungs from liver and the rest of the abdominal compartment by the post-hepatic septum evolved, which prevents the stomach, liver and gut from impinging on lung expansion during inspiration [355–357, 359]. In more advanced reptiles such as varanoid lizards, chameleons, crocodilians and many turtles, a post-pulmonary septum, separating the lung from both the pericardium and the liver evolved, which partially stabilizes the lungs against the liver, providing a viscera-free compartment [155, 502]. Thus, in some reptiles and all mammals, the lungs are located in a thoracic cavity separated by a partition (post-pulmonary septa for reptiles and in the mammalian case, the DIAm) from the abdominal cavity (i.e., the thoracic cavity contains the peritoneal and pleural cavities and the abdominal cavity contains the peritoneal cavity) [351]. In some turtle species, the post-pulmonary septum contains skeletal muscle [226].

It is important to note that neither the bilateral skeletal muscle diaphragmaticus in the crocodile, nor the striatum pulmonalis in the turtle have a principal inspiratory function [503]. In crocodiles, piston action of the diaphragmaticus muscle against the liver increases the thoracic volume and decouples ventilation from locomotion restraints on chest wall expansions [169, 171, 211, 212, 473], and provides a functional advantage during increased metabolic demands of exercise, low temperature or hypercapnea [170, 263, 264, 469]. In turtles, when the striatum pulmonalis muscles contract, they increase P_{ab} for active expiration [213, 214]. In addition, these muscles contribute to buoyancy compensation by displacing the lungs and viscera when the animals are submerged, to help maintain desired pitch and yaw orientations [664]. Importantly, these muscles are not phylogenetically or ontogenetically related to the DIAm of mammals [503]. Furthermore, in crocodiles that have a post-pulmonary septum partitioning the thoracic and abdominal cavities, internal circulation of blood is enhanced, which allows some internal physiologic control of body temperature and thermo-stability [579, 584, 634]. It is tempting to speculate that the larger dinosaurs may have had similar muscularized partitions or piston-like apparatus to facilitate P_{th} and P_{ab} generation. Indeed detailed descriptions of this possibility have previously been discussed in the literature [547–549]. Alternatively, diaphragmaticus muscle like piston functions arguably require a kinetic pubis bone, found only in crocodilofoms [169], whereas dinosaurs have an immovable pubis [103, 270]. Furthermore, the undoubted relationship of sauropods to birds and the avian-like nature of their breathing [111], suggests that the evolution of the air sac, and the unidirectional crosscurrent gaseous exchange system [683, 684], evident in some alligators and lizards [167, 168, 172, 571], meant O_2 delivery was not a limiting factor in ever-more gigantic sauropods [501, 559–561], and helps overcome the dead-space constraints due to excessively long necks.

Of course, the diaphragm muscle is only one way to match respiratory function requirements to anatomical structure. Instead of inflating the thoracic cavity like mammals, the avian respiratory system instead decouples the pump (air sacs and diverticula of the postcranial skeleton) from the site of gaseous exchange (the parabronchi) [78]. Thus, the avian respiratory system allows for oxygenated air to flow constantly in a single direction throughout the entire breath cycle. The gaseous exchange at the parabronchi is also highly efficient, with the direction of pulmonary blood flow at right angles to the direction of airflow. These adaptations allow for the adequate oxygenation of blood at high altitudes

during flight, including over the Himalayan mountain range [266, 576, 577] and compensate for the increased respiratory dead space created by the elaborate and elongated necks and beaks of some species [277]. Indeed, the defining components of an avian-like respiration system, namely the unidirectional airflow, air sacs, the pneumacity of bony structures and countercurrent gaseous exchange, are not interdependent, and may have arisen separately during evolution [559, 572], as evidenced by observations of unidirectional airflow in Nile crocodiles, despite the lack of postcranial pneumacity or air sacs [572]. The aforementioned unidirectional airflow in crocodiles and some other reptiles [168, 172, 571, 572] satisfies the first component, and modern phylogenetic classification schemes would thus indicate their likelihood in other sauropods [559, 654, 685]. The pneumacity of the postcranial skeleton would serve two purposes in dinosaurs: the first would serve to reduce the mass of the skeleton and return the center of mass towards the center of gravity, thus facilitating balance [41, 89, 685]; the second to allow for the growth of neck length, allowing for the exploitation of new ecological niches [559]. Regardless of whether or not dinosaur vertebrae were pneumatised or not, the extremely long neck does pose a respiratory dead space problem, particularly for tidal breathing. Regardless, in many sauropods, evolution towards continuous O_2 uptake, air sacs and pneumaticised postcranial skeletons would undoubtedly confer selective advantages for not only gigantism, but also for flight in pterosaurs, incidentally the largest flying vertebrates to grace the earth [104, 700]. Obviously, these adaptations are some of the defining features of avian species.

In summary, effective partitioning of the thoracic cavity from the abdominal cavity promotes P_{ab} generation and prevents impingement of abdominal viscera on the lungs during the inspiratory phase of aspiration breathing. Positive P_{ab} facilitates venous return of blood to the heart as well as several other important physiological functions. The development of a physical partition between abdominal and thoracic cavities enhances the development of P_{ab}. In reptiles, negative intra-coelomic cavity pressure generation during aspiration breathing creates another problem of incursion of gut viscera and impingement of lung expansion. A physical partition of thoracic and abdominal cavities solves this problem. Muscle action on this partition in crocodiles and turtles evolved to enhance positive P_{ab} generation and facilitate non-respiratory function, not to promote inspiratory efforts. By contrast, evolution of intrinsic DIAm in mammals serves both as a partition and an inspiratory pump, playing an important role in facilitating both P_{ab} and P_{th} generation. This increased efficiency of both P_{ab} and P_{th} generation and the functions they serve presents a major evolutionary advantage for mammals.

Diaphragm Muscle as a Pressure Pump

As noted above, the DIAm separates the abdominal and thoracic cavities of the body. As the DIAm contracts it moves caudally, creating a negative P_{th} and inspiratory airflow. This downward motion of the DIAm also produces a positive P_{ab}. The resulting transdiaphragmatic pressure ($P_{di} = P_{ab} – P_{th}$) reflects DIAm force generation (Figure 5).

We assert that in the context of symmorphosis, evolution of the structure/function relationships in the DIAm involves a tale of two diaphragms, one serving as a partition separating thoracic and abdominal cavities and the second serving as a muscular pump for

pressure generation. Even when considering the pump function of the DIAm, there are two evolutionary paths: 1) the DIAm as an inspiratory pump for the generation of persistent, non-fatiguing negative P_{th} to sustain the high duty cycle requirements of ventilating the lungs day in and day out; and 2) the DIAm as a pump for generating positive P_{ab} that are more infrequent (lower duty cycle) but typically require higher forces (i.e., requiring near maximal activation of the DIAm). Below, we consider the structural and functional design of two types of muscle fibers (or motor units): one a lower force but fatigue resistant set of muscle fibers (type I and IIa comprising slow-twitch - type S and fast-twitch fatigue resistant - type FR motor units) that are efficiently designed for generating negative P_{th} necessary to sustain breathing behaviors, and a second set of higher force but fatigable muscle fibers (type IIx and/or IIb comprising type fast-twitch fatigue intermediate – type FInt and fast-twitch fatigable – type FF motor units) that are optimally designed for short duration high force motor behaviors involving maximal P_{ab} generation.

In complex animals, the generation of positive P_{ab} and negative P_{th} impacts two circulations that are necessary to sustain life. The first “external” circulation is designed to intake and distribute raw materials from outside the body to within the body, where they can be processed and utilized by the organism. Generation of a negative pressure in the thoracic cavity facilitates this intake and thus, there is a distinct biological advantage. A primary example of this type of circulation is the respiratory system in aspiration breathing, where a negative P_{th} facilitates airflow from the environment into the lungs for gas exchange. Another example is the alimentary tract and swallowing, which shuttles food, water and nutrients to stomach and gut epithelia for absorption and digestion. The external circulation is also important in facilitating the voiding of waste products from the body. This is true in the respiratory tract, where positive P_{ab} helps move expired air from the lungs thereby eliminating carbon dioxide as the byproduct of metabolism. Generation of positive P_{ab} is also important in defecation and micturition and the elimination of waste products.

The second “internal” circulation distributes energy substrates (nutrients and O_2) to tissues throughout the body and eliminates metabolic waste products from the tissues delivering them to points of excretion. This internal circulation is provided by the cardiovascular and lymphatic systems. In the abdominal and thoracic cavities, these blood and lymphatic vessels are located in the peritoneal and pleural spaces and thus subject to pressure gradients (difference between P_{ab} and P_{th}). In the cardiovascular system, the heart acts as a pump to generate pressures in order to distribute oxygenated blood to the tissues. Venous blood returning to the heart, is lower pressure and thus proportionally more affected by gravity, which is mitigated by skeletal muscle contractions [20, 406] and a pressure gradient generated by a pressure differential between the thoracic and abdominal cavities. In mammals, the DIAm elegantly provides the partition necessary to simultaneously generate a negative P_{th} and a positive P_{ab}. Thus, both ventilation of the lungs and the ablution of abdominal contents is achieved by a single muscle, with multiple demands for P_{th} and P_{ab} generation.

The earliest strategy for distributing fresh air into the lungs was buccal breathing (Figure 4) [64, 66, 69, 399, 414, 415]. In this scenario, the oral cavity expands and compresses, with air forced into the lung under positive pressure. In ray-finned fishes, buccal breathing serves to

perfuse the gill with water. In lungfish and the extant amphibians, it serves to inflate the lung [64, 66, 69, 399, 414, 415]. At some point in the early natural history of the amniotes (reptiles, mammals and birds), aspiration breathing evolved, a strategy whereby the lungs are inflated by the generation of a sub-atmospheric negative pressure to cause influx of atmospheric air [64, 66, 69, 399, 414, 415, 503]. The efficiency of this mechanism is enhanced by partitioning the thoracic and abdominal cavities (seen in some reptiles). Muscularization of this partition in the DIAm of mammals further increased pressure generation capacity and efficiency. There is no living intermediate form between buccal pump and aspiration breathing, and the abrupt shift from the cranial and hyobranchial musculature providing for ventilation remains puzzling [64, 66, 69]. However, this view has been challenged, with axial musculature involved in active exhalation maneuvers of salamanders [65, 67, 68, 70]. This suggests that aspiration breathing did not evolve suddenly, but in two phases, the first with axial musculature powering active exhalation (while buccal movements remain required for inhalation), followed by axial muscles being used for inhalation and exhalation. Further support of this notion is the buccal and gular breathing of some lizards and geckoes to assist in lung ventilation during and after bouts of locomotion [494]. Certainly, the interactive mechanisms for the neuromotor control required to coordinate the upper respiratory muscles were present in reptiles and amphibians before the emergence of muscularized DIAm, as evidenced by the conservation of rhythmic respiratory pattern generators in the medulla and brainstem of various animal kingdom phylogenetic lineages [531, 642, 665, 666, 697]. Furthermore, in the medulla and brainstem is where one finds the respiratory-related pre-motor neurons that project bilaterally to the phrenic motor pool [186], in many ways making the neuromotor control and ventilator function of the DIAm an extension of the rhythmic upper airway opening and closures related to buccal ventilation, while lung ventilation in amphibians is analogous to active expiration in aspiration breathers (Figure 4).

In many respects, the trunk and abdominal stabilization maneuvers are essential adaptations for both efficient mammalian respiration and locomotion, and there is an abundance of information for locomotor-respiratory coupling [500]. This coupling is facilitated by the ribs, which allow for improved energetics in locomotion and reduce the breathlessness apparent in the pausing of buccal breathers (between jumps) and in reptiles where the side-to-side locomotion impinges on the ability to inflate the lungs [110, 358]. In quadrupeds, there is synchrony integrating one breath per stride (1:1 ratio) [71], and in hopping mammals, such as wallabies a 1:1 pattern is also observed [32]. In humans during walking, locomotor-respiratory coupling is also in 1:1 [524]. However, while running, there is more variability, with synchronization following various patterns (4:1, 3:1, 2:1, 1:1, 5:2 and 3:2) [71]. Trained individuals exhibit markedly more stable coupling between respiratory patterns and locomotor patterns [437]. During locomotion, while parasternal activity remains associated with inspiration, activity of the interosseous intercostals becomes uncoupled from ventilation and instead the activity becomes associated with leg movement [92]. Thus, during locomotor tasks, the intercostal efficiency for ventilatory maneuvers is reduced, underlining the importance of locomotor–respiratory coupling of the DIAm during exercise.

Exercise increases muscle tissue demand for oxygen and thus increases the requirement for ventilation. Indeed, exercise is likely the greatest stressor on ventilation. Respiratory minute

volumes for male adults during eupnea (quiet breathing) are ~6–10 L min^{-1}, assuming a tidal volume of ~500–1000 ml [1, 590] and a respiratory rate of 12–20 breaths min^{-1} [1, 590]. The P_{di} generated by the DIAm during these events is ~4–8 cmH_20 [3, 311, 603], which represents only ~3–5% of maximum P_{di} generation (~150 cmH_2O) [508, 657]. During exercise, minute ventilation increases to ~100–170 L min^{-1}, respiratory rates increasing to ~40–70 breaths min^{-1} and tidal volumes increasing to ~3 L [46, 108, 250, 328, 435]. Using a modified version of Ohm's Law, and assuming the resistance to airflow within the respiratory system is equal between eupnea and exercise, the requirement for P_{di} generation during maximum exercise is ~50 cmH_20, representing only ~33% of maximum DIAm force production, and likely to be less given the increased contribution of the intercostals and other accessary inspiratory muscles [139, 699]. Indeed, ~30–40% of maximum P_{di} is in good agreement with the P_{di} generated during sustain airway occlusion in rodents [347], which likely represents the ceiling of DIAm pressure generation for ventilatory efforts. In humans such P_{di} may be achieved with inspiratory efforts associated with obstructive sleep apnea before arousal.

If the DIAm is only an "inspiratory muscle" as many believe, this raises the question of overdesign and violation of the symmorphosis hypothesis. It is clear that although exercise does utilize some of the 'reserve capacity' of the DIAm, these increased ventilatory requirements for P_{di} generation do not approach the maximum pressure generating capacity of the DIAm. However, expulsive/straining maneuvers require near maximum P_{di} generation and, we will endeavor to highlight the underappreciated non-ventilatory functions of the DIAm.

As the superior wall of the abdominal cavity, the DIAm is essential in the generation of positive P_{ab} in a variety of motor behaviors (Figure 6). The highest P_{ab} are generated during straining maneuvers that involve very high levels of DIAm activation with co-contraction of abdominal and external intercostal muscles and simultaneous closing of the glottis by coordinated activation of the lateral cricoarytenoid and transverse arytenoid muscles of the larynx [317]. Such straining maneuvers occur with vomiting [4, 5], defecation [203, 204] and parturition [271].

Depending on the thoracic or abdominal nature of the expulsive behavior, and the orifice of ejection, an increase in P_{ab} may induce reflex activation of the anal or urethral sphincters. This reflex activation typically depends on the rate of rise of P_{ab} [317]. During coughing, a rapid increase in P_{ab} occurs, which leads to augmentation of anal sphincter activity, thus preventing incontinence [585–588]. By contrast, slower rate of increase in P_{ab}, such as rates observed during defecation, results in a decrease or the abolishment of anal sphincter activity [586]. Many of the non-ventilatory behaviors involving DIAm activation correspond to the generation of very high forces and thus extensive recruitment of phrenic motor neurons and DIAm motor units. Reflex straining maneuvers may be elicited by distension of the rectal wall, vaginal wall, bladder wall, or by stimulation of pelvic afferent nerves [203, 204]. In pregnant rats, stimulation of vaginal afferent nerves also elicits substantial DIAm activation and the generation of higher P_{ab}, leading to expulsion of the fetus [271]. Interestingly, when the abdominal muscles are paralyzed in quadriplegic patients, activation of the DIAm is still preserved during high-force efforts of coughing. This indicates that

neither abdominal muscle contractions or reflexes are required to initiate cough-related DIAm contractions [165].

Expulsive straining behaviors require the generation of very high P_{ab} but these pressures do not need to be maintained for long-periods of time; thus, fatigue is not typically a factor. To generate higher P_{ab} participation of all abdominal wall muscles is required including the DIAm, which forms the superior wall of the abdomen. Synchronous co-contraction of antagonistic muscle groups prevents their relative shortening [7, 269]. This ensures that the lengths of these muscles are maintained within an optimal portion of their force-length relationship throughout activation. Preservation of optimal length explains why P_{di} pressures generated voluntarily in humans are highest during expulsive Valsalva maneuvers, where generation of an P_{ab} ranges from ~90 to 220 cmH_2O [109, 253, 591]. During the Valsalva maneuver, co-contraction of the DIAm and abdominal muscles prevents both the DIAm and abdominal muscles from shortening (i.e., maintaining maximum isometric condition) thereby maximizing DIAm force generation. In contrast, P_{ab} are lower in isolated voluntary maneuvers, where co-contraction of abdominal muscles with the DIAm does not occur [384]. Synchronous contraction of the DIAm and abdominal muscles during expulsive maneuvers also prevents cranial displacement of the abdominal organs toward the thoracic cavity.

The important role of DIAm activation in expulsive maneuvers is supported by a variety of clinical reports. In patients with severe DIAm weakness, difficulties with defecation are often concomitant [503]. In horses, the severing of the phrenic nerve leads to the accumulation of feces in the rectum [332]. In quadriplegic patients, DIAm pacing is associated with less difficulty during defecation [503]. In addition, diaphragmatic ruptures may occur during other high-force expulsive efforts such as coughing [100, 123, 227, 335, 540], vomiting [391], or during parturition [61, 255, 257, 275, 542, 550, 580, 713]. Indeed, the generation of higher P_{ab} during straining behaviors is a common factor in non-traumatic diaphragmatic hernia [157]. Among all expulsive straining behaviors, parturition inarguably requires the highest, most prolonged and repeated activations of the DIAm. During this effort, the coordinated and sustained contractions of the abdominal muscles and the DIAm generate incredibly high intra-uterine pressures, greater than ~130–220 mmHg (~170–300 cmH_2O) [84, 506, 521]. In humans, where the dimensions of the birth canal and the head of the fetus are very similar, hence there is a necessity for generation of high P_{ab} in addition to uterine contractions. In addition to humans, herniation of the DIAm during parturition has also been observed in other mammalian species including horses, buffaloes and goats [120, 630, 645]. Perhaps even more significant, DIAm fatigue may occur during the repetitive maximal contractions of normal human labor [476]. From an evolutionary standpoint, the development of a muscularized DIAm may have been a key adaptation in mammals to allow the bearing and birth of living offspring. Indeed, the high-force generating capacity of the DIAm may be a key facilitator favoring the evolution of increased cranial size in humans and thus the increased volume of the “disproportionate” human brain.

The DIAm is also active during non-respiratory activities that involve adjustments in trunk posture, including those that occur during rapid upper limb movements [279–281] and other motor activities such as weightlifting [9]. Anticipatory crural and costal DIAm contractions,

initiated in response to visual stimulation, occur before rapid flexions of the shoulder [279]. Swift and repetitive motions of the upper limbs induce expiratory activity of DIAm relaxation, upon which a layer of phasic modulation is added at frequencies corresponding to both limb and respiratory movements [281]. Abdominal muscles (e.g., the transversus abdominis muscle) are subject to similar modulatory activities [279, 281], and likewise for pelvic floor muscles [283]. Importantly, the activation of pelvic floor muscles is linked to DIAm activity through polysynaptic reflex pathways that facilitate voiding behaviors. These reflexes are triggered by high-force expiratory (e.g., cough) or inspiratory (e.g., sniff) pressures that increase P_{ab} [102].

Intra-abdominal pressure increases during postural tasks [268], a result of the co-activation of the abdominal muscles and the DIAm, together with various pelvic muscles. A marked elevation of P_{ab} occurs during weight lifting behaviors and reflects the contribution of the DIAm to core strength and the tight coordination among the abdominal wall muscles [268]. Activation of the DIAm is the most important determinant of the maximum P_{ab} achieved, which is enhanced with a closed glottis. A rise in P_{ab} also increases spinal stiffness, reduces lumbar intervertebral motions [282, 595], and stabilizes the trunk, thereby optimizing posture and the efficiency of movement. As mentioned, rupture of the DIAm following high P_{ab}, closed glottis maneuvers may occur [434]. The mechanisms involved in such injuries range from DIAm avulsion from the muscle origin or insertion, the shearing of overstretched fibers or blunt/sudden force transmission through the abdominal viscera acting in a projectile manner.

Symmorphosis: Skeletal Muscle Design and Function

The structural properties of muscle are designed to efficiently accomplish force generation and contraction (change in length) while avoiding fatigue of these motor properties. The striated appearance of skeletal (and cardiac) muscle fibers is due to the presence of repeated sarcomeres in series arranged along the length of myofibrils [252, 398, 441] (Figure 7). The DIAm is a striated (skeletal) muscle with sarcomeric organization of contractile proteins. There is some controversy regarding the number of muscle fibers within the DIAm although very few studies have systematically examined this. Krnjevic and Miledi estimated that the rat DIAm comprises ~10,000 individual muscle fibers [373]. Since there are ~480 phrenic motor neurons in the rat spinal cord [190], this would represent a mean innervation ratio (muscle fibers per motor neuron) of ~21 fiber per motor neuron. However, the innervation ratio is likely closer to 100 fibers per motor unit [196], which would correspond to a total of ~48,000 muscle fibers in the rat diaphragm.

Similar to all skeletal muscle fibers, DIAm fibers are multinucleated, with nuclei located peripherally [237, 598, 615, 620]. Thus, each myonucleus controls gene expression within a restricted volume of the muscle fiber, termed the myonuclear domain [18, 430, 668]. Some investigators have suggested that myonuclear domain size is regulated via apoptotic elimination of myonuclei during atrophy and addition of myonuclei (satellite cell fusion) during hypertrophy. However, in the rat DIAm, we found that myonuclear domain size was not controlled during conditions of atrophy and hypertrophy and changed proportionately with muscle fiber cross-sectional area [233].

Although the basic sarcomeric structure of muscle fibers is similar, the sub-sarcomeric structural design of muscle fibers varies to enhance certain features in the form of different fiber types. In addition, the volume density of organelles such as the sarcoplasmic reticulum and mitochondria can vary across fibers enhancing performance features that are well aligned to functional demands.

Sarcomeric Structure of Striated Muscle

In eukaryotes, actin-based myosin motors evolved to facilitate a variety of movement-related functions including the trafficking of intracellular organelles, cellular division, and muscle contraction. Among the myosin motor protein superfamily, class-II myosins are distinguished by their ability to assemble into thick filaments [116]. Within the rod domain of the myosin heavy chain (MyHC) there is an interface for dimerization into a coiled-coil configuration [405], which contributes to a higher order assembly first into filaments [439, 440] and further into sarcomeres [122] found in skeletal and cardiac muscles (Figure 7).

Different MyHC isoforms are found that determine both the contractile and energetic properties of muscle fibers. In humans, skeletal muscle MyHC isoforms are encoded by six genes (chromosome 17p13) [596, 691, 692] and two genes (chromosome 14q12) encode cardiac muscle MyHC isoforms [410, 556]. In addition, in mammals three other class-II MyHC genes exist: 1) the smooth muscle MyHC gene that encodes, via alternative RNA splicing processes, four distinct proteins [25]; 2) non-muscle A MyHC; and 3) non-muscle B MyHC. These class-II MyHC proteins in non-muscle cells are responsible for a variety of actin-dependent motor functions [25, 344]. There is structural similarity between myofilaments comprising smooth muscle MyHC (thought to be the most primitive) and non-muscle MyHC [10], suggesting an evolutionary relationship among class-II MyHCs. It is likely that the evolution of smooth muscle MyHC and non-muscle MyHCs emerged from a common ancestral gene before the evolution of sarcomeric MyHC isoforms.

The sarcomere, which is the essential functional unit of myofibrils, consists of contractile proteins interspersed between Z-discs. The Z-discs are typically aligned orthogonally to the long axis of each myofibril and also aligned in parallel across myofibrils to form Z-disc (Figure 7). Thin filaments are anchored to the Z-discs and project toward a midline (M-line). Thick filaments are interposed between the thin filaments in a highly-organized, crystalline fashion with six actin filaments surrounding each myosin filament.

Thin filaments comprise polymerized actin molecules together with tropomyosin and troponin. Thick filaments comprise MyHC and myosin light chain (MyLC) molecules (together called the myosin head) with a longer myosin tail. Cross-bridges are formed by the chemical binding of myosin heads to the actin filament, and cross-bridge formation provides the molecular basis for force generation and contraction (i.e., shortening) [507] (Figure 7).

When muscle fibers contract, the ratcheting action of cross-bridge attachment and detachment (cross-bridge cycling) requires energy (ATP hydrolysis) and establishes the velocity of shortening depending on the external load (load-velocity relationship of striated muscle). The interactions between thick and thin filaments cause the Z-disc to move toward

the midline of sarcomeres without a change in thick or thin filament length; first described as the sliding filament theory [313] (Figure 7).

Within a muscle fiber, the sarcoplasmic reticulum is a loose network between myofibrils that connects to T-tubules located near each Z-disc. The sarcoplasmic reticulum network serves as an intracellular storage depot for Ca^{2+}, whose release can be triggered to initiate contraction through a process termed excitation-contraction coupling. Deep invaginations of the plasma membrane called T-tubules are juxtaposed to the sarcoplasmic reticulum at each Z-disc. These T-tubules transmit depolarization of the plasma membrane deep into the interior of the muscle fiber allowing the organization of myofibrils in parallel and larger diameter muscle fibers. With T-tubule depolarization, Ca^{2+} is released from internal stores (the sarcoplasmic reticulum). The resulting elevated of intracellular Ca^{2+} facilitates binding to troponin C (TnC) on the thin filament, thereby removing the steric hindrance of the binding site of the myosin head on the actin filament. This regulation of myosin attachment to actin and cross-bridge formation also involves troponin T (TnT), which binds the troponin complex to the tropomyosin molecule and troponin I (TnI) that actually blocks the actin binding site (Figure 8). Through this Ca^{2+} regulatory process, the attachment of myosin heads to actin and force generation is regulated, as reflected by a sigmoidal force-Ca^{2+} relationship (Figure 8).

Evolution of Excitation-Contraction Coupling

In striated muscle (both cardiac and skeletal), a process of excitation-contraction coupling evolved to control muscle contraction. In this process, the electrical charge stored on the membrane capacitor is discharged during an action potential. Muscle fiber action potentials are propagated along the length of the sarcolemma (muscle fiber membrane) and depolarization is passively transmitted down the T tubule where dihydropyridine receptors (DHPRs; voltage sensitive L-type Ca^{2+} channels) are located. In vertebrate skeletal muscle fibers, DHPRs are linked at tetrad structures to a subset of ryanodine receptors (RyRs), which are Ca^{2+} release channels located in the sarcoplasmic reticulum membrane. T-tubule depolarization activates DHPRs, which in turn induces an initial RyR-mediated Ca^{2+} release. The open probability of the RyRs is also sensitive to Ca^{2+} such that initial DHPR-mediated Ca^{2+} induces further Ca^{2+} release in a positive feedback process (i.e., Ca^{2+}-induced Ca^{2+} release). This process rapidly floods the cytosolic space surrounding contractile proteins with free Ca^{2+}. The elevated cytosolic Ca^{2+} binds to TnC leading to removal of steric hindrance and cross-bridge formation (Figure 8). In cardiac muscle and in body muscles of invertebrates, RyR and DHPRs are also present, but tetrads are not present and their interaction is indirect. Muscle fiber depolarization triggers opening of DHPRs and Ca^{2+} influx. This Ca^{2+} influx triggers Ca^{2+}-induced Ca^{2+} release through RyRs in the sarcoplasmic reticulum.

Functional Properties of Striated Muscle

The two major inter-related functions of muscle are to generate force and cause shortening or contraction. Contraction of muscle typically occurs in opposing an external load. When the load equals or exceeds the force generation capacity of a muscle, no contraction occurs (isometric condition). With a lesser external load, the ability of the muscle to shorten

depends on the force generated (force/load - velocity relationship; Figure 9). Thus, the generation of force is central to the overall function of muscle.

The force (F) generated by a muscle fiber is estimated by the following equation:

$$\mathbf{F = n \bullet \mathit{f} \bullet \alpha_{fs}}$$

Where n is the MyHC concentration per half sarcomere, f is the force contributed by each cross-bridge and α_{fs} is the fraction of MyHC forming strongly bound cross-bridges. At optimal sarcomere length (i.e., greatest extent of overlap of myosin heads and actin binding sites), the primary determinant of α_{fs} is Ca^{2+}-dependent regulation of the myosin head binding site on the thin filament (this forms the basis of the force-Ca^{2+} relationship in muscle fibers). At sub-optimal length, myosin heads cannot bind to actin; thus, α_{fs} is also reduced and less force is generated (Figure 9). This forms the basis of the force-length relationship of striated muscle (both skeletal and cardiac muscle). During muscle contraction sarcomere length changes thus affecting the overlap of thin and thick filaments, α_{fs}, the number of cross-bridge formed and the force generated. Thus, as sarcomere shortening velocity gets faster, force decreases and this dependency is reflected by the force-velocity relationship of muscle (Figure 9).

The force generated by an individual cross-bridge (f) is mainly determined by MyHC isoform composition. Myosin is a hexameric protein comprising two MyHC molecules (each weighing ~200 kDa), and four MyLC molecules (weighing ~17–20 kDa). The MyHC molecules are intertwined to form a double helix. A myosin head is at the end of each MyHC that acts as an enzyme to hydrolyze ATP during cross-bridge cycling. There are also two MyLCs at each myosin head; one “regulatory” and one “structural”. The functional role of the MyLC isoforms varies, but it is thought that they help stabilize the myosin head during contraction.

Several isoforms of MyHC exist, some present only during embryonic ($MyHC_{Emb}$) and neonatal development ($MyHC_{Neo}$). In the adult rat DIAm, MyHC isoforms $MyHC_{slow}$, $MyHC_{2A}$, $MyHC_{2X}$, $MyHC_{2B}$ correspond to different fiber types [195, 610, 613, 625], a phenomenon conserved across all species studied, though the $MyHC_{2B}$ isoform is not present adult human DIAm. Each DIAm fiber typically expresses only a single MyHC isoform, although some co-expression of $MyHC_{2X}$ with $MyHC_{2B}$ occurs in varying proportions in a variety of mammalian species. With muscle injury, it has been reported that expression of $MyHC_{Emb}$ and $MyHC_{Neo}$ reappears, possibly due to the fusion of satellite cells, into the injured fiber for repair. Differences in the relative proportions and expression of MyHC isoforms determine the contractile and fatigue properties of the DIAm across species.

Sir Andrew Huxley introduced the sliding filament theory of muscle contraction in 1957 [313]. Based on this general model, it is now widely accepted that cross-bridge cycling determines the mechanical properties of muscle fibers. When myosin heads strongly bind to actin, there is a “power stroke” that involves bending at the junction of the “head” and “neck” regions of the myosin molecule. As a result, the strong binding of the myosin head

transitions to a weaker bond, and cross-bridges detach. During this power stroke force is generated and the sarcomere shortens depending on the external load. This process then repeats during cross-bridge cycling, and with each transition there is hydrolysis of one ATP molecule and chemical energy (ATP) is converted into mechanical energy (force and/or shortening). When ATP is removed, myosin and actin do not dissociate and consequently the muscle fiber stiffens (i.e., rigor mortis). It appears that the power stroke varies across MyHC isoforms, being greater in fibers comprising $MyHC_{2A}$, $MyHC_{2X}$, $MyHC_{2B}$ isoforms compared to those comprising the $MyHC_{slow}$ isoform. Thus, both the greater force per cross-bridge (f) and faster shortening velocity of "fast" muscle fibers relates to their MyHC isoform composition. The consumption of ATP for any MyHC isoform is described by the following equation:

$$\textbf{ATP Consumption} = \mathbf{n} \bullet \mathbf{b} \bullet \alpha_{\mathbf{fs}} \bullet g_{\mathbf{app}}$$

Where n is MyHC concentration per half sarcomere, b is the number of half sarcomeres in series, α_{fs} is the fraction of MyHC that is strongly bound forming cross-bridges, and g_{app} is the apparent rate constant for cross bridge detachment. Velocity of shortening and g_{app} are dependent on external loading; thus, ATP consumption changes with external load and velocity of shortening reaching a maximum at peak power output of a muscle fiber [259, 261, 616]. This relationship was first quantitatively described by W. O. Fenn, who measured heat production in contracting muscle, and is known as the Fenn effect (Figure 10). The maximum velocity of the ATPase reaction can be determined using quantitative histochemistry [50, 52] and varies with DIAm fiber type due to MyHC concentration and differences in g_{app} [259–261]. During peak power output of DIAm fibers, the rate of ATP consumption is close to the maximum velocity of the ATPase reaction (Figure 10).

Cross-bridge cycling rates (shortening velocities) and maximum ATP consumption rates of muscle fibers are associated with the expression of different MyHC isoforms. Muscle fibers comprising $MyHC_{2B}$ and $MyHC_{2X}$ isoforms display faster rates of force development (faster f_{app}; Figure 11) and faster cross-bridge cycling rates and maximum shortening velocities (associated with faster g_{app}; Figure 11) and have the highest ATP hydrolysis (consumption) rates followed by fibers comprising $MyHC_{2A}$ and $MyHC_{slow}$ isoforms [259, 543, 619].

Consistent with the Fenn effect, ATP consumption within a muscle fiber increases with power output or work performed [177]. In order to fulfill the considerable range of ATP consumption demands across muscle fibers, a range of ATP production reserve capacity by mitochondria and glycolytic pathways is necessary. Due to the lower mitochondrial volume density in muscle fibers expressing $MyHC_{2X}$ and $MyHC_{2B}$ (type IIx and/or IIb) and thus the lower capacity for oxidative phosphorylation, the reserve capacity for ATP production oxidative phosphorylation in these fibers is lower compared to fibers expressing $MyHC_{2A}$ and $MyHC_{slow}$ [543, 621]. These type IIx and/or IIb fibers depend more on glycolytic pathways for ATP production, which has much lower functional reserve capacity. It is likely that the greater fatigue susceptibility of type IIx and/or IIb fibers is due to their higher rate of

ATP consumption, fewer mitochondria and lower total reserve capacity for ATP production [195, 614].

Throughout life, skeletal muscle is constantly remodeling, adjusting to changes in activity, load, or innervation. Thus, within limits, muscle can change its structure and function to adapt to environmental conditions, natural or imposed. We see this commonly in sports, where athletes train to achieve muscle adaptations that optimize specific performance needs. This can be in the form of increasing the number and velocity of muscular contractions to promote mitochondrial biogenesis (increased oxidative capacity via increasing mitochondrial density and surface area) and endurance (e.g., marathon runners) or increasing the external loading on muscle contraction to increase force and power (e.g., body builders). Marathon runners and body builders obviously do not have the same physiques. Generally, muscles in marathon runners are smaller, weaker but with greater endurance. In contrast, the training regimen of body builders results in muscle hypertrophy and an increase in force by adding sarcomeres in parallel.

The importance of skeletal muscle remodeling extends far beyond exercise physiology to many clinical conditions and diseases. The strength and endurance of muscle changes throughout life, initially as mature muscle forms and alters through age-related sarcopenia. However, chronic diseases often induce cachexia or muscle wasting and weakening. There are also neuromuscular or muscular diseases such as muscular dystrophy and other congenital muscular disorders, amyotrophic lateral sclerosis (ALS), and spinal cord injury that impair muscle activation or muscle performance. Just as exercise varies for marathon runners versus body builders, there is not a single therapeutic approach for musculoskeletal diseases. In general, the structure and function of different motor unit and muscle fiber types in respiratory muscles are the same those of other skeletal muscles and the training effects are the same.

Evolution of Muscle and Myogenesis

The development of mechanisms for movement within cells, tissues and the whole organism is a key feature of evolution. Some motor proteins such as MyHC found in striated muscle were already present in unicellular organisms before the evolution of multicellular animals. Indeed, orthologs of MyHC were expressed in sponges, suggesting functional diversification of paralogs of myosin motor proteins before the origin of true striated muscles. Similarly, in jellyfish and other animals of the Cnidarian phylum, there were orthologs of Z-disc proteins, but they were not associated with striated muscles. Thus, it appears that vertebrate skeletal muscle evolved through the separate independent evolution of constituent proteins that may or may not have been part of a pre-existing, ancestral contractile apparatus. The combined components of striated muscle, including MyHC, filamentous actin, the troponin complex and titin appear in bilaterian Metazoan animals, which have three germ layers endoderm, mesoderm, and ectoderm. Muscle cells derive from the mesoderm layer in these animals.

All skeletal muscle fibers, both axial and limb, including those of the DIAm, undergo myogenesis consisting of two stages: 1) the determination phase, a temporal switch when myoblasts emerge from mesodermal progenitor cells; and 2) the terminal differentiation

phase, when myoblasts fuse to form the nascent myotubes followed by the formation of myofibers that express contractile proteins in ordered sarcomeres (Figure 12).

Potential mechanisms for myogenesis include the procession of an intrinsic genetic program, removal of inhibitory regulatory signals or the presence or promotion of positive extrinsic signals [19]. However, current knowledge indicates that myogenesis is programmed by the timed expression of muscle regulatory factors (MRFs), including MyoD [129], myogenin [73], Myf-5 [74] and MRF4 [534]. Furthermore, MRFs also appear to be involved in determining MyHC isoform expression in adult muscle fibers [306]. Thus, they are a parsimonious regulatory factor in both pre- and postnatal development.

The MRFs initiate myogenesis through their function as molecular switches, triggering the expression of muscle specific genes. This occurs via the binding of MRFs to the genomic control elements (E-boxes) of muscle specific genes [484]. These CANNTG sequence motifs are located in promoter regions of a variety of genes specific to skeletal muscle [82]. Removing the inhibitory signals that dampen MRF expression results in myoblast determination (commitment). In certain classes of helix-loop-helix (HLH) transcriptional regulators, termed Id factors (Id1-Id4), the formation of heterodimers with E2 products (HLH-containing proteins ubiquitously expressed) inhibits the activity of MRF. This prevents the activation of genes specific to skeletal muscle [38]. Calcineurin reduces Id inhibitory protein expression, and thus indirectly activates MyoD via removal of inhibition [199]. Twist proteins also prevent MRF-E protein heterodimer formation, and thus they inhibit MRF activity [638]. In a similar manner, another HLH-containing protein, Mist1 binds with MyoD to form an inactive heterodimer, and thus it inhibits myogenesis [394]. Nuclear factor 1X (Nfix) binds to MEF2A, and through this mechanism, it plays a role in the transition of embryonic to fetal MyHC isoform expression [445, 639]. Overall, the balance between pro-myogenic and anti-myogenic inhibitory signals determines the location and the developmental timing of skeletal muscle precursor cells.

The first MRF to be expressed in the DIAm and other hypaxial skeletal muscles is MyoD, which initiates a cascade involving subsequent expression of Myf-5, MRF4 and myogenin within skeletal muscle precursor cells [555]. The specific timing of specific MRF expression is important for the normal development of skeletal muscle. In proliferating myoblasts, MyoD and Myf-5 are highly expressed, underscoring their importance at this stage of myogenesis [129]. By contrast, lack of MyoD, MRF4 and Myf-5 has no known deleterious effect on the development of normal skeletal muscle [75, 552, 709]. However, in mutant mice lacking both Myf-5 and MyoD, the absence of myoblasts suggests that the expression of these particular MRFs is necessary for myoblast commitment [553]. By contrast, myoblast formation occurs in the absence of myogenin but myotubes and myofibers fail to develop [265, 471]. This suggests that myogenin is obligatory for the terminal differentiation of myoblasts into myotubes and subsequent formation of myofibers.

The irreversible exit of mononucleated proliferating myoblasts from the cell cycle occurs with terminal differentiation, when transformed myoblasts fuse into multinucleated myotubes and subsequently into myofibers with expression of contractile proteins. In adults some myoblasts persist as satellite cells with the ability to proliferate, and thus play a role in

regenerative processes involved in injury repair [417]. These satellite cells remain susceptible to apoptosis until they are terminally differentiated [417]. In DIAm and other hypaxial muscles, terminal differentiation of myoblasts occurs only after migration to their final destination [417]. In the DIAm, myoblast migration begins at ~E10 and continues through ~E12 and during this time, the migrating myoblasts express Myf-5, MyoD and c-MET, a tyrosine protein kinase encoded by the MET gene [83]. As mentioned, the timed expression of Myf-5, MyoD and c-MET is important in the process of myoblast differentiation and fusion into myotubes.

Myoblast fusion to form multinucleated myotubes is essential for the subsequent formation of myofibers with expression of contractile proteins organized into sarcomeres. Phrenic nerve outgrowth and arrival at the DIAm is coincident with the period of myoblast migration and formation of myotubes (Figure 13) [425].

However, terminal differentiation of myoblasts and formation of myotubes and myofibers is not dependent on innervation. Instead, myotube and myofibers formation is influenced by mechanical properties and proteins expressed in the cell membrane (e.g., β1-integrin), the cytoskeleton (e.g., actin and desmin), the basal lamina (e.g., muscle cell adhesion molecule - M-CAM), and the extracellular matrix (e.g., fibronectins, laminins, M-cadherin and neural cell adhesion molecule - N-CAM) [361, 371]. Thus, terminal differentiation of myoblasts and subsequent formation of myotubes and myofibers is a very complex process that involves interactions of the cells with their surrounding environment.

During embryonic and neonatal development, there is a transit0069on in the expression of MyHC isoforms with considerable co-expression of isoforms (Figure 12) [376, 377, 680, 681]. During the embryonic period, muscle fibers in the DIAm express an embryonic MyHC isoform ($MyHC_{Emb}$) as well as $MyHC_{Slow}$ and $MyHC_{2A}$. This period corresponds with very low heterogeneity in the size of motor neurons innervating muscle fibers [191]. During the perinatal period, expression of the $MyHC_{Emb}$ switches to a neonatal isoform ($MyHC_{Neo}$), with continued expression of $MyHC_{Slow}$ and $MyHC_{2A}$. In the first two postnatal weeks in rodents, expression of the $MyHC_{Neo}$ isoform in the DIAm gradually disappears and there is an emergence in the expression of $MyHC_{2X}$ and $MyHC_{2B}$ isoforms. Singular expression of MyHC isoforms in DIAm fibers, and thus the final proportions of fiber types does not occur until about 28 days of age [219]. Beginning at postnatal day 14 in the rodent DIAm, there is disproportionate growth of fibers expressing $MyHC_{2X}$ and/or $MyHC_{2B}$ isoforms (~2–3 fold greater increase in cross sectional area compared to fibers expressing $MyHC_{Slow}$ and $MyHC_{2A}$ isoforms) [331, 512]. This period also corresponds to an increase in specific force and velocity of shortening of the DIAm (Figure 14). It remains unclear whether specific innervation of DIAm fibers plays a role in the differential growth of type IIx and/or IIb fibers. However, it is of interest that this period corresponds with a period of growth of phrenic motor neurons [513, 517].

Diaphragm Muscle Structure

Diaphragm muscle structure serves two roles: as a partition separating the thoracic and abdominal cavities and as a muscular pump affecting both P_{th} and P_{ab}. Although the gross

anatomy of the DIAm is generally similar across mammalian species, there are differences that reflect adaptation to specific environmental needs.

Gross Anatomy of the Diaphragm Muscle

Based on muscle fiber origins, the DIAm is typically separated into three major regions (Figure 15): 1) the sternal region in which muscle fibers originate from the posterior portion of xyphoid process and xyphisternal junction and insert into the central tendon; 2) the costal region in which fibers originate from the broad expanse of the lower rib cage (ribs 7–12 and their costal cartilage) and insert into the central tendon; and 3) the crural region in which fibers originate from the broad expanse of intervertebral fibrocartilages of the upper lumbar vertebrae, and the arcuate ligaments overlying the aorta, vena cava and psoas major and quadratus lumborum muscles, and insert into the central tendon.

The DIAm comprises right and left sides (reflecting mammals as bilaterian Metazoan animals), which are generally symmetrical with some differences in the crural region based on structures that pass behind or through the DIAm. Obviously, there is some right/left asymmetry in DIAm structure due to the asymmetry of associated structures including the heart, lungs, esophagus, abdominal organs (e.g., liver) and major vessels.

The orientation of muscle fibers in the two sternal regions of the DIAm are parallel, such that unilateral contraction of one side leads to passive shortening of the opposite side [707]. By contrast, the radiating orientation of fibers in the left and right costal regions of the DIAm are generally in series, such that unilateral contraction of fibers on one side lead to passive lengthening of the contralateral side (Figure 15). In addition, the orientation of fibers in the costal regions of the DIAm are complicated by curvature to form a dome shape. Contraction of muscle fibers in the costal regions causes this curvature to flatten downward, thereby pushing on the abdominal cavity and increasing P_{ab}. Diaphragm contractile mechanics combines muscle tension and curvature with generation of pressures directed orthogonal to the axis of muscle fibers. In contrast, skeletal muscles of the limb exert forces parallel to the muscle fiber axis, with force production and joint movement in line with the direction of muscle fibers [302, 349, 390, 698].

The orientation of muscle fibers in the right and left crural regions of the DIAm is far more complex and displays the greatest asymmetry. The right side is larger and longer compared to the left side. The medial margins of the right and left crural regions encompass the esophagus and act as a lower esophageal sphincter during inspiratory contractions, decreasing the risk of gastric reflux. The descending aorta passes dorsal behind the right crural DIAm, whereas the inferior vena cava passes through the central tendon such that blood flow in both structures is unimpaired by DIAm contractions (Figure 15). Indeed, the negative transdiaphragmatic pressure generated during inspiration promotes an increase in venous return to the right atrium.

Blood flow is heterogeneous in the DIAm at rest, with the sternal portion of the DIAm receiving less blood flow than mid-costal and crural regions [511]. In dogs, increased blood flow is observed in the medial costal region of the DIAm, where the greatest shortening occurs [72]. This is consistent with the relationship between DIAm fiber power output and

ATP consumption rate (Fenn effect; Fig x). During exercise, blood flow increases five-fold and heterogeneity persists, indicating that costal and crural regions of the DIAm may display differential loading, different shortening velocities and different contributions to inspiratory pressure generation [583]. However, there is no evidence of regional differences in fiber type proportions [527], or oxidative capacities [623].

Comparative Anatomy of the Diaphragm Muscle

In general, the gross morphology of the DIAm is conserved across species; however certain differences exist in relation to the relative area and shape of the central tendon, whether or not individual muscle fibers span the entire distance between the costal wall and central tendon, and the orientation of the DIAm in relation to the long axis of the body. These gross variations are likely due to various ecological niches inhabited by different mammals, indeed the successful adaptation of the mammalian clade to some of the most diverse environments on planet Earth, i.e., from pole to pole, from the oceans depths to the tallest peaks and from the driest desert to the wettest jungles is unique in vertebrates.

The central tendon is prevalent in all mammals, except for marine mammals [308, 316, 506], though the shape of the central tendon is variable across species, with pigs having a remarkably large proportion of tendon and ferrets having a relatively small proportion [503]. For example, most mammals have a “V”-shaped central tendon, though “I-” and “U-” shaped configurations do occur. On the right side, a foramen in the central tendon allows passage of the vena cava. Importantly, the relative proportion of central tendon to individual DIAm fiber length has little bearing on pressure generation, though it can have an effect on shortening.

In smaller mammals such as rats, mice and hamsters, DIAm fibers extend from their origin at the costal border to insertion at the central tendon, reaching lengths of ~20 mm [162, 234, 235, 245, 528], which may be a physiological limit of muscle fiber length. In larger species such as cats, dogs, monkeys and humans, DIAm fibers do not extend the full span between the costal margin and the central tendon but instead, have intramuscular tendinous origins and insertions [59, 232, 350, 466, 622]. These differences are evident in the pattern of neuromuscular junction distribution in the DIAm In rodents, neuromuscular junctions are distributed along a clear central line in the middle of the muscle (i.e., at the mid-point of each muscle fiber). In contrast, in larger mammals including humans, neuromuscular junctions are widely distributed as the mid-point of muscle fibers varies with intramuscular tendinous origins and insertions. The presence of intramuscular tendinous origins and insertions is also evident by the pattern of secondary branching of the phrenic nerve. In rodents this secondary branching pattern is very linear corresponding with the location of neuromuscular junctions. However, in larger mammals there is greater variation and elaboration of secondary branches, corresponding with the wider distribution of neuromuscular junctions [14, 59, 85, 152, 350, 386, 387, 443, 466, 578] (Figure 15).

Typically, the DIAm is oriented obliquely in the body, with the origin of fibers in costal and crural regions located more caudally than the origin of fibers in the sternal region. The central tendon insertion of fibers is located more rostral than origin of fibers in the costal and crural regions, thus fibers generally have a rostral projection. In many cases, the thickness of

the diaphragm muscle in excised tissue does not match that of the *in situ* scenario, suggestive of potential differences in regional tensions and thus pressure generation, particularly in dogs [676]. Along the same line, horses exhibit increased length and thickness within the medial costal portion of the DIAm [510]. In horses and elephants, the orientation of the DIAm is more parallel [79, 389], with an almost complete parallel orientation (in relation to the long axis of the body) achieved in the whale in whales [503, 632, 633]. The structure and orientation of the DIAm in the manatee is highly atypical, with distinct hemi-diaphragms that are separated and positioned in the dorsal part of the body cavity, behind the heart, liver and gut, extending to the caudal end of the body cavity with no sternal attachments [541]. In the manatee, the septum transversum still partitions the heart from the liver, but is not muscularized, and actually these two structures are oriented orthogonally to each other. With the lungs distributed dorsally along the entire length of the body cavity, it is speculated that DIAm contractions can help maintain buoyancy [541].

In general, the largest pressures generated by the DIAm involve expulsive behaviors generating high P_{ab} following maximal DIAm contractions. By contrast, the elephant is likely to use near-maximal DIAm activation to fill its trunk with water, requiring a pressure of ~200–300 cm H_2O [79, 694]. The DIAm in the elephant is oriented obliquely between the thorax and abdomen, in contrast to the perpendicular orientation in most mammals, although it is unknown if this orientation serves to enhance pressure generation required for trunk water snorkel function or to alleviate gravitational stresses within the lung alveoli [79, 392, 393].

In diving and marine mammals, the design concerns are not related to gravitational stress, but to the considerable requirement for buoyancy control. In addition, some marine mammalian species dive ~2–3 km below the ocean's surface [109, 495], and experience severe lung compression [48, 398]. As mentioned previously, pressure differentials between the intra-thoracic and intra-abdominal compartments affect both the cardiovascular and respiratory systems [400, 633]. In general, DIAm adaptations in diving marine mammals include a severe reduction in the size of the central tendon, increasing relative muscularization and helping to stabilize the DIAm [389, 400, 633] or alternatively, provide extra shortening potential for muscle fiber contractility [400]. In whales, the DIAm is oriented almost parallel to the long axis of the body [503, 632, 633], which in humpbacks is likely to account for some of their incredible stability in the water column without torso, flipper or fluke movement [210]. During the underwater activities of cetaceans (dolphins), both locomotor function [118, 495] and ambient oceanic pressure differentials load the DIAm [400]. By contrast, pinnipeds (seals), which do not load the DIAm as much during locomotion (generating thrust using hind flippers) [505], however they do experience marked oceanic pressures on dives. Accordingly, the DIAm of cetaceans has substantial subserosal collagen fibers, the amount of which correlated to locomotion velocities of different species [400]. This collagen layer stabilizes the DIAm during locomotion in cetaceans and prevents the intra-thoracic compartment from experiencing sinusoidal pressure waves due to spinal flexion and extension cycles [400].

Embryological Development of the Diaphragm Muscle

The DIAm derives from myoblasts that migrate along the pleuroperitoneal fold [24], which initially appears as bilateral folds of mesenchyme that project into the undivided thoracic cavity. The pleuroperitoneal fold ultimately fuses with the dorsal mesentery surrounding the esophagus and with the dorsal part of the septum transversum (formed from folds caudal to the developing heart and pericardium) to complete the partitioning of the thoracic and abdominal cavities (Figure 3).

With embryonic growth, there is a progressive caudal displacement of the pleuroperitoneal fold, with eventual attachments spanning from mid to lower thoracic levels. Myoblasts that will form the DIAm migrate along the pleuroperitoneal fold [417]. At the same time, the phrenic nerves emerge from the cervical spinal cord and grow following the trajectory of the septum transversum and migrating myoblasts [385, 388] (Figure 3). What chemical factor(s) drive or guide axonal growth of phrenic nerve is unclear, but the coincidental growth of phrenic nerve axons with formation of the pleuroperitoneal fold and migrating myoblasts suggests a linkage [12, 241]. Although the exact mechanisms remain elusive, branching of phrenic motor axons begins within the descending pleuroperitoneal fold at the same time that myoblasts migrate into the sternal, costal and crural regions of the DIAm [24]. Thus, somatotopic innervation of the DIAm is established early in embryonic development.

As mentioned above, the sternal and more ventral aspects of both costal and crural regions are innervated by phrenic motor neurons located in more rostral segments of the phrenic motor neuron pool in the cervical spinal cord, while more dorsal portions of the costal and crural regions are innervated by more caudal segments of the phrenic motor neuron pool [194] (Figure 16). This somatotopic pattern of DIAm innervation develops before initial synapse formation likely reflects the pattern of phrenic nerve outgrowth and branching on the pleuroperitoneal fold.

In rodents, the phrenic nerve emerges onto the pleuroperitoneal fold at about the 11^{th} day of embryonic development (E11) (Figure 13) [241]. As mentioned branching of phrenic motor axons occurs early with Schwann cells in close proximity, which actually appear to precede motor axon terminals. Guidance of Schwann cell and phrenic axon terminal outgrowth may involve a series of complex regulatory processes. Clearly, the phrenic nerve must initially target the pleuroperitoneal fold before contacting myoblasts and myotubes or myofibers. Subsequently, specialized axon terminals must form in association with myotubes and/or myofibers, where cholinergic receptor aggregation occurs in close proximity to form synapses. These events occur in a relatively short period of time within 2–3 days (E11-E14) in rodents, and the timing of the regulatory processes involved is critical. These events may be affected by muscle or nerve activity [30, 191, 192], mechanical properties the extracellular matrix, and/or the release of trophic factors and/or chemotactic substances by muscle or extracellular matrix [417, 487–492].

Agrin derived from motor neurons is important for development of neuromuscular junctions and thus, for development of excitation-contraction coupling mechanisms [29, 647]. Neuregulin [166, 563, 659, 712], expressed by motor neurons during embryonic development activates ErbB tyrosine kinase receptors located on DIAm myoblasts,

myotubes and myofibers [267]. Neuregulin/ErbB signaling promotes protein synthesis in developing DIAm fibers [267] and also induces acetylcholine receptor expression and clustering [479, 480] at embryonic neuromuscular junctions via its effects on Schwann cells [325].

Diaphragm Muscle Innervation

In DIAm fibers, a series of electro- chemical- and mechanical transduction processes underlie neuromotor control of muscle activation by the nervous system. This excitation-contraction signaling process is begins with a nerve action potential (electrical signal), which is transduced at the neuromuscular junction to a chemical signal transmitted to receptors on the muscle fiber. This chemical signal then initiates another electrical signal (action potential) in the muscle fiber that is propagated and leads to another chemical signal (Ca^{2+} release from the sarcoplasmic reticulum), with subsequent binding of Ca^{2+} to TnC. This chemical signaling process results in cross-bridge formation and transduction to mechanical force or shortening (Figure 7). The interface between nerve and muscle fiber is the neuromuscular junctions, with specialized structures on the presynaptic nerve terminal and postsynaptic, motor endplate sides to mediate electrochemical transduction.

Neuromuscular Junctions

In animals, there are two different types of locomotor systems: one based on ciliary motion and the second that is based on muscle activation. Muscle-based locomotion is present in all metazoans except sponges (eumetazoan). Interestingly, sponges are the most primitive animals in the metazoan tree, and they lack a nervous system. The nervous system evolved in the eumetazoans (comprising cnidarians, ctenophores and bilaterians), and enabled these animals to sense their environment, process this information and then initiate a response that involved either neurosecretory or muscle-based (motor) systems. Response elements involving neurosecretion appear to have evolved first in early eumetazoan phylogeny. In contrast, the neural control of muscles and locomotion required the evolution of mechanisms mediating faster propagation of electrical signals, likely in bilaterian metazoan animals. Thus, there was a convergence in the evolution of striated muscle and neural control.

The nervous system controls skeletal muscle fiber force generation through neuromuscular synaptic transmission (Figure 17). Typically, multiple muscle fibers are innervated by a single motor neuron through branching of the motor axon. Collectively, the motor neuron and group of muscle fibers it innervates is called the motor unit [397, 594].

Neuromuscular synaptic transmission begins with the generation and propagation of an action potential in a motor neuron. The propagating action potential invades the presynaptic terminal, and the resulting depolarization activates voltage-dependent Ca^{2+} channels, resulting in Ca^{2+} influx, which triggers the release of synaptic vesicles containing acetylcholine (ACh).

At the presynaptic terminal, the influx of Ca^{2+} binds to synaptotagmin located on synaptic vesicles, which regulates fusion of synaptic vesicles to the presynaptic terminal membrane. Typically, during an action potential, a number of synaptic vesicles fuse to the presynaptic

terminal membrane and the combined release of ACh diffuses across the synaptic cleft, i.e., the space between the presynaptic terminal and postsynaptic muscle membrane, where ACh binds to nicotinic cholinergic receptors (nAChR) located in a specialized region called the endplate. Binding of ACh to its receptor opens cation channels that results in depolarization of the muscle fiber membrane (an endplate potential - EPP). There can also be spontaneous synaptic vesicle release of ACh, and these events are reflected by a miniature end-plate potential (mEPP) [143, 173, 342]. The action potential mediated EPP is the quantal summation of mEPPs. The larger EPP depolarizes the sarcolemma surrounding the neuromuscular junction leading to the opening of voltage-gated Na^+ channels and the generation of an action potential that propagates along the muscle fiber membrane. This electrical event can be measured using electromyography (EMG). Using discrete electrodes, the activation of a single motor unit can be measured which provides a window on the central nervous system control of muscle contraction.

Phrenic Motor Neurons

Diaphragm muscle fibers are innervated by phrenic motor neurons located within the ventral horn (lamina IX) of the cervical spinal cord, segments C_3-C_5 in rats [13, 431, 522, 637], echidnas [453], and humans [346]. While in the mouse the pool spans C_3-$_6$ [520] and C_4-$_6$ in cats [682] and rabbits [663]. In the rat, there are ~240 phrenic motor neurons on each side of the cervical spinal cord (Figure 18) [13, 190, 513, 522], bilaterally innervating the DIAm (providing a total of ~480 motor units).

As mentioned above, phrenic innervation of the DIAm displays a somatotopic organization with more rostral cervical segments of the phrenic motor neuron pool innervating more ventral regions of the costal and crural regions of the DIAm, whereas more caudal segments innervate more dorsal portions of both the costal and crural regions (Figure 16) [622].

Adult phrenic motor neurons display a wide range of sizes, matching the range of DIAm motor unit types. In the rat, the somal surface areas of phrenic motor neurons range from 1,000 to 8,000 μm^2 with a median of 4,500 μm^2 (Figure 16) [190, 513, 515, 522]. In ~80% of cases, somal surface areas of phrenic motor neurons display a significant biomodal distribution, perhaps reflecting differences between phrenic motor neurons innervating type S and FR motor units (possibly including some relatively more fatigue resistant type FInt units) and larger phrenic motor neurons innervating type FInt and FF motor units.

During late embryonic and early postnatal development, ~50% of motor neurons within the mammalian spinal cord undergo pruning or programmed cell death [382]. Within the phrenic motor pool of the rat, this motor neuron loss occurs days before birth and numbers remain stable during late embryogenesis and early postnatal life within the mammalian spinal cord [12, 262]. In older animals, an age-related loss of phrenic motor neurons has been observed, and may underlie sarcopenia of old age [190, 347].

Embryological Development of the Diaphragm Muscle Innervation

Myoblast migration and myotubes formation is concurrent with the outgrowth of phrenic motor axons (Figure 13). Similarly, myotubes transformation into myofibers with contractile protein expression and sarcomeric organization is concurrent with the development of pre-

and postsynaptic specialization, including the aggregation of cholinergic receptors. In the rodent (mouse and rat) DIAm, cholinergic receptors aggregate into clusters by ~E13-E14. This aggregation process for cholinergic receptors involves agrin secretion by the nerve terminal, which activates skeletal muscle specific kinase (MuSK) receptors at the postsynaptic membrane [215, 564, 565]. Following cholinergic receptor aggregation the postsynaptic membrane is further specialized by the formation of junctional folds (Figure 17).

In adult DIAm fibers, the morphology of neuromuscular junctions varies across different fiber types, with increased complexity and size at type IIx and/or IIb fibers compared to type I and IIa fibers (Figure 19) [421, 514].

At the time of synapse formation, each myotube or myofiber is contacted by multiple motor neurons (termed polyneuronal innervation) (Figure 20). Subsequently during late embryonic and early postnatal development, synapse elimination occurs and polyneuronal innervation disappears. The adult pattern of innervation of DIAm fibers by a single phrenic motor neuron is present by about the second postnatal week in the mouse and rat (Figure 13) [39, 40, 76, 504, 526, 564].

The mechanism(s) underlying perinatal synapse elimination remains unclear. A leading theory is that synapse elimination reflects a competition among motor neurons that depends on activity and/or efficacy of neurotransmission (Hebbian competition) [323, 504, 526]. This fundamental concept for synaptic neuroplasticity and assembly of cellular connections in the nervous system was introduced in 1949 by Donald Hebb, a Canadian psychologist/ neuroscientist. The concept can be simply paraphrased as “cells that fire together, wire together”. In Hebb’s theory a synapse between two cells (e.g., a motor neuron and a muscle fiber) is strengthened if the synaptic transmission is effective as evidence by repeated and persistent stimulation of the postsynaptic cell. Accordingly, during the period of polyneuronal innervation of muscle fibers, the synaptic transmission of one motor neuron is more effective in activating the muscle fiber than other synapses and thus, this synapse is subsequently strengthened while other synapses are further weakened. Contrary to what some have argued, it is not a matter of a more active motor neurons persisting at the expense of less active motor neurons (i.e., purely activity dependent). Synapse elimination driven by activity alone during development is inconsistent with the fact that in adults, type FInt and FF motor units, with the largest motor neurons tending to have the largest innervation ratios (i.e., the number of muscle fibers innervated by a single motor neuron). In adults, these larger motor neurons are the least active [54, 195, 601]. Thus, during development, either the size and excitability of these motor neurons must change dramatically (transitioning from most to least active), or something other than activity alone accounts for the persistence of synaptic contacts of these motor neurons. However, differences in motor unit innervation ratios are entirely consistent with Hebb’s theory if there is something associated with improved synaptic efficacy that results in the strengthening of synaptic connections at larger motor units. One possibility is the release of neurotrophic factors (e.g., BDNF) that stabilizes the neuromuscular junction. Another possibility is the production of some trophic factor (“synaptomedin”) by the active muscle fiber that is then retrogradely transported by

the presynaptic terminal and thus serves as an intracellular signal to facilitate and maintain the synaptic contact [28].

In mammals, including humans, respiratory movements are observed in the fetus indicating intact inspiratory drive to the DIAm and functional neuromuscular transmission. In the rat, fetal respiratory movements are present by E17 [244], but these movements may occur earlier since they are not easily detected. Functional synapses and excitation-contraction coupling in DIAm fibers (i.e., evoked intracellular Ca^{2+} and contractile responses to nerve stimulation) can be seen as early as E12.5 in rodents. It is possible that the transition of myotubes to myofibers and the establishment of the conventional sarcomeric organization in the DIAm may be influenced by mechanical responses evoked by neural signals.

It is not surprising that the efficacy of neuromuscular transmission in the fetal and neonatal DIAm differs from that in adults. For example, with repetitive phrenic nerve stimulation, neuromuscular transmission failure is more pronounced in the neonatal rat DIAm [34, 174, 193, 618]. It is possible that the more extensive branching of phrenic motor axons in the neonate due to polyneuronal innervation may increase susceptibility to branch point failure - a form of neuromuscular transmission failure [33, 45, 164, 193, 330, 432, 454, 618]. In addition, during the process of synapse elimination, weaker synapses are present that are more susceptible to neuromuscular transmission failure [193, 372, 374, 618]. In support, the frequency and amplitude of spontaneous mEPPs is reduced in the neonatal rat DIAm, and the amplitude of evoked EPPs is also reduced [34, 174, 193].

Motor Unit and Muscle Fiber Types in the Diaphragm Muscle

Diaphragm muscle force generation is dependent on the interplay between phrenic motor neurons and the muscle fibers they innervate. Motor units are commonly classified into four types (type S, FR, FInt and FF), according to the mechanical and fatigue properties of their constituent muscle fibers [195, 223, 224, 598, 608, 610–614] (Figure 21). Importantly, within an individual motor unit, all of the muscle fibers display homogeneous contractile protein expression and biochemical properties that define a specific muscle fiber type [195, 256, 477, 478]. This homogeneity of muscle fiber type within motor units has been confirmed in the adult cat DIAm [163, 331, 613, 622].

In modern classification schemes, different muscle fiber types are identified by the expression of different MyHC isoforms. Type I muscle fibers in slow-twitch (type S) motor units express $MyHC_{Slow}$. These type I muscle fibers have a high mitochondrial volume density and capacity for oxidative phosphorylation that contributes to their fatigue resistance [163, 614]. Furthermore, type I muscle fibers have smaller cross-sectional areas [395, 455, 513, 617, 708], and generate less force per cross-sectional area (specific force) [221–224]. Due to the enzymatic properties of the $MyHC_{Slow}$ isoform, type I fibers display lower rates of ATP hydrolysis, slower cross-bridge cycling rats and slower maximum velocity of shortening compared to type II muscle fibers [221–224]. Fast-twitch, fatigue resistant (type FR) DIAm motor units comprise type IIa muscle fibers that express the $MyHC_{2A}$ isoform [219, 220, 222, 223]. Type IIa muscle fibers have higher mitochondrial volume density and oxidative capacity comparable to type I fibers, which may account for their greater fatigue resistance in some species [259, 261, 621]. The cross-sectional areas of type IIa fibers is

small, similar to that of type I fibers, but the specific force they generate is of similar magnitude to other type II muscle fibers [221–224]. The maximum ATP hydrolysis rate of type IIa fibers is lower than other type II fibers but higher than type I fibers (Figure 10) [625]. Accordingly, the maximum velocity of shortening of type IIa fibers is faster than type I fibers but slower than other type II fibers [221–224]. Type IIx and IIb DIAm fibers generally co-express $MyHC_{2X}$ and/or $MyHC_{2B}$ isoforms in varying proportions and comprise type FInt and FF motor units. In general, the higher proportionate expression of the $MyHC_{2B}$ isoform in type IIx/IIb fibers, the greater is their susceptibility to fatigue. The relative co-expression of $MyHC_{2X}$ and $MyHC_{2B}$ isoforms in DIAm fibers also appears to underlie differences in mechanical and energetic properties [614]. Type IIx/IIb DIAm fibers have higher ATP hydrolysis rates and faster cross-bridge cycling rates and faster maximum shortening velocities than other DIAm fiber types [224, 259, 260]. Type IIx/IIb DIAm fibers also have both larger cross-sectional areas [246, 395, 455, 513, 597, 617, 708] and higher specific forces [221–224]; thus they have a greater contribution to muscle force generation (Figure 21).

An important factor in the force generation when recruited by a motor unit is the number of muscle fibers comprising the motor unit (innervation ratio). In limb muscles, the largest innervation ratios occur in type FInt and FF motor units and smaller ratios occur in type S and FR units [101, 336]. However, in the cat DIAm, there is no difference in the innervation ratio between motor unit types [194, 602, 604]. Taken together, the larger muscle fiber cross-sectional areas and the greater specific forces of type FInt and FF DIAm motor units result in markedly greater levels of force contributed by these motor units compared to type S and FR units [195, 423, 428, 609, 610, 612].

Although it was suggested that the costal and the crural regions of the DIAm were actually two separate muscles, with different embryological origin, and different in fiber type composition [140], this was subsequently shown to be incorrect in both respects [558, 622]. Firstly, all regions of the DIAm have been shown to derive from shared embryological origins [12, 24, 241, 242]. Secondly, systematic evaluations of the phrenic nerve innervation of the DIAm using glycogen depletion techniques clearly demonstrated considerable overlap in the cervical segmental innervation of DIAm fibers across sternal costal and crural regions [196, 603]. For a given species, the costal and crural regions of the DIAm have similar mixed fiber type composition. The relative fiber type proportions and cross-sectional areas for a given DIAm fiber type may vary across species [126, 251, 278, 348]. Similarly, DIAm fiber lengths and orientation may differ across species [558, 622]. Indeed, type I muscle fibers take up a very large proportion of DIAm fibers in some species of dolphin [141], whose rapid ventilation, ~90% lung volume exchange in under ~0.3 s [316, 368, 539], occurs mainly via epaxial, hypaxial and abdominal muscles [118]. For comparison to a terrestrial mammal, a galloping horse exchanges ~20% of its lung volume in 0.5 s [703], despite the horse being somewhat atypical, with a small tidal volume for its body size and exercise induced pulmonary hemorrhage [509]. For comparison, a trained human male during near maximal exercise will exchange ~50% of their total lung volume in ~1 s [250].

Like all skeletal muscles, DIAm force is related to the relative proportions of different fiber types (I, IIa, and IIx/IIb) and their cross sectional areas. A variety of conditions, including

spinal cord injury, myasthenia gravis, spinal muscle atrophy, amyotrophic lateral sclerosis, corticosteroid treatment, mechanical ventilation and aging, lead to type-specific atrophy (reduced cross sectional area), force decline and fiber-type conversion or co-expression in the DIAm [186, 237, 416, 424, 426, 427, 429, 543]. Remarkably, in hibernating mammals, retention of type I muscle fibers and increased muscle mass is evident, despite uniform reduction in muscle mass and decreased protein levels in almost all other muscles, including those of mixed fiber types similar to DIAm [119].

From the standpoint of symmorphosis, it is interesting that the basic differences in contractile, fatigue and metabolic properties defining fiber types persist across species. Differences in the proportion and cross-sectional areas of these different fiber types will underlie difference in performance features of the DIAm across species. Accordingly, if there is a requirement for greater endurance of the DIAm (more fatigue resistance during ventilatory behaviors), the proportion of type I and IIa fibers and/or their cross-sectional areas may be greater in a particular species. Thus, the relative proportion of type I and type IIa fibers compared to type IIx and/or IIb fibers in the DIAm provides insight into its dual functional role in generating negative P_{th} versus P_{ab}, respectively. For example, in species where offspring size and maturity at birth are relatively greater (e.g., elephants, sea mammals), there may be a need for greater P_{ab} generation during childbirth. By contrast, in similarly sized animals where offspring are smaller and less precocial (e.g., monotremes and marsupials), there may not be as great of a demand for P_{ab} generation at childbirth. Accordingly, there may be difference in the proportion and size of type IIx and/or IIb fibers in the DIAm of these different species. However, in all of the mammalian species tested to date, the requirements of ventilation appear to be well met by the relative contribution of type I and IIa fibers in the DIAm.

The mean cross-sectional area of DIAm fibers scales with body weight, i.e., as body mass increases the size of all DIAm fibers increases [59, 126, 251, 278]. Sadly, many of these earlier observations did not determine cross-sectional areas specific to fiber type. When fiber type is taken into account, type IIx and/or IIb fibers have ~1.5–3 times greater cross-sectional areas than type I and type IIa fibers [222, 223]. Importantly, the specific force (force normalized to cross-sectional area) of different DIAm fiber types appears to be highly conserved across all species. In permeabilized rat DIAm fibers maintained at 15°C, the maximum specific force (at pCA 4.0 activation) of type I fibers is ~10 N cm^{-2}, type IIa fibers ~12 N cm^{-2}, and type IIx and/or IIB fibers ~15 N cm^{-2}. Considering the Q10 for force generation is ~2.0, at normal body temperature (i.e., ~37°C), specific forces would range between ~22–25 N cm^{-2} in type I and IIa fibers to 32–35 N cm^{-2} in type IIx and/or IIb fibers. These differences in specific force across fiber types are due in part to differences in contractile protein content per half sarcomere (n in the force equation) [222–224, 259, 621]. In the rat DIAm, we showed that type I and IIa fibers have lower MyHC content per half sarcomere compared to type IIx and/or IIb fibers. When isometric force is normalized for MyHC content per half sarcomere, the force per MyHC content of fibers expressing $MyHC_{slow}$ is only ~ half that generated by all type II fibers regardless of type II MyHC isoform (i.e., $MyHC_{2A}$, $MyHC_{2X}$ and/or $MyHC_{2B}$) (Figure 21). These results suggest that each MyHC head contributes a quantal level of force during cross-bridge cycling that only differs between slow (type I) and fast (type II) MyHC isoforms. Accordingly, the total

amount of force contributed by a DIAm fiber depends on MyHC isoform (type I or II) and the fraction of MyHC heads that are attached to the actin filament to form cross-bridges (α_{fs} in force equation). Thus, differences in P_{th} and P_{ab} generation across species are likely to be associated with the thickness of the DIAm. For example, in elephants the DIAm is ~3 cm [79], an order of magnitude greater than that observed in humans, ~3 mm [21, 22], an order of magnitude difference. Additional considerations include proportions of muscle fiber types (i.e., motor unit types) within the DIAm, and the patterning of activation of costal and abdominal wall musculature when performing different maneuvers.

Neuromotor Control of the Diaphragm Muscle

Although much is still to be defined in regard to phrenic motor neuron inputs, it remains immutable that individual phrenic motor neurons are the final common output as well as the integrators of signals from pattern generators and other neural circuits. The DIAm motor unit remains the final executor of neuromotor control and produces motor force output across a range of ventilatory and higher force, non-ventilatory behaviors. It still remains unclear whether phrenic motor neurons constituting the different types of DIAm motor units receive diverse premotor inputs. Regardless, neuromotor control of the DIAm during different motor behaviors requires production of graded levels of force generation, a property dependent on recruitment and rate coding of motor units themselves (Figure 22).

Motor Unit Recruitment and Frequency Coding

The intrinsic size-dependent electrophysiological properties of motor neurons determine the recruitment order of motor units [87, 345, 610]. Mathematically, the relationship between motor neuron size and excitability (recruitment order) may be expressed as the following equation:

$$\mathbf{dV_m/dt = I_{syn}/C_m}$$

Where dV_m/dt is the change in membrane potential with time, I_{syn} is the net synaptic inward (depolarizing) current and C_m is membrane capacitance. Thus, for a given I_{syn}, smaller motor neurons with a lower C_m have a greater dV_m/dt compared to larger motor neurons, reaching a threshold for action potential generation sooner (Figure 23).Smaller motor neurons have smaller C_m; thus, for a given amount of I_{syn}, the dV_m/dt is greater, reflecting greater excitability [179, 644, 704, 706]. Accordingly, if synaptic input is comparable across phrenic motor neurons, smaller more excitable motor neurons (presumably type S and FR) are recruited before larger motor neurons (presumably type FInt and FF) (Figure 22).

Motor unit recruitment order generally matches motor unit type, with initial recruitment of type S and FR motor units followed by type FInt and FF motor units (Figure 22) [86, 442, 644]. In agreement, it has been shown that motor units recruited first contribute less force compared to those units recruited later [704]. In the DIAm, it is very likely that type S and FR motor units are initially recruited to accomplish the lower force, high duty cycle (active vs. inactive) behavior of breathing. During rhythmic breathing, inspiration typically has a duty cycle of 30–40%, which would cause marked fatigue if type FInt and FF motor units

were recruited. Higher force, expulsive sneezing and coughing behaviors of the DIAm have very short durations allowing sufficient time for recovery from any fatigue that might occur.

Based on these observations, a model of DIAm motor unit recruitment was formulated based on an orderly recruitment of type S, FR, FInt and FF motor units (Figure 22) [195, 423, 428, 581, 602, 604, 605, 610]. In the initial model developed for the cat DIAm, the force contribution of each motor unit type was based on direct measurements of motor unit mechanical properties [195, 598, 601, 604, 609, 610]. Subsequently, in the rat DIAm, the force contributed by different motor unit types was estimated based on measurements of Ca^{2+} activated specific force generated by single permeabilized muscle fibers of different types [221–224], the mean cross-sectional area [395, 455, 513, 617, 708] and proportions [163, 195, 598, 613, 614] of these muscle fiber types, and the assumption that innervation ratios are comparable across motor unit types [194, 602, 604]. In each of these models, ventilatory behaviors (i.e., eupnea and response to hypoxia/hypercapnea) were assumed to be accomplished by the recruitment of only fatigue resistant type S and FR motor units [423, 428, 599, 600, 602, 604, 610]. Based on these assumptions, it was estimated that in cats, ~23% of the total phrenic motor neuron pool is recruited during eupnea [326], corresponding to the relative proportions of type S and FR motor units in the DIAm [195, 610, 613]. To perform higher force, expulsive behaviors (i.e., coughing and sneezing), the recruitment of additional type FInt and FF motor units is required [423, 428, 599, 600, 602, 604, 610]. The progressions in force generated by DIAm motor units (type FF > FInt > FR > S) [195, 221–224, 609, 610] results in various slopes of force development during the sequential recruitment of motor units (Figure 22).

With increasing rates of activation, skeletal muscle force increases, reaching a plateau reflecting maximum tetanic force. As frequency of activation increases, force responses fuse into larger summated forces, thus the force-frequency response curve is sigmoidal. In type S and FR motor units, the force-frequency response is shifted leftward, such that tetanic fusion of force occurs at lower activation frequencies compared to type FInt and FF motor units (Figure 22) [195, 624]. Using fine wire electrodes implanted into the DIAm the discharge of motor unit action potentials was recorded during ventilatory behaviors [87, 367, 624]. For motor units recruited during these ventilatory behaviors, the onset discharge rate was lower compared to the peak discharge rate occurring later within the inspiratory burst [318, 624]. In the cat DIAm, motor unit discharge rates were compared to the force frequency response curves of different motor unit types [195]. Consistently, it was observed that the onset discharge rate of low threshold motor units (i.e., those recruited early during inspiration) was ~8–10 Hz with discharge peaking at ~25 Hz toward the end of inspiration. This range of discharge rates corresponds to the steepest part of the force-frequency response curves of type S and FR motor units. In contrast, DIAm motor units with higher recruitment thresholds (i.e., those recruited later during more forceful inspiratory efforts) had higher onset (~15 Hz) and peak (~60 Hz) discharge rates, which corresponded to the steep part of the force-frequency response curves for type FInt and FF motor units [624]. Based on these results, a modified model for DIAm motor unit recruitment was developed, which included frequency coding of different motor unit types (Figure 22) [422, 423, 581].

In the DIAm, motor units are likely recruited systematically depending on motor unit type (fatigue resistant to more fatigable) to accomplish a range of forces and different motor behaviors [423, 428, 582, 599, 600, 602, 604, 605]. Recruitment order is maintained even with increasing neural drive (I_{syn}), with a decrease in recruitment delay and an increase in discharge rate [582]. For those low threshold DIAm motor units that are recruited consistently across all ventilatory behaviors (i.e., eupnea and hypoxia-hypercapnia), onset discharge rates are comparable [581, 582]. We assume these low threshold DIAm motor units are type S and FR, which develop lower forces but are fatigue resistant, and thus, especially appropriate for high duty cycle repetitive motor behaviors such as breathing [367, 422, 423, 581]. In contrast, to achieve higher force, shorter duration (lower duty cycle) motor behaviors, it is more appropriate to recruit higher force but more fatigable type FInt and FF motor units. The size principle for motor unit recruitment in the DIAm has been confirmed [145, 326, 423, 581, 599, 600, 604, 605, 610, 620] and underlies neuromotor control of force generation across a range of motor behaviors.

Components of Neuromotor Control System

There are five main motor components of the neuronal circuitry of the phrenic/DIAm motor system: 1) a central pattern generator (for ventilatory – P_{th} generation; or expulsive/straining – P_{ab} generation - motor behaviors); 2) premotor neurons responsible for transmitting the output of the central pattern generator; 3) interneurons responsible for modulating or coordinating premotor neuron and/or phrenic motor neuron excitability – these interneurons also serve to integrate sensory feedback (e.g., chemoreceptive, lung stretch, propriospinal or other afferent inputs); 4) direct cortical premotor input to motor neurons via the corticospinal pathway; and 5) phrenic motor neurons as the final common output for generating the forces necessary for the desired motor behaviors (Figure 24).

The central pattern generator for locomotion in the spinal cord was characterized much earlier than that for respiration. Indeed, initial studies were performed by the French physiologist Marie-Jean-Pierre Flourens, who in 1824 conducted brain and spinal cord lesion studies to determine the origin of motor behaviors. Subsequent work in the early 1900's by Charles Sherrington, Thomas Graham Brown and others showed that stereotypical rhythmic motor behaviors such as walking were controlled by a spinal cord neuronal network, a central pattern generator.

Sherrington's seminal research examining the effects of spinal cord transection showed that locomotor movements are modulated by spinal segmental reflexes [593]. However, it was the work of Thomas Graham Brown, who provided clear evidence for the local control of locomotion behaviors within the spinal cord [80]. In dogs with thoracic spinal cord transections preventing descending cortical control, spontaneous rhythmic locomotor patterns of the hindlimb were generated by a local spinal neuronal network, independent of peripheral input, i.e., these patterns were the result of a central pattern generator for locomotion [80].

It is likely that several distinct central pattern generators affect activation of the DIAm to accomplish motor behaviors, e.g., separate central pattern generators for breathing, sighing, sneezing, coughing, swallowing, vomiting, vocalization, defecation, etcetera (Figure 24). Of

these, the neuronal circuitry responsible for generating the rhythmic behavior of breathing (ventilation) is the best characterized central pattern generator affecting phrenic motor neurons and DIAm activation. For ventilatory behaviors, this central pattern generator plays an indispensable role in determining the timing and duration of the different phases of the respiratory pattern.

Other central pattern generators affecting DIAm neuromotor control may also exist in the brainstem and spinal cord, e.g., for sighing [396], swallowing [146], coughing [56, 447], sneezing, vomiting [364, 447], defecation and parturition (Figure 24). The output of these other pattern generators is transmitted to premotor neurons and then phrenic and other motor neurons. In addition, the output of different central pattern generators that affect DIAm activation, such as those for swallowing or vomiting, must be integrated with the respiratory pattern generator that sets the baseline of activation and relaxation of DIAm activity.

Neuromotor Control for Intra-Thoracic Pressure Generation

The major functional demand for negative P_{th} generation is ventilation of the lungs for gas exchange. Lung ventilation consists of three main phases, inspiration, post inspiration and expiration [536, 537]. The precise mechanisms underlying the central pattern generator for respiration are still debated, but it is now generally agreed that the Pre-Bötzinger Complex (PreBötC) in the medulla provides the spontaneously active ‘kernel’ of neurons for the metronomic drive for the inspiratory phase of respiration, via interactions of various membrane channels (Figure 24) [35]. It now appears that the PreBötC is essential for inspiration [438], and is the prime source of inspiratory excitatory drive to respiratory premotor neurons [635] via a core subpopulation of glutamatergic (Glu) pacemaker cells that project bilaterally to premotor neurons in the medulla (Figure 24) [365]. Inhibitory neurotransmission at premotor neurons also plays an important role in modulating respiratory pattern generator outputs [42, 228].

The Bötzinger Complex actually located rostral to the PreBötC provides for switching from inspiration to expiration [536, 537], possibly via inhibitory inputs to the PreBötC [538]. Normally, expiration is passive; however, during increased respiratory efforts, active expiration involves activation of intercostal and abdominal muscle and this activation has a distinct central pattern generator located in the region of the retrotrapezoid nucleus (RTN) [322].

Premotor neurons providing monosynaptic drive to phrenic motor neurons during inspiration (ventilatory behavior) are located primarily in the ventrolateral medulla (ventral respiratory group – VRG), although there is some contribution from a dorsal respiratory group (DRG) in the dorsomedial medulla (Figure 24) [324, 493]. These descending excitatory (Glu) premotor inputs for inspiratory-related activation of phrenic motor neurons are located predominantly ipsilateral in the spinal cord [147, 160, 176], transmitted via bulbospinal pathways in the ventrolateral and ventromedial funiculi [175, 176, 635]. These excitatory premotor inputs for respiratory-related activation of phrenic motor neurons are generally thought to be widely distributed [113, 127], with recruitment of phrenic motor neurons (DIAm motor units) dependent on intrinsic electrophysiological properties of phrenic motor neurons rather than a specific pattern of premotor input.

It remains unclear whether the other central pattern generators that affect phrenic motor neuron and DIAm activation during other non-ventilatory motor behaviors share common or distinct premotor neurons. It is clear that the central pattern generator involved in breathing is different from that involved in generating the patterns of expulsive/straining motor behaviors of the DIAm. However, these different pattern generators may have a certain degree of overlap in their inputs to the medullary premotor neurons affecting phrenic motor neuron activation [554, 635]. For ventilatory behaviors, it is generally thought that phrenic motor neurons receive distributed descending medullary premotor input that is predominantly ipsilateral. However, retrograde tracing studies that examine the connectivity of phrenic motor neurons have indicated a variety of premotor inputs both from the brainstem and spinal cord [145, 160, 161, 303, 326, 403, 557]. Perhaps these connections reflect distinct premotor inputs mediating the output of central pattern generators that are different from those involved in respiratory drive to phrenic motor neurons. For higher force non-ventilatory behaviors of the DIAm, premotor input to larger (higher threshold) phrenic motor neurons may be different compared to premotor input mediating the output of the respiratory central pattern generator, which activates primarily smaller, lower threshold phrenic motor neurons (i.e., those innervating fatigue resistant type S and FR motor units). In support, we recently found that unilateral spinal cord hemisection at C_2, which silenced respiratory-related activation of the DIAm, predominantly affected Glu synaptic input to smaller phrenic motor neurons, while Glu synaptic input to larger phrenic motor neurons was far less affected. This differential effect of C_2 spinal hemisection on Glu input to phrenic motor neurons was consistent with the persistence of DIAm activation associated with higher force motor behaviors [62, 149–151, 207, 208, 236, 238, 239, 418, 562]. These results suggest that small versus large phrenic motor neurons may be involved in different motor behaviors – smaller phrenic motor neurons in ventilatory behaviors; larger phrenic motor neurons in expulsive/straining behaviors (Figure 24). If true, the larger phrenic motor neurons may be primarily influenced by central pattern generators and premotor neurons involved in expulsive/straining behaviors, which are located in the spinal cord (Figure 24).

Phrenic motor neurons also receive input from spinal cord interneurons (Figure 24), including those involved in proprioception. However, in stark contrast to muscles involved in locomotor behaviors [519], the DIAm has very few, if any, muscle spindles [156]. Thus, in contrast to well-studied limb muscles, direct muscle spindle proprioceptive feedback from the DIAm does not contribute substantially to modulation of phrenic motor neuron excitability [117, 321]. However, phrenic motor neurons do receive feedback from muscle spindles in intercostal muscles, and this input has primarily inhibitory effects on phrenic motor neuron excitability [158, 529]. In particular, an intercostal to phrenic reflex has been characterized, which suppresses phrenic nerve activity following strain on the chest wall [142, 530], an effect that appears to involve both disfacilitation of VRG premotor input [55, 530, 589] and interneuronal inhibition of phrenic motor neurons [36]. Additional local inhibition of phrenic motor neurons from interneurons within the spinal cord has been characterized [36, 37, 153, 154, 404]. Remodeling of local interneurons within the spinal cord may partially account for the spontaneous recovery of ventilatory and non ventilatory behaviors following cervical spinal cord injury [383, 711].

In humans, direct corticospinal inputs onto phrenic motor neurons allow for voluntary control of breathing [209, 407] and the interplay between ventilation and behaviors such as speech [592] (Figure 24). Neuromodulatory inputs (e.g., serotonergic – 5-HT) also affect changes in phrenic motor neuron excitability during sleep-waking states. For example, it is well documented that there is resilience to apnea during the waking state and an increased response to hypoxic and hypercapnic stimulation of ventilation [125, 178]. By contrast, sleep predisposes to episodes of apnea even during hypoxic, hypercapnic conditions [125, 631].

The depression of respiratory activity during sleep is remarkably similar to the depression of respiratory activity during diving [96, 97]. Apnea is a vital aspect of the diving response, which also includes bradycardia and peripheral vasoconstriction, in all air breathing vertebrates [15, 63, 88]. Mammals and other endotherms are constrained in their diving lengths and durations [63, 88], though many species are capable of extended dives ~2 hours in some seals and whales [276, 575]. Tolerance of hypoxia during extended dive durations are largely due to blood and tissue adaptations, including locomotor muscle fiber-type differences [626, 667], unrelated to the neural control of breathing [130, 369, 481, 636]. Obviously, limiting the chemoreceptor associated inspiratory drive is pertinent while submerged, yet, during sleep, seals experience bouts of apnea that can exceed 20 min, with no pathology or deleterious effects [97], and do not awaken in order to cease these bouts of apnea, with sleeping eupnea-apnea-eupnea cycles occurring uninterrupted [98]. Indeed, many seals sleep submerged, and rapid eye movement sleep of some seals involves complete cessation of ventilation, regardless of whether sleeping on land or submerged, perhaps due to muscle atonia of sleep extending to the DIAm in these species [97]. In longitudinal studies, the durations of apnea increased with age, correlating with the establishment of marked sinus arrhythmias [48, 99]. From a neural control standpoint, apneas in seals do not involve movements of the respiratory muscles, nor do they attempt to breathe [97]. In contrast, human apneas involve the movement of respiratory musculature and involve tissue damage, and apnea-related sudden infant death syndrome may involve impaired cardiorespiratory sinus arrhythmia development [97, 341]. Though many human apneas are obstructive, many are initiated centrally and related to arousal. The investigation of routine, repeated and extended periods of diving and sleeping apnea in the absence of deleterious consequences in seals and the random and pathological human episodes of apnea may provide more detailed information about the neuromotor control of ventilatory function.

Although much is still to be defined in regard to phrenic motor neuron inputs and the central pattern generation of ventilatory and other straining and expulsive motor behaviors of the DIAm, the individual phrenic motor neuron is the final integrator of these signals. The DIAm motor unit remains the final executor of neuromotor control and produces motor force output across a range of ventilatory and higher force, straining and expulsive behaviors. It remains unclear whether phrenic motor neurons innervating different types of DIAm motor units receive different premotor inputs. Regardless, neuromotor control of the DIAm during different motor behaviors requires production of different levels of force generation, a property dependent on recruitment and rate coding of motor units themselves.

Modulation of the respiratory pattern and/or of phrenic motor neuron activity may occur directly or indirectly in response to afferent inputs to phrenic motor neurons, from signaling initiated by mechanoreceptors in the lung and airway, peripheral and central chemoreceptors, to behavioral state influence mediated by serotonergic projections emanating from the raphe (Figure 24). Mechanoreceptors in the lung respond to lung inflation, are sensitive to the mechanical loading of breathing and prevent airway over-inflation by increasing their afferent activity – peaking at the end of inspiration [90, 474]. These afferent inputs exert effects on ventilatory phrenic motor neuron discharge indirectly, via vagal nerve inputs in the nucleus tractus solitarius (NTS) [43, 148]. Laryngeal mechanoreceptors also exert an indirect effect on phrenic motor neurons, decreasing inspiratory drive during upper airway collapse [566].

The carotid bodies, peripheral chemoreceptors, that respond to hypoxia and hypercapnea by increasing ventilation [2, 378, 379, 671] act indirectly via signaling to brainstem respiratory centers through the carotid sinus nerve [710]. Many brainstem areas contain central chemoreceptors [475], which are exquisitely sensitive to deviation of pH and pCO_2 [497], and act in response to hypercapnea to increase ventilation [254]. The field is full of intense debate regarding the particulars of the interactivity of peripheral and central chemoreceptors. Regardless of their precise activities, the indirect modulatory action of chemoreceptors (likely acting via medullary premotor neurons) leads to a heightening of the overall drive to phrenic motor neurons.

Serotinergic neurons located in the caudal raphe project to brainstem respiratory regions and to phrenic motor neurons [273], and thus may have effects on rhythmic central pattern generator and premotor outputs [380, 381] as well as on phrenic motor neuron excitation [401, 458]. Catecholamine modulation of respiration also occurs via activation of the α_1 or α_2 adrenoreceptors, enhancing or inhibiting, respectively respiratory rhythmic central pattern generation [272, 661, 669, 670].

Neuromotor Control for Intra-Abdominal Pressure Generation

As previously mentioned, activation of the DIAm is also involved in the generation of positive P_{ab} required for straining behaviors, such as vomiting, defecation and child birth. Expulsive behaviors that require near-maximal inspirations before perform effectively, such as coughing and sneezing, that are essential to maintaining a patent airway for breathing also require more forceful activation of the DIAm and generation of increased P_{ab}. Similar to inspiration, these expulsive maneuvers involve the coordinated activation of various abdominal wall muscles (including the DIAm), sphincter muscles, and upper airway muscles. For example, vomiting requires the coordinated contraction of the DIAm and other abdominal wall muscles, relaxation of pharyngeal muscles, protrusion of the tongue and the relaxation of the lower esophageal sphincters. By contrast, defecation, which involves the generation of P_{ab} ranging between 150–200 cm H_2O [93]) requires coordinated contraction of the DIAm and other abdominal wall muscles and pharyngeal muscles in order to close the glottus. A similar voluntary effort is the Valsalva maneuver, where after a deep inspiration, an individual attempts a forceful expiratory effort against a closed airway, thereby generating maximum positive P_{ab} ~90 to 220 CmH_2O [109, 253, 591]. This maneuver was

introduced by a 17th century Italian anatomist/physician, Antonia Valsalva who applied this procedure to clear the Eustachian tube. The reverse is the Müller's maneuver, where, following a forced expiration, an individual attempts a forceful inspiratory effort against closed airway, thereby generating a maximum negative intrathoracic pressure. This maneuver was introduced by the 19th century physiologist Johannes Peter Müller during which he demonstrated dramatic effects on the cardiovascular system due to increased venous blood return to the heart.

Extensive coordination between abdominal and pelvic musculature and the respiratory musculature have been observed during straining and voiding behaviors, including vomiting, defecation and child birth. Vomiting behavior is initiated by various stimuli, including motion, repugnant events, pregnancy, gastric irritation, toxins and drug effects [301]. Vomiting behavior is conserved across multiple species, including invertebrates, fish, amphibia, reptiles, birds and mammals [16, 17, 60, 114, 436]. Vomiting requires two phases; i) retching and ii) expulsion. The retching phase consists of cycles of co-contraction followed by simultaneous relaxation of DIAm and abdominal wall muscles [301]. During retching, P_{th} are reduced and P_{ab} are increased [300]. The expulsion phase consists of prolonged abdominal muscle contractions, coordinated with relaxation of the DIAm, and activation of intercostal muscles, the larynx and the pharynx. The maneuver occurs with a closed glottis and an elevated soft palate [301]. P_{ab} during vomiting have been estimated using gastric pressures, with positive pressures ranging from a mean of ~155 to a maximum of ~400 CmH_2O [315]. The initiation of vomiting involves the integration within the NTS of cortical, vestibular, area postrema and vagal afferents [23, 300, 301]. Due to the complicated orchestration of contractions of upper airway, DIAm, thoracic and abdominal musculature, and the remarkable range of stimuli provoking emesis, the control of vomiting is distributed throughout the medulla [301] and the phases are governed by a central pattern generator [364, 447]. Results from lesion, pharmacological and electrical stimulation studies show that regardless of how vomiting is elicited, the NTS is coordinating the response [138, 319, 363, 449, 450, 486, 525, 533], likely via axonal projections to motor control targets within the dorsal motor nucleus of the vagus, nucleus ambiguus and phrenic motor nucleus [319, 448, 450].

Defecation maneuvers often involve co-activation of the DIAm and the abdominal wall muscles. These straining efforts are characterized by the Valsalva maneuver, whereby maximal inspiratory efforts are followed by generation of P_{ab} against a closed glottis [202–205]. This coordination of the DIAm and abdominal musculature is likely to use the same pattern generation and reflex pathways that co-activate these muscles during vomiting behaviors, particularly projections from the nucleus retroambiguus [176, 284, 285, 289–291]. In spontaneous defecations, the EMG activities of the DIAm and abdominal muscles exceeds that of coughing [128]. In addition, projections from the nucleus retroambiguus onto Onuf's motor nucleus within the sacral spinal cord ensures external anal sphincter opening during defecation, the only straining behavior where rectal continence is absent [180]. Currently, very little is known about the central control of defection, with the existence and location of a central pattern generator unknown, although central pattern generators have been observed for other pelvic functions, such as ejaculation [660]. Despite these limitations, though there is evidence for supraspinal brainstem defecation centers in

the pons [200, 201, 206], though spinal cord lesion studies in rats and man indicate these supraspinal influences are superimposed over existing spinal reflexes [230, 409, 472, 672]. In accordance, studies have confirmed co-activation of DIAm and abdominal muscles following distension of the rectum [204], a reflex mediated by the K**ö**lliker-Fuse nucleus, a well-described pneumotaxic center [44, 112, 702]. We assert that descending voluntary controls, in concert with central pattern generators within the spinal cord co-activate the DIAm and abdominal wall muscles to generate high P_{ab} (Figure 24).

Rhythmic straining behaviors of DIAm and abdominal wall muscles are elicited by distension of the vaginal walls [202, 205], similar to voiding behaviors initiated by bladder or colon distension. Currently there is an astonishing paucity of reliable studies into the neural and/or reflex control of increased P_{ab} generation. Hints as to the necessity of an 'emotional nervous system' [286–288], have shown that pathways within the periaquiductal grey region provide a level of supraspinal control for pelvic expulsive functions, including micturition and defecation, and sexual functions in females and males [286, 287, 314], however none have dealt specifically with parturition. Clearly, expulsive behaviors such as parturition may be facilitated by Valsalva maneuvers, however spontaneous expulsive contractions also occur during labor, with little knowledge of their neural control.

Overall, the neural control of low-force rhythmic motor behaviors (locomotion) and low to moderate intra-thoracic ventilatory pressures (eupnea and hypoxia/hypercapnea) are well established and increasingly defined in terms of specific central pattern generation circuitry. In our opinion, far less progress has been made in the characterization of the central pattern generators necessary to co-ordinate for high P_{ab} generation in expulsive and straining behaviors. These high-force behaviors are often impaired in neuromotor conditions, such as ALS, and during normal aging [181, 182, 190, 247, 248, 347]. Understanding the fundamentals of the neural control of expulsive behaviors will provide us with targets to alleviate some of the more deleterious consequences of neuromotor disease, injury or aging, many of which affect multiple components of the neuromotor system [185, 187–189, 347, 418–420, 516, 522, 640].

Development of Diaphragm Motor Behaviors

The maturation and adaptation of the respiratory system of newborn mammals following birth must be regarded as one of Nature's all-time greatest achievements. The abrupt abandonment of the liquid uterine environment, to the air-breathing scenario is perilous. Indeed, not only is the change of environment a shock, but mammalian neonates generally (excepting some very small mammals, and the marsupials/monotremes) have a higher resting O_2 consumption (VO_2) requirement compared to adults of the same species [6, 27, 31, 47, 53, 121, 274, 307, 451, 459, 464, 465, 641, 655]. The exquisitely tailored structural and functional changes in mammalian neonates in adaptation to this shock begin *in utero* [240], with fetal breathing movements thought to prime neuromotor control of the respiratory muscles [12, 24, 243, 244, 362, 532], required for both ventilation and suckling in the newborn. The structural and functional dimensions of the first breath and the establishment of a steady and effective ventilatory behavior will be examined.

During *in utero* development, the lungs are not collapsed but maintained in a distended state [295, 459]. This distension is provided by fetal lung liquid [295], secreted by the pulmonary epithelium and serving to expand the lungs [485], particularly during the final trimester [295]. The amount of fetal lung fluid has direct effects on the development of lung size, with increased fluid increasing lung size [11, 91] and decreased fluid reducing lung size [11]. The latter has particularly disastrous consequences, as neonates born with pulmonary hypoplasia have a poor prognosis for morbidity and mortality [310, 360, 456]. Indeed, pulmonary hypoplasia as sequelae from congenital diaphragmatic hernia is the main concern for neonatal health following surgical correction of the defect [8, 470, 545, 546, 705]. Secretion of fetal lung liquid is tightly regulated. The inhibition of fetal lung liquid occurs by the action hormones such as adrenalin and vasopressin [77, 94, 95, 293, 498, 499, 677, 678, 701] and by O_2-dependent mechanisms, with hypoxaemia a particularly potent inhibitor [292, 294]. Fetal breathing movements are essential to the development of effective neuromotor circuits to control DIAm motor units [106, 131, 240] and to release episodically fetal lung liquid out of the trachea to be swallowed or absorbed by the amniotic fluid [295]. Episodic bouts of fetal breathing movements are essential for normal lung growth – possibly due to a relationship with fetal lung liquid [295].

Despite the essential function of fetal lung liquid during embryonic development, this accumulated fluid must be removed at birth for effective gaseous exchange to occur. Interestingly, by the onset of labor, the amount of fetal lung liquid accumulating in the lungs is ~30 ml kg^{-1} [459, 482], very similar to the volume of air (functional residual capacity) present in the lung after birth ~20–25 ml kg^{-1} [320, 544]. During labor, production of fetal lung liquid ceases, likely in response to adrenalin and vasopressin, due to an inhibitory effect that is exponentially more potent in late gestational ages [77, 94, 95, 293, 498, 499, 677, 678, 701]. Reabsorption is achieved through lymphatic drainage and diffusion into the pulmonary circulation [81, 231], both of which are enabled by the high permeability of the pulmonary endothelia and reduced vascular resistance of the pulmonary circulation in the newborn [312, 482]. It is important to note that fluid clearance during birth is not contingent on P_{th} generated by passage of the fetus through the pelvic canal in delivery, even though this does cause some expulsion of fetal lung fluid [58, 338, 567], caesarian deliveries display no appreciable rise in leftover fluids within the lung [26]. Overall, regardless of the mode of delivery, fetal lung liquid is reabsorbed during labor and the primary action of the newborn after birth is the first inspiratory breath.

A profound event in both the philosophical development of parents and the physiological development of the newborn is the first neonatal breath. The first breath involves the same stages as every breath thereafter, the inspiratory phase and the expiratory phase. The P_{di} pressures generated during the first breath (between 30 and 100 cmH_2O) approach that of maximal forces generated by adults, and dwarf the forces of neonatal steady-state ventilation (5–7 cmH_2O) established soon after birth [459]. There are many hypotheses proposed for the enlarged pressure generation of the first neonatal breath, ranging from the DIAm contractile forces being applied across a smaller surface area, motor control differences, i.e. the breathing centers not being attuned to inhibitory activity, and mechanical factors. The surface tension of the lung also plays a significant role in the larger forces required to inflate the lung during the first inspiration. Indeed, animal studies have shown that without

surfactant, the volume inhaled with a first breath pressure generation of ~35 cmH_20 is only ~10% of neonates with surfactant [375].

The first expiratory phase is often longer in duration than the later steady-state neonatal breathing and often involves periodic opening and closing of the upper respiratory tract, in order to promote fluid clearance from the lungs [340, 461]. There is a remarkable amount of air left in the lung following the first expiratory phase, which can be ~10–20% of the equivalent functional reserve capacity of a newborn a few days old [57, 340, 452, 461, 567, 673]. This air retention is primarily due to the formation of foam within the airways. In addition to the surface tension-overcoming properties of surfactant, it provides for the formation of foam within the newborn lung and allows for effective air retention in the newborn lung. The importance of surfactant is underscored by the observations that immature lungs, with less surfactant production, retain less air and have less foam than mature lungs [309, 370, 375, 569, 570].

The progressive establishment of a steady respiratory pattern occurs within a few hours after birth and requires three main adaptations; the clearing of pulmonary fluids, the matching of lung and respiratory mechanical properties to ventilation and the establishment of a functional reserve capacity. The clearing of the airways of pulmonary fluids is likely due to intermittent positive airway pressures (increased P_{th}) and fluid resorption [459]. Progressive increases in the compliance of the lungs, and progressive decreases in the resistance of the lungs and respiratory system occur concomitantly with the clearance of pulmonary fluids [339, 460]. Therefore, mechanical changes in the lung in the immediate hours after birth cause the pressures required to inflate the lung to steadily decrease [132, 308]. These changes allow the establishment of a functional reserve capacity [352, 452], ventilation-perfusion matching [518] and the normalization of blood gas partial pressures [483].

In the context of development, negative P_{th} development is inarguably essential for surviving the transition from the liquid-filled lung to the air-breathing scenario. If the principles of symmorphosis are to hold, than the more immature mammalian neonates, such as those found in marsupials with incredibly low basal metabolic rates, have extremely low requirement for P_{di} pressure generation and ventilatory capacity when compared to the more precocial mammalians. Importantly, the marsupials range from ~3–850 mg at birth (or hatching) [249, 662] are not uniformly all tiny species by at maturity, with further pouch gestation lasting up to ~7–11 months postpartum for larger wallaby and kangaroo species [662]. In newborn marsupials, the upper airway musculature (required for effective suckling behaviors [183, 184, 337]) and rib structures are well developed, with intercostal muscles innervated by motor neurons [304, 305]. However, the DIAm is a thin sheet and plays little, if any, role in the generation of negative P_{th} for respiration [304, 305], there is an impaired/lack of descending respiratory drive [197, 627], reduced chemosensitivity [628] and the lungs are similarly immature when compared to other mammals, with the extent of compartmentalization and vascularization ranging from canalicular to rudimentary [197, 408, 627]. Consequently, these muscular and alveolar deficiencies necessitate alternative modes of gaseous exchange, particularly via transcutaneous mechanisms [197, 198, 408, 462, 627]. Despite these developmental constraints, the athletic capacity of many marsupials scales with those of placental mammals (though there is large variability in this regard),

including large tidal volumes [115, 135–137, 467, 468], providing further evidence for the overall utility of the symmorphosis concept, with markedly low neonatal marsupial ventilation requirements matched to functional capacity prior to exiting the pouch.

Conclusion

In this comprehensive review of the evolution of the DIAm, we have adopted the conceptual framework of symmorphosis by which the structural properties of the DIAm were matched to functional demands. In this context, the evolution of the DIAm should be viewed in relation to its two major functions: serving as a partition between the thoracic and abdominal cavities, and serving as a muscular pump to generate a negative P_{th} and a positive P_{ab}. These two functions are not exclusive but interrelated. In evolution, partitioning of the coelemic cavity into separate thoracic and abdominal cavities promoted the efficacy of aspiration breathing. Before partitioning the negative intra-coelemic pressure required to ventilate the lung caused incursion of the thoracic space by abdominal viscera. The impingement of viscera impeded lung expansion; thus the primordial DIAm membrane/partition promoted lung expansion and increased ventilation. Of course, improving respiratory efficiency by partitioning the abdominal and visceral compartments is not the only solution Nature has devised. An alternative is the development of the avian unidirectional air sac system.

Muscularization of the DIAm *per se* is unique to mammals. There were major evolutionary advantages in muscularizing the DIAm in order to provide an active pump for improved pressure generation in both intra-thoracic and intra-abdominal cavities. We often think of the DIAm as the major inspiratory muscle for ventilating the lung. This is certainly the case, and improved lung ventilation provided a major evolutionary advantage for mammals, especially considering the coincident evolution of the lung subdivision into alveoli to increase the surface area for gas exchange. However, even under extreme conditions, less than half of the force generating capacity of the DIAm is used to accomplish ventilatory behaviors. There is less consideration of the fact that the DIAm comprises the superior boundary of the abdominal cavity. Thus, DIAm contraction increases P_{ab}. Indeed, near maximum contraction of the DIAm occurs during straining behaviors that included defecation, vomiting, coughing sneezing and parturition. As with other skeletal muscles, contraction of the DIAm is under neural control. The motor unit, comprising a motor neuron and the muscle fibers it innervates is the fundamental unit of neuromotor control. Two groups of motor units are present in the DIAm to accomplish the range of motor functions involving P_{th} and P_{ab} generation. Fatigue resistant type S and FR motor units are well designed (with a high capacity for oxidative phosphorylation) to accomplish breathing behaviors that require lower forces but are repetitive and have a long duty cycle. In contrast, type FInt and FF motor units generate greater forces but are susceptible to fatigue. These motor units are well designed to accomplish higher force but more infrequent straining motor behaviors associated with increased P_{ab} generation.

Acknowledgements

This work is supported by NIH grants (AG044615, AG057052, HL96750, HL146114) and the Mayo Clinic.

References

1. Introduction to Pulmonary Structure & Mechanics, in Ganong's Review of Medical Physiology, Barrett KE, et al., Editors. 2018, McGraw-hill: New York.
2. Aaron EA and Powell FL, Effect of chronic hypoxia on hypoxic ventilatory response in awake rats. J Appl Physiol (1985), 1993 74(4): p. 1635–40. [PubMed: 8514677]
3. Abdallah SJ, Chan DS, Glicksman R, Mendonca CT, Luo Y, Bourbeau J, Smith BM, and Jensen D, Abdominal Binding Improves Neuromuscular Efficiency of the Human Diaphragm during Exercise. Front Physiol, 2017 8: p. 345. [PubMed: 28620310]
4. Abe T, Kieser TM, Tomita T, and Easton PA, Respiratory muscle function during emesis in awake canines. J Appl Physiol (1985), 1994 76(6): p. 2552–60. [PubMed: 7928883]
5. Abe T, Kusuhara N, Katagiri H, Tomita T, and Easton PA, Differential function of the costal and crural diaphragm during emesis in canines. Respir Physiol, 1993 91(2–3): p. 183–93. [PubMed: 8469843]
6. Adamsons K, Blumberg E, and Joelsson I, The effect of ambient temperature upon post-natal changes in oxygen consumption of the guinea-pig. J Physiol, 1969 202(2): p. 261–9. [PubMed: 5784287]
7. Ait-Haddou R, Binding P, and Herzog W, Theoretical considerations on cocontraction of sets of agonistic and antagonistic muscles. J Biomech, 2000 33(9): p. 1105–11. [PubMed: 10854883]
8. Akinkuotu AC, Sheikh F, Cass DL, Zamora IJ, Lee TC, Cassady CI, Mehollin-Ray AR, Williams JL, Ruano R, Welty SE, and Olutoye OO, Are all pulmonary hypoplasias the same? A comparison of pulmonary outcomes in neonates with congenital diaphragmatic hernia, omphalocele and congenital lung malformation. J Pediatr Surg, 2015 50(1): p. 55–9. [PubMed: 25598093]
9. Al-Bilbeisi F and Mc CF, Diaphragm recruitment during nonrespiratory activities. Am J Respir Crit Care Med, 2000 162(2 Pt 1): p. 456–9. [PubMed: 10934070]
10. Alberts GF, Peifley KA, Johns A, Kleha JF, and Winkles JA, Constitutive endothelin-1 overexpression promotes smooth muscle cell proliferation via an external autocrine loop. J Biol Chem, 1994 269(13): p. 10112–8. [PubMed: 8144511]
11. Alcorn D, Adamson TM, Lambert TF, Maloney JE, Ritchie BC, and Robinson PM, Morphological effects of chronic tracheal ligation and drainage in the fetal lamb lung. J Anat, 1977 123(Pt 3): p. 649–60. [PubMed: 885780]
12. Allan DW and Greer JJ, Embryogenesis of the phrenic nerve and diaphragm in the fetal rat. J Comp Neurol, 1997 382(4): p. 459–468. [PubMed: 9184993]
13. Alvarez-Argote S, Gransee HM, Mora JC, Stowe JM, Jorgenson AJ, Sieck GC, and Mantilla CB, The Impact of Midcervical Contusion Injury on Diaphragm Muscle Function. J Neurotrauma, 2016 33(5): p. 500–9. [PubMed: 26413840]
14. An X, Yue B, Lee JH, Lee MS, Lin C, and Han SH, Intramuscular distribution of the phrenic nerve in human diaphragm as shown by Sihler staining. Muscle Nerve, 2012 45(4): p. 522–6. [PubMed: 22431085]
15. Andersen HT, Physiological adaptations in diving vertebrates. Physiol Rev, 1966 46(2): p. 212–43. [PubMed: 5325969]
16. Andrews PL, Axelsson M, Franklin C, and Holmgren S, The emetic reflex in a reptile (Crocodylus porosus). J Exp Biol, 2000 203(Pt 10): p. 1625–32. [PubMed: 10769224]
17. Andrews PL, Okada F, Woods AJ, Hagiwara H, Kakaimoto S, Toyoda M, and Matsuki N, The emetic and anti-emetic effects of the capsaicin analogue resiniferatoxin in Suncus murinus, the house musk shrew. Br J Pharmacol, 2000 130(6): p. 1247–54. [PubMed: 10903962]
18. Aravamudan B, Mantilla CB, Zhan WZ, and Sieck GC, Denervation effects on myonuclear domain size of rat diaphragm fibers. J Appl Physiol, 2006 100(5): p. 1617–22. [PubMed: 16410375]
19. Arnold HH and Braun T, Genetics of muscle determination and development. Curr Top Dev Biol, 2000 48: p. 129–165. [PubMed: 10635459]
20. Arnoldi CC, The Venous Return from the Lower Leg in Health and in Chronic Venous Insufficiency. A Synthesis. Acta Orthop Scand Suppl, 1964 64: p. SUPPL64:1–75.

21. Arora NS and Rochester DF, Effect of body weight and muscularity on human diaphragm muscle mass, thickness, and area. J Appl Physiol, 1982 52(1): p. 64–70. [PubMed: 7061279]
22. Arora NS and Rochester DF, COPD and human diaphragm muscle dimensions. Chest, 1987 91(5): p. 719–24. [PubMed: 3568775]
23. Babic T and Browning KN, The role of vagal neurocircuits in the regulation of nausea and vomiting. Eur J Pharmacol, 2014 722: p. 38–47. [PubMed: 24184670]
24. Babiuk RP, Zhang W, Clugston R, Allan DW, and Greer JJ, Embryological origins and development of the rat diaphragm. J Comp Neurol, 2003 455(4): p. 477–87. [PubMed: 12508321]
25. Babu GJ, Warshaw DM, and Periasamy M, Smooth muscle myosin heavy chain isoforms and their role in muscle physiology. Microsc Res Tech, 2000 50(6): p. 532–40. [PubMed: 10998642]
26. Bachofen H and Duc G, Lung tissue resistance in healthy children. Pediatr Res, 1968 2(2): p. 119–24. [PubMed: 5659210]
27. Balbir A, Lande B, Fitzgerald RS, Polotsky V, Mitzner W, and Shirahata M, Behavioral and respiratory characteristics during sleep in neonatal DBA/2J and A/J mice. Brain Res, 2008 1241: p. 84–91. [PubMed: 18817755]
28. Balice-Gordon RJ and Lichtman JW, In vivo observations of pre- and postsynaptic changes during the transition from multiple to single innervation at developing neuromuscular junctions. J Neurosci, 1993 13(2): p. 834–55. [PubMed: 8426240]
29. Bandi E, Jevsek M, Mars T, Jurdana M, Formaggio E, Sciancalepore M, Fumagalli G, Grubic Z, Ruzzier F, and Lorenzon P, Neural agrin controls maturation of the excitation-contraction coupling mechanism in human myotubes developing in vitro. Am J Physiol Cell Physiol, 2008 294(1): p. C66–73. [PubMed: 18003748]
30. Banks GB, Kanjhan R, Wiese S, Kneussel M, Wong LM, O'Sullivan G, Sendtner M, Bellingham MC, Betz H, and Noakes PG, Glycinergic and GABAergic synaptic activity differentially regulate motoneuron survival and skeletal muscle innervation.[Erratum appears in J Neurosci. 2005 Mar 16;25(11):3018–21]. Journal of Neuroscience, 2005 25(5): p. 1249–59. [PubMed: 15689563]
31. Bartlett D Jr. and Areson JG, Quantitative lung morphology in newborn mammals. Respir Physiol, 1977 29(2): p. 193–200. [PubMed: 866814]
32. Baudinette RV, Gannon BJ, Runciman WB, Wells S, and Love JB, Do cardiorespiratory frequencies show entrainment with hopping in the tammar wallaby? J Exp Biol, 1987 129: p. 251–63. [PubMed: 3585241]
33. Bazzy AR, Developmental changes in rat diaphragm endplate response to repetitive stimulation. Brain Res Dev Brain Res, 1994 81(2): p. 314–7. [PubMed: 7813051]
34. Bazzy AR and Donnelly DF, Failure to generate action potentials in newborn diaphragms following nerve stimulation. Brain Res, 1993 600: p. 349–352. [PubMed: 8382101]
35. Bellingham MC, Driving respiration: the respiratory central pattern generator. Clin Exp Pharmacol Physiol, 1998 25(10): p. 847–56. [PubMed: 9784928]
36. Bellingham MC, Synaptic inhibition of cat phrenic motoneurons by internal intercostal nerve stimulation. J Neurophysiol, 1999 82(3): p. 1224–32. [PubMed: 10482742]
37. Bellingham MC and Lipski J, Respiratory interneurons in the C5 segment of the spinal cord of the cat. Brain Res, 1990 533(1): p. 141–6. [PubMed: 2085725]
38. Benezra R, Davis RL, Lassar A, Tapscott S, Thayer M, Lockshon D, and Weintraub H, Id: a negative regulator of helix-loop-helix DNA binding proteins. Control of terminal myogenic differentiation. Ann N Y Acad Sci, 1990 599: p. 1–11.
39. Bennett MR and Lavidis NA, Segmental motor projections to rat muscles during the loss of polyneuronal innervation. Dev Brain Res, 1984 13: p. 1–7.
40. Bennett MR and Pettigrew AG, The formation of synapses in striated muscle during development. J Physiol, 1974 241: p. 515–545. [PubMed: 4443927]
41. Benson RB, Butler RJ, Carrano MT, and O'Connor PM, Air-filled postcranial bones in theropod dinosaurs: physiological implications and the 'reptile'-bird transition. Biol Rev Camb Philos Soc, 2012 87(1): p. 168–93. [PubMed: 21733078]
42. Berger AJ, Phrenic motoneurons in the cat: subpopulations and nature of respiratory drive potentials. J Neurophysiol, 1979 42: p. 76–90. [PubMed: 430115]

43. Berger AJ and Averill DB, Projection of single pulmonary stretch receptors to solitary tract region. J Neurophysiol, 1983 49(3): p. 819–30. [PubMed: 6300354]
44. Bertrand F, Hugelin A, and Vibert JF, Quantitative study of anatomical distribution of respiration related neurons in the pons. Exp Brain Res, 1973 16(4): p. 383–99. [PubMed: 4693624]
45. Bigland-Ritchie B, Kukulka CG, Lippold OCJ, and Woods JJ, The absence of neuromuscular transmission failure in sustained maximal voluntary contractions. J Physiol, 1982 330: p. 265–278. [PubMed: 6294288]
46. Blackie SP, Fairbarn MS, McElvaney NG, Wilcox PG, Morrison NJ, and Pardy RL, Normal values and ranges for ventilation and breathing pattern at maximal exercise. Chest, 1991 100(1): p. 136–42. [PubMed: 1905613]
47. Blackmore D, Body size and metabolic rate in newborn lambs of two breeds. J Appl Physiol, 1969 27(2): p. 241–5. [PubMed: 5796315]
48. Blackwell SB and Le Boeuf BJ, Developmental aspects of sleep apnoea in northern elephant seals, Mirounga angustirostris. J. Zool. Lond, 1993 231: p. 437–447.
49. Blanco CE, Fournier M, and Sieck GC, Metabolic variability within individual fibres of the cat tibialis posterior and diaphragm muscles. Histochemical Journal, 1991 23(8): p. 366–374. [PubMed: 1917565]
50. Blanco CE and Sieck GC, Comparison of succinate dehydrogenase activity between the diaphragm and medial gastrocnemius muscles of the rat, in Respiratory Muscles and Their Neuromotor Control, Sieck GC, Gandevia SC, and Cameron WE, Editors. 1987, Alan R. Liss, Inc.: New York p. 281–289.
51. Blanco CE and Sieck GC, Quantitative determination of calcium-activated myosin adenosine triphosphatase activity in rat skeletal muscle fibres. Histochem J, 1992 24(7): p. 431–444. [PubMed: 1387125]
52. Blanco CE, Sieck GC, and Edgerton VR, Quantitative histochemical determination of succinic dehydrogenase activity in skeletal muscle fibres. Histochem J, 1988 20: p. 230–243. [PubMed: 3209423]
53. Blix AS and Lentfer JW, Modes of thermal protection in polar bear cubs--at birth and on emergence from the den. Am J Physiol, 1979 236(1): p. R67–74. [PubMed: 434189]
54. Bodine SC, Roy RR, Eldred E, and Edgerton VR, Maximal force as a function of anatomical features of motor units in the cat tibialis anterior. J Neurophysiol, 1987 57(6): p. 1730–1745. [PubMed: 3598628]
55. Bolser DC, Lindsey BG, and Shannon R, Medullary inspiratory activity: influence of intercostal tendon organs and muscle spindle endings. J Appl Physiol (1985), 1987 62(3): p. 1046–56. [PubMed: 3571061]
56. Bolser DC, Pitts TE, Davenport PW, and Morris KF, Role of the dorsal medulla in the neurogenesis of airway protection. Pulm Pharmacol Ther, 2015 35: p. 105–10. [PubMed: 26549786]
57. Boon AW, Ward-McQuaid JM, Milner AD, and Hopkin IE, Thoracic gas volume, helium functional residual capacity and air-trapping in the first six hours of life: the effect of oxygen administration. Early Hum Dev, 1981 5(2): p. 157–66. [PubMed: 7018885]
58. Borell U and Fernstrom I, The shape of the foetal chest during its passage through the birth canal. A radiographic study. Acta Obstet Gynecol Scand, 1962 41: p. 213–22. [PubMed: 14013904]
59. Boriek AM, Miller CC 3rd, and Rodarte JR, Muscle fiber architecture of the dog diaphragm. J Appl Physiol (1985), 1998 84(1): p. 318–26. [PubMed: 9451652]
60. Borison HL, Borison R, and McCarthy LE, Phylogenic and neurologic aspects of the vomiting process. J Clin Pharmacol, 1981 21(8–9 Suppl): p. 23S–29S. [PubMed: 6117573]
61. Boufettal R, Lefriyekh MR, Boufettal H, Fadil A, and Zerouali NO, [Spontaneous diaphragm rupture during delivery. Case report]. J Gynecol Obstet Biol Reprod (Paris), 2008 37(1): p. 93–6. [PubMed: 18077103]
62. Boulenguez P, Gauthier P, and Kastner A, Respiratory neuron subpopulations and pathways potentially involved in the reactivation of phrenic motoneurons after C2 hemisection. Brain Res, 2007 1148: p. 96–104. [PubMed: 17379194]
63. Boyd IL, The behavioural and physiological ecology of diving. Trends Ecol Evol, 1997 12(6): p. 213–7. [PubMed: 21238044]

64. Brainerd EL, The evolution of lung-gill bimodal breathing and the homology of vertebrate respiratory pumps. Am. Zool, 1994 34: p. 289–299.

65. Brainerd EL, Mechanics of lung ventilation in a larval salamander Ambystoma tigrinum. J Exp Biol, 1998 201(Pt 20): p. 2891–901.

66. Brainerd EL, New Perspectives on the Evolution of Lung Ventilation Mechanisms in Vertebrates. Exp. Biol. Online, 1999 4: p. 11–28.

67. Brainerd EL, Ditelberg JS, and Bramble DM, Lung ventilation in salamanders and the evolution of vertebrate air-breathing mechanisms. Biol. J. Linn. Soc, 1993 49: p. 163–183.

68. Brainerd EL and Monroy JA, Mechanics of lung ventilation in an aquatic salamander, Siren lacertina. J. Exp. Biol, 1998 201: p. 673–682. [PubMed: 9450976]

69. Brainerd EL and Owerkowicz T, Functional morphology and evolution of aspiration breathing in tetrapods. Respir Physiol Neurobiol, 2006 154(1–2): p. 73–88. [PubMed: 16861059]

70. Brainerd EL, Page BN, and Fish FE, Opercular jetting during fast-starts by flatfishes. J. Exp. Biol, 1997 200: p. 1179–1188. [PubMed: 9319024]

71. Bramble DM and Carrier DR, Running and breathing in mammals. Science, 1983 219(4582): p. 251–6. [PubMed: 6849136]

72. Brancatisano A, Amis TC, Tully A, Kelly WT, and Engel LA, Regional distribution of blood flow within the diaphragm. J Appl Physiol, 1991 71: p. 583–589. [PubMed: 1938731]

73. Braun T, Bober E, Buschhausen-Denker G, Kohtz S, Grzeschik KH, Arnold HH, and Kotz S, Differential expression of myogenic determination genes in muscle cells: possible autoactivation by the Myf gene products. EMBO J, 1989 8(12): p. 3617–3625. [PubMed: 2583111]

74. Braun T, Buschhausen-Denker G, Bober E, Tannich E, and Arnold HH, A novel human muscle factor related to but distinct from MyoD1 induces myogenic conversion in 10T1/2 fibroblasts. EMBO J, 1989 8(3): p. 701–709. [PubMed: 2721498]

75. Braun T, Rudnicki MA, Arnold H-H, and Jaenisch R, Targeted inactivation of the muscle regulatory genes Myf-5 results in abnormal rib development and perinatal death. Cell, 1992 71: p. 269–282.

76. Brown MC, Jansen JKS, and Van Essen D, Polyneuronal innervation of skeletal muscle in new-born rats and its elimination during maturation. J Physiol, 1976 261: p. 387–422. [PubMed: 978579]

77. Brown MJ, Olver RE, Ramsden CA, Strang LB, and Walters DV, Effects of adrenaline and of spontaneous labour on the secretion and absorption of lung liquid in the fetal lamb. J Physiol, 1983 344: p. 137–52. [PubMed: 6655575]

78. Brown RE, Brain JD, and Wang N, The avian respiratory system: a unique model for studies of respiratory toxicosis and for monitoring air quality. Environ Health Perspect, 1997 105(2): p. 188–200. [PubMed: 9105794]

79. Brown RE, Butler JP, Godleski JJ, and Loring SH, The elephant's respiratory system: adaptations to gravitational stress. Respir Physiol, 1997 109(2): p. 177–94. [PubMed: 9299649]

80. Brown TG, On the nature of the fundamental activity of the nervous centres; together with an analysis of the conditioning of rhythmic activity in progression, and a theory of the evolution of function in the nervous system. The Journal of physiology, 1914 48(1): p. 18–46. [PubMed: 16993247]

81. Brumley GW, Chernick V, Hodson WA, Normand C, Fenner A, and Avery ME, Correlations of mechanical stability, morphology, pulmonary surfactant, and phospholipid content in the developing lamb lung. J Clin Invest, 1967 46(5): p. 863–73. [PubMed: 6025487]

82. Buckingham M, Which myogenic factors make muscle? Curr Biol, 1994 4(4): p. 61–63. [PubMed: 7922315]

83. Buckingham ME, Lyons GE, Ott MO, and Sassoon DA, Myogenesis in the mouse. CIBA Found Symp, 1992 165: p. 111–24. [PubMed: 1516464]

84. Buhimschi CS, Buhimschi IA, Malinow A, and Weiner CP, Use of McRoberts' position during delivery and increase in pushing efficiency. Lancet, 2001 358(9280): p. 470–1. [PubMed: 11513914]

85. Burgess RW, Jucius TJ, and Ackerman SL, Motor axon guidance of the mammalian trochlear and phrenic nerves: dependence on the netrin receptor Unc5c and modifier loci. J Neurosci, 2006 26(21): p. 5756–66. [PubMed: 16723533]

86. Burke RE, Levine DN, Tsairis P, and Zajac FE 3rd, Physiological types and histochemical profiles in motor units of the cat gastrocnemius. J Physiol, 1973 234(3): p. 723–48. [PubMed: 4148752]

87. Butler JE, McKenzie DK, and Gandevia SC, Discharge properties and recruitment of human diaphragmatic motor units during voluntary inspiratory tasks. J Physiol, 1999 518 (Pt 3): p. 907–20. [PubMed: 10420024]

88. Butler PJ and Jones DR, Physiology of diving of birds and mammals. Physiol Rev, 1997 77(3): p. 837–99. [PubMed: 9234967]

89. Butler RJ, Barrett PM, and Gower DJ, Reassessment of the evidence for postcranial skeletal pneumaticity in Triassic archosaurs, and the early evolution of the avian respiratory system. PLoS One, 2012 7(3): p. e34094. [PubMed: 22470520]

90. Canning BJ, Chang AB, Bolser DC, Smith JA, Mazzone SB, McGarvey L, and Panel CEC, Anatomy and neurophysiology of cough: CHEST Guideline and Expert Panel report. Chest, 2014 146(6): p. 1633–1648. [PubMed: 25188530]

91. Carmel JA, Friedman F, and Adams FH, Fetal Tracheal Ligation and Lung Development. Am J Dis Child, 1965 109: p. 452–6. [PubMed: 14280143]

92. Carrier DR, Function of the intercostal muscles in trotting dogs: ventilation or locomotion? J Exp Biol, 1996 199(Pt 7): p. 1455–65. [PubMed: 8699153]

93. Carry PY and Banssillon V, [Intra-abdominal pressure]. Ann Fr Anesth Reanim, 1994 13(3): p. 381–99. [PubMed: 7992945]

94. Cassin S, DeMarco V, Perks AM, Kuck H, and Ellis TM, Regulation of lung liquid secretion in immature fetal sheep: hormonal interaction. J Appl Physiol (1985), 1994 77(3): p. 1445–50. [PubMed: 7836151]

95. Cassin S and Perks AM, Amiloride inhibits arginine vasopressin-induced decrease in fetal lung liquid secretion. J Appl Physiol (1985), 1993 75(5): p. 1925–9. [PubMed: 8307841]

96. Castellini M, Life under water: physiological adaptations to diving and living at sea. Compr Physiol, 2012 2(3): p. 1889–919. [PubMed: 23723028]

97. Castellini MA, Dreaming About Diving: Sleep Apnea in Seals. NiPS, 1996 11: p. 208–214.

98. Castellini MA, Milsom WK, Berger RJ, Costa DP, Jones DR, Castellini JM, Rea LD, Bharma S, and Harris M, Patterns of respiration and heart rate during wakefulness and sleep in elephant seal pups. Am J Physiol, 1994 266(3 Pt 2): p. R863–9. [PubMed: 8160882]

99. Castellini MA, Rea LD, Sanders JL, Castellini JM, and Zenteno-Savin T, Developmental changes in cardiorespiratory patterns of sleep-associated apnea in northern elephant seals. Am J Physiol, 1994 267(5 Pt 2): p. R1294–301. [PubMed: 7977857]

100. Chaar CI, Attanasio P, and Detterbeck F, Disruption of the costal margin with transdiaphragmatic abdominal herniation induced by coughing. Am Surg, 2008 74(4): p. 350–3. [PubMed: 18453304]

101. Chamberlain S and Lewis DM, Contractile characteristics and innervation ratio of rat soleus motor units. J Physiol, 1989 412: p. 1–21. [PubMed: 2600827]

102. Chan CL, Ponsford S, and Swash M, The anal reflex elicited by cough and sniff: validation of a neglected clinical sign. J Neurol Neurosurg Psychiatry, 2004 75(10): p. 1449–51. [PubMed: 15377694]

103. Claessens LP, Archosaurian respiration and the pelvic girdle aspiration breathing of crocodyliforms. Proc Biol Sci, 2004 271(1547): p. 1461–5. [PubMed: 15306317]

104. Claessens LP, O'Connor PM, and Unwin DM, Respiratory evolution facilitated the origin of pterosaur flight and aerial gigantism. PLoS One, 2009 4(2): p. e4497. [PubMed: 19223979]

105. Clarke A, Rothery P, and Isaac NJ, Scaling of basal metabolic rate with body mass and temperature in mammals. J Anim Ecol, 2010 79(3): p. 610–9. [PubMed: 20180875]

106. Clewlow F, Dawes GS, Johnston BM, and Walker DW, Changes in breathing, electrocortical and muscle activity in unanaesthetized fetal lambs with age. J Physiol, 1983 341: p. 463–76. [PubMed: 6413680]

107. Clugston RD and Greer JJ, Diaphragm development and congenital diaphragmatic hernia. Semin Pediatr Surg, 2007 16(2): p. 94–100. [PubMed: 17462561]
108. Coast JR, Rasmussen SA, Krause KM, O'Kroy JA, Loy RA, and Rhodes J, Ventilatory work and oxygen consumption during exercise and hyperventilation. J Appl Physiol (1985), 1993 74(2): p. 793–8. [PubMed: 8458797]
109. Cobb WS, Burns JM, Kercher KW, Matthews BD, James Norton H, and Todd Heniford B, Normal intraabdominal pressure in healthy adults. J Surg Res, 2005 129(2): p. 231–5. [PubMed: 16140336]
110. Codd JR and Klein W, Breathing, locomotion and everything in-between. Comp Biochem Physiol A Mol Integr Physiol, 2010 156(3): p. 301–2.
111. Codd JR, Manning PL, Norell MA, and Perry SF, Avian-like breathing mechanics in maniraptoran dinosaurs. Proc Biol Sci, 2008 275(1631): p. 157–61. [PubMed: 17986432]
112. Cohen MI, Neurogenesis of respiratory rhythm in the mammal. Physiol Rev, 1979 59(4): p. 1105–73. [PubMed: 227004]
113. Cohen MI, Piercey MF, Gootman PM, and Wolotosky P, Synaptic connections between medullary inspiratory neurons and phrenic motoneurons as revealed by cross-correlation. Brain Res, 1974 81: p. 319–324. [PubMed: 4373128]
114. Colby ED, McCarthy LE, and Borison HL, Emetic action of xylazine on the chemoreceptor trigger zone for vomiting in cats. J Vet Pharmacol Ther, 1981 4(2): p. 93–6. [PubMed: 7349332]
115. Cooper CE and Withers PC, Ventilatory physiology of the numbat (Myrmecobius fasciatus). J Comp Physiol B, 2004 174(2): p. 107–11. [PubMed: 14628148]
116. Cope MJ, Whisstock J, Rayment I, and Kendrick-Jones J, Conservation within the myosin motor domain: implications for structure and function. Structure, 1996 4(8): p. 969–87. [PubMed: 8805581]
117. Corda M, von Euler C, and Lennerstrand G, Proprioceptive innervation of the diaphragm. J Physiol, 1965 178: p. 161–177. [PubMed: 14298107]
118. Cotten PB, Piscitelli MA, McLellan WA, Rommel SA, Dearolf JL, and Pabst DA, The gross morphology and histochemistry of respiratory muscles in bottlenose dolphins, Tursiops truncatus. J Morphol, 2008 269(12): p. 1520–38. [PubMed: 18777569]
119. Cotton CJ, Skeletal muscle mass and composition during mammalian hibernation. J Exp Biol, 2016 219(Pt 2): p. 226–34. [PubMed: 26792334]
120. Cran HR, Uterine rupture in the mare. Vet Rec, 1985 116(20): p. 550.
121. Crighton GW and Pownall R, The homeothermic status of the neonatal dog. Nature, 1974 251(5471): p. 142–4. [PubMed: 4420883]
122. Cripps RM, Suggs JA, and Bernstein SI, Assembly of thick filaments and myofibrils occurs in the absence of the myosin head. EMBO J, 1999 18(7): p. 1793–804. [PubMed: 10202143]
123. Daniel R, Naidu B, and Khalil-Marzouk J, Cough-induced rib fracture and diaphragmatic rupture resulting in simultaneous abdominal visceral herniation into the left hemithorax and subcutaneously. Eur J Cardiothorac Surg, 2008 34(4): p. 914–5. [PubMed: 18715797]
124. Darveau CA, Suarez RK, Andrews RD, and Hochachka PW, Allometric cascade as a unifying principle of body mass effects on metabolism. Nature, 2002 417(6885): p. 166–70. [PubMed: 12000958]
125. Datta AK, Shea SA, Horner RL, and Guz A, The influence of induced hypocapnia and sleep on the endogenous respiratory rhythm in humans. J Physiol, 1991 440: p. 17–33. [PubMed: 1804960]
126. Davies AS and Gunn HM, Histochemical fibre types in the mammalian diaphragm. J Anat, 1972 112(Pt 1): p. 41–60. [PubMed: 4263892]
127. Davies JG, Kirkwood PA, and Sears TA, The distribution of monosynaptic connexions from inspiratory bulbospinal neurones to inspiratory motoneurones in the cat. J Physiol, 1985 368: p. 63–87. [PubMed: 4078753]
128. Davis JN and Plum F, Separation of descending spinal pathways to respiratory motoneurons. Exp Neurol, 1972 34(1): p. 78–94. [PubMed: 5009511]

129. Davis RL, Weintraub H, and Lassar B, Expression of a single transfected cDNA converts fibrobalsts to myoblasts. Cell, 1987 51: p. 987–1000. [PubMed: 3690668]
130. Davis RW, Polasek L, Watson R, Fuson A, Williams TM, and Kanatous SB, The diving paradox: new insights into the role of the dive response in air-breathing vertebrates. Comp Biochem Physiol A Mol Integr Physiol, 2004 138(3): p. 263–8. [PubMed: 15313479]
131. Dawes GS, Gardner WN, Johnston BM, and Walker DW, Breathing in fetal lambs: the effect of brain stem section. J Physiol, 1983 335: p. 535–53. [PubMed: 6875894]
132. Dawes GS, Mott JC, Widdicombe JG, and Wyatt DG, Changes in the lungs of the new-born lamb. J Physiol, 1953 121(1): p. 141–62. [PubMed: 13085305]
133. Dawson TH, Scaling laws for capillary vessels of mammals at rest and in exercise. Proc Biol Sci, 2003 270(1516): p. 755–63. [PubMed: 12713751]
134. Dawson TH, Modeling of vascular networks. J Exp Biol, 2005 208(Pt 9): p. 1687–94. [PubMed: 15855400]
135. Dawson TJ, Mifsud B, Raad MC, and Webster KN, Aerobic characteristics of red kangaroo skeletal muscles: is a high aerobic capacity matched by muscle mitochondrial and capillary morphology as in placental mammals? J Exp Biol, 2004 207(Pt 16): p. 2811–21. [PubMed: 15235010]
136. Dawson TJ and Needham AD, Cardiovascular characteristics of two resting marsupials: an insight into the cardio-respiratory allometry of marsupials. J. Comp. Physiol, 1981 145: p. 95–100.
137. Dawson TJ, Webster KN, Lee E, and Buttemer WA, High muscle mitochondrial volume and aerobic capacity in a small marsupial (Sminthopsis crassicaudata) reveals flexible links between energy-use levels in mammals. J Exp Biol, 2013 216(Pt 7): p. 1330–7. [PubMed: 23239895]
138. De Jonghe BC and Horn CC, Chemotherapy agent cisplatin induces 48-h Fos expression in the brain of a vomiting species, the house musk shrew (Suncus murinus). Am J Physiol Regul Integr Comp Physiol, 2009 296(4): p. R902–11. [PubMed: 19225146]
139. De Troyer A, Legrand A, Gevenois PA, and Wilson TA, Mechanical advantage of the human parasternal intercostal and triangularis sterni muscles. J Physiol, 1998 513 (Pt 3): p. 915–25. [PubMed: 9824728]
140. De Troyer A, Sampson M, Sigrist S, and Macklem PT, The diaphragm: two muscles. Science, 1981 213(4504): p. 237–238. [PubMed: 7244632]
141. Dearolf JL, Diaphragm muscle development in bottlenose dolphins (Tursiops truncatus). J Morphol, 2003 256(1): p. 79–88. [PubMed: 12616575]
142. Decima EE, von Euler C, and Thoden U, Intercostal-to-phrenic reflexes in the spinal cat. Acta Physiol Scand, 1969 75(4): p. 568–79. [PubMed: 4243231]
143. del Castillo J and Katz B, Quantal components of the end-plate potential. J Physiol, 1954 124(3): p. 560–573. [PubMed: 13175199]
144. Demetrius L, Of mice and men. When it comes to studying ageing and the means to slow it down, mice are not just small humans. EMBO Rep, 2005 6 Spec No: p. S39–44. [PubMed: 15995660]
145. Dick TE, Kong FJ, and Berger AJ, Correlation of recruitment order with axonal conduction velocity for supraspinally driven diaphragmatic motor units. J Neurophysiol, 1987 57(1): p. 245–259. [PubMed: 3559674]
146. Dick TE, Oku Y, Romaniuk JR, and Cherniack NS, Interaction between central pattern generators for breathing and swallowing in the cat. J Physiol, 1993 465: p. 715–30. [PubMed: 8229859]
147. Dobbins EG and Feldman JL, Brainstem network controlling descending drive to phrenic motoneurons in rat. J Comp Neurol, 1994 347(1): p. 64–86. [PubMed: 7798382]
148. Donoghue S, Garcia M, Jordan D, and Spyer KM, The brain-stem projections of pulmonary stretch afferent neurones in cats and rabbits. J Physiol, 1982 322: p. 353–63. [PubMed: 7069621]
149. Doperalski NJ and Fuller DD, Long-term facilitation of ipsilateral but not contralateral phrenic output after cervical spinal cord hemisection. Exp Neurol, 2006 200(1): p. 74–81. [PubMed: 16647702]
150. Doperalski NJ, Sandhu MS, Bavis RW, Reier PJ, and Fuller DD, Ventilation and phrenic output following high cervical spinal hemisection in male vs. female rats. Respir Physiol Neurobiol, 2008 162(2): p. 160–7. [PubMed: 18586119]

151. Dougherty BJ, Lee KZ, Gonzalez-Rothi EJ, Lane MA, Reier PJ, and Fuller DD, Recovery of inspiratory intercostal muscle activity following high cervical hemisection. Respir Physiol Neurobiol, 2012 183(3): p. 186–92. [PubMed: 22705013]

152. Downey R, Anatomy of the normal diaphragm. Thorac Surg Clin, 2011 21(2): p. 273–9, ix. [PubMed: 21477776]

153. Duffin J and Douse MA, Botzinger expiratory neurones inhibit propriobulbar decrementing inspiratory neurones. Neuroreport, 1993 4(11): p. 1215–8. [PubMed: 8219016]

154. Duffin J and Iscoe S, The possible role of C5 segment inspiratory interneurons investigated by cross-correlation with phrenic motoneurons in decerebrate cats. Exp Brain Res, 1996 112(1): p. 35–40. [PubMed: 8951404]

155. Duncker HR, [Coelom organization of vertebrates--functional aspects]. Verh Anat Ges, 1978(72): p. 91–112. [PubMed: 746827]

156. Duron B, Jung-Caillol MC, and Marlot D, Myelinated nerve fiber supply and muscle spindles in the respiratory muscles of cat: quantitative study. Anatomy and embryology, 1978 152(2): p. 171–92. [PubMed: 147637]

157. Edwin F, Tettey MM, Sereboe L, and Frimpong-Boateng K, eComment: Spontaneous or effort diaphragmatic rupture. Interact Cardiovasc Thorac Surg, 2009 9(2): p. 376. [PubMed: 19628553]

158. Eldridge FL, Gill-Kumar P, Millhorn DE, and Waldrop TG, Spinal inhibition of phrenic motoneurones by stimulation of afferents from peripheral muscles. J Physiol, 1981 311: p. 67–79. [PubMed: 7264986]

159. Elgar MA, Predator vigilance and group size in mammals and birds: a critical review of the empirical evidence. Biol Rev Camb Philos Soc, 1989 64(1): p. 13–33. [PubMed: 2655726]

160. Ellenberger HH and Feldman JL, Monosynaptic transmission of respiratory drive to phrenic motoneurons from brainstem bulbospinal neurons in rats. J Comp Neurol, 1988 269: p. 47–57. [PubMed: 3361003]

161. Ellenberger HH and Feldman JL, Brainstem connections of the rostral ventral respiratory group of the rat. Brain Res, 1990 513: p. 35–42 [PubMed: 2350683]

162. Elliott JE, Omar TS, Mantilla CB, and Sieck GC, Diaphragm muscle sarcopenia in Fischer 344 and Brown Norway rats. Experimental physiology, 2016 101(7): p. 883–94. [PubMed: 27126607]

163. Enad JG, Fournier M, and Sieck GC, Oxidative capacity and capillary density of diaphragm motor units. J Appl Physiol, 1989 67((2)): p. 620–627. [PubMed: 2529236]

164. Ermilov LG, Pulido JN, Atchison FW, Zhan WZ, Ereth MH, Sieck GC, and Mantilla CB, Impairment of diaphragm muscle force and neuromuscular transmission after normothermic cardiopulmonary bypass: effect of low dose inhaled CO. Am J Physiol Regul Integr Comp Physiol, 2010 298(3): p. R784–9. [PubMed: 20089713]

165. Estenne M and Gorini M, Action of the diaphragm during cough in tetraplegic subjects. J Appl Physiol (1985), 1992 72(3): p. 1074–80. [PubMed: 1568963]

166. Falls DL, Rosen KM, Corfas G, Lane WS, and Fischbach GD, ARIA, a protein that stimulates acetylcholine receptor synthesis, is a member of the neu ligand family. Cell, 1993 72(5): p. 801–15. [PubMed: 8453670]

167. Farmer CG, The provenance of alveolar and parabronchial lungs: insights from paleoecology and the discovery of cardiogenic, unidirectional airflow in the American alligator (Alligator mississippiensis). Physiol Biochem Zool, 2010 83(4): p. 561–75. [PubMed: 20377411]

168. Farmer CG, The evolution of unidirectional pulmonary airflow. Physiology (Bethesda), 2015 30(4): p. 260–272. [PubMed: 26136540]

169. Farmer CG and Carrier DR, Pelvic aspiration in the American alligator (Alligator mississippiensis). J Exp Biol, 2000 203(Pt 11): p. 1679–87. [PubMed: 10804158]

170. Farmer CG and Carrier DR, Respiration and gas exchange during recovery from exercise in the American alligator. Respir Physiol, 2000 120(1): p. 81–7. [PubMed: 10786647]

171. Farmer CG and Carrier DR, Ventilation and gas exchange during treadmill locomotion in the American alligator (Alligator mississippiensis). J Exp Biol, 2000 203(Pt 11): p. 1671–8. [PubMed: 10804157]

172. Farmer CG and Sanders K, Unidirectional airflow in the lungs of alligators. Science, 2010 327: p. 338–340. [PubMed: 20075253]

173. Fatt P and Katz B, An analysis of the end-plate potential recorded with an intra-cellular electrode. J Physiol, 1951 115: p. 320–370. [PubMed: 14898516]
174. Feldman JD, Bazzy AR, Cummins TR, and Haddad GG, Developmental changes in neuromuscular transmission in the rat diaphragm. J Appl Physiol, 1991 71: p. 280–286. [PubMed: 1655690]
175. Feldman JL and Cohen MI, Relation between expiratory duration and rostral medullary expiratory neuronal discharge. Brain Res, 1978 141: p. 172–178. [PubMed: 624073]
176. Feldman JL, Loewy AD, and Speck DF, Projections from the ventral respiratory group to phrenic and intercostal motoneurons in cat: an autoradiographic study. J Neurosci, 1985 5(8): p. 1993–2000. [PubMed: 3926961]
177. Fenn WO, A quantitative comparison between the energy liberated and the work performed by the isolated sartorius muscle of the frog. J. Physiol. (London), 1923 58: p. 175–203. [PubMed: 16993652]
178. Fink BR, Influence of cerebral activity in wakefulness on regulation of breathing. J Appl Physiol, 1961 16: p. 15–20. [PubMed: 13699604]
179. Fleshman JW, Munson JB, Sypert GW, and Friedman WA, Rheobase, input resistance, and motor-unit type in medial gastrocnemius motoneurons in the cat. J Neurophysiol, 1981 46(6): p. 1326–1338. [PubMed: 6275043]
180. Floyd WF and Walls EW, Electromyography of the sphincter ani externus in man. J Physiol, 1953 122(3): p. 599–609. [PubMed: 13118564]
181. Fogarty MJ, The bigger they are the harder they fall: size-dependent vulnerability of motor neurons in amyotrophic lateral sclerosis. J Physiol, 2018 596(13): p. 2471–2472. [PubMed: 29719046]
182. Fogarty MJ, Driven to decay: Excitability and synaptic abnormalities in amyotrophic lateral sclerosis. Brain Res Bull, 2018 140: p. 318–333. [PubMed: 29870780]
183. Fogarty MJ, Kanjhan R, Bellingham MC, and Noakes PG, Glycinergic Neurotransmission: A Potent Regulator of Embryonic Motor Neuron Dendritic Morphology and Synaptic Plasticity. J Neurosci, 2016 36(1): p. 80–7. [PubMed: 26740651]
184. Fogarty MJ, Kanjhan R, Yanagawa Y, Noakes PG, and Bellingham MC, Alterations in hypoglossal motor neurons due to GAD67 and VGAT deficiency in mice. Exp Neurol, 2017 289: p. 117–127. [PubMed: 27956032]
185. Fogarty MJ, Klenowski PM, Lee JD, Drieberg-Thompson JR, Bartlett SE, Ngo ST, Hilliard MA, Bellingham MC, and Noakes PG, Cortical synaptic and dendritic spine abnormalities in a presymptomatic TDP-43 model of amyotrophic lateral sclerosis. Sci Rep, 2016 6: p. 37968. [PubMed: 27897242]
186. Fogarty MJ, Mantilla CB, and Sieck GC, Breathing: Motor Control of Diaphragm Muscle. Physiology (Bethesda), 2018 33(2): p. 113–126. [PubMed: 29412056]
187. Fogarty MJ, Mu EW, Noakes PG, Lavidis NA, and Bellingham MC, Marked changes in dendritic structure and spine density precede significant neuronal death in vulnerable cortical pyramidal neuron populations in the SOD1(G93A) mouse model of amyotrophic lateral sclerosis. Acta Neuropathol Commun, 2016 4(1): p. 77. [PubMed: 27488828]
188. Fogarty MJ, Mu EWH, Lavidis NA, Noakes PG, and Bellingham MC, Motor Areas Show Altered Dendritic Structure in an Amyotrophic Lateral Sclerosis Mouse Model. Front Neurosci, 2017 11: p. 609. [PubMed: 29163013]
189. Fogarty MJ, Noakes PG, and Bellingham MC, Motor cortex layer V pyramidal neurons exhibit dendritic regression, spine loss, and increased synaptic excitation in the presymptomatic hSOD1(G93A) mouse model of amyotrophic lateral sclerosis. J Neurosci, 2015 35(2): p. 643–7. [PubMed: 25589758]
190. Fogarty MJ, Omar TS, Zhan WZ, Mantilla CB, and Sieck GC, Phrenic Motor Neuron Loss in Aged Rats. J Neurophysiol, 2018.
191. Fogarty MJ, Smallcombe KL, Yanagawa Y, Obata K, Bellingham MC, and Noakes PG, Genetic deficiency of GABA differentially regulates respiratory and non-respiratory motor neuron development. PLoS ONE, 2013 8(2): p. e56257. [PubMed: 23457538]

192. Fogarty MJ, Yanagawa Y, Obata K, Bellingham MC, and Noakes PG, Genetic absence of the vesicular inhibitory amino acid transporter differentially regulates respiratory and locomotor motor neuron development. Brain Struct Funct, 2015 220(1): p. 525–40. [PubMed: 24276495]

193. Fournier M, Alula M, and Sieck GC, Neuromuscular transmission failure during postnatal development. Neurosci Lett, 1991 125(1): p. 34–36. [PubMed: 1649983]

194. Fournier M and Sieck GC, Topographical projections of phrenic motoneurons and motor unit territories in the cat diaphragm, in Respiratory Muscles and Their Neuromotor Control, Sieck GC, Gandevia SC, and Cameron WE, Editors. 1987, Alan R. Liss, Inc.: New York p. 215–226.

195. Fournier M and Sieck GC, Mechanical properties of muscle units in the cat diaphragm. J Neurophysiol, 1988 59(3): p. 1055–1066. [PubMed: 3367195]

196. Fournier M and Sieck GC, Somatotopy in the segmental innervation of the cat diaphragm. J Appl Physiol, 1988 64: p. 291–298. [PubMed: 3356649]

197. Frappell PB and MacFarlane PM, Development of the respiratory system in marsupials. Respir Physiol Neurobiol, 2006 154(1–2): p. 252–67. [PubMed: 16781204]

198. Frappell PB and Mortola JP, Respiratory function in a newborn marsupial with skin gas exchange. Respir Physiol, 2000 120(1): p. 35–45. [PubMed: 10786643]

199. Friday BB, Mitchell PO, Kegley KM, and Pavlath GK, Calcineurin initiates skeletal muscle differentiation by activating MEF2 and MyoD. Differentiation, 2003 71(3): p. 217–27. [PubMed: 12694204]

200. Fukuda H and Fukai K, Convergence of visceral afferents on candidate units for the pontine defecation reflex center of the dog. Jpn J Physiol, 1982 32(6): p. 1007–10. [PubMed: 7169695]

201. Fukuda H and Fukai K, The afferent and efferent pathways of the recto-colonic reflex in the dog. Jpn J Physiol, 1985 35(5): p. 795–801. [PubMed: 4079135]

202. Fukuda H and Fukai K, Ascending and descending pathways of reflex straining in the dog. Jpn J Physiol, 1986 36(5): p. 905–20. [PubMed: 3560538]

203. Fukuda H and Fukai K, Location of the reflex centre for straining elicited by activation of pelvic afferent fibres of decerebrate dogs. Brain Res, 1986 380(2): p. 287–96. [PubMed: 3756481]

204. Fukuda H and Fukai K, Postural change and straining induced by distension of the rectum, vagina and urinary bladder of decerebrate dogs. Brain Res, 1986 380(2): p. 276–86. [PubMed: 3756480]

205. Fukuda H and Fukai K, Discharges of bulbar respiratory neurons during rhythmic straining evoked by activation of pelvic afferent fibers in dogs. Brain Res, 1988 449(1–2): p. 157–66. [PubMed: 3395844]

206. Fukuda H, Fukai K, Yamane M, and Okada H, Pontine reticular unit responses to pelvic nerve and colonic mechanical stimulation in the dog. Brain Res, 1981 207(1): p. 59–71. [PubMed: 7470906]

207. Fuller DD, Doperalski NJ, Dougherty BJ, Sandhu MS, Bolser DC, and Reier PJ, Modest spontaneous recovery of ventilation following chronic high cervical hemisection in rats. Exp Neurol, 2008 211(1): p. 97–106. [PubMed: 18308305]

208. Fuller DD, Golder FJ, Olson EB Jr., and Mitchell GS, Recovery of phrenic activity and ventilation after cervical spinal hemisection in rats. J Appl Physiol, 2006 100(3): p. 800–6. [PubMed: 16269524]

209. Gandevia SC and Rothwell JC, Activation of the human diaphragm from the motor cortex. J Physiol, 1987 384: p. 109–118. [PubMed: 3656144]

210. Gandilhon N, Adam O, Cazau D, Laitman JT, and Reidenberg JS, Two new theoretical roles of the laryngeal sac of humpback whales. Marine Mammal Science, 2015 21(2): p. 774–781.

211. Gans C, Respiration in early tetrapods - the frog is a red herring. Evolution, 1971 24: p. 740–751.

212. Gans C and Clark B, Studies on ventilation of Caiman crocodilus (Crocodilia: Reptilia). Respir Physiol, 1976 26(3): p. 285–301. [PubMed: 951534]

213. Gans C and Hughes GM, The mechanism of lung ventilation in the tortoise Testudo graeca Linne. J Exp Biol, 1967 47(1): p. 1–20. [PubMed: 6058978]

214. Gaunt AS and Gans C, Mechanics of respiration in the snapping turtle, Chelydraserpentina (Linne). J. Morphol, 1969 128: p. 195–228.

215. Gautam M, DeChiara TM, Glass DJ, Yancopoulos GD, and Sanes JR, Distinct phenotypes of mutant mice lacking agrin, MuSK, or rapsyn. Brain Res Dev Brain Res, 1999 114(2): p. 171–178. [PubMed: 10320756]
216. Gehr P, Bachofen M, and Weibel ER, The normal human lung: ultrastructure and morphometric estimation of diffusion capacity. Respir Physiol, 1978 32(2): p. 121–40. [PubMed: 644146]
217. Gehr P, Mwangi DK, Ammann A, Maloiy GM, Taylor CR, and Weibel ER, Design of the mammalian respiratory system. V. Scaling morphometric pulmonary diffusing capacity to body mass: wild and domestic mammals. Respir Physiol, 1981 44(1): p. 61–86. [PubMed: 7232887]
218. Gehr P, Sehovic S, Burri PH, Claassen H, and Weibel ER, The lung of shrews: morphometric estimation of diffusion capacity. Respir Physiol, 1980 40(1): p. 33–47. [PubMed: 7394364]
219. Geiger PC, Bailey JP, Mantilla CB, Zhan WZ, and Sieck GC, Mechanisms underlying myosin heavy chain expression during development of the rat diaphragm muscle. J Appl Physiol, 2006 101(6): p. 1546–55. [PubMed: 16873604]
220. Geiger PC, Bailey JP, Zhan WZ, Mantilla CB, and Sieck GC, Denervation-induced changes in myosin heavy chain expression in the rat diaphragm muscle. J Appl Physiol, 2003 95(2): p. 611–619. [PubMed: 12704093]
221. Geiger PC, Cody MJ, Han YS, Hunter LW, Zhan WZ, and Sieck GC, Effects of hypothyroidism on maximum specific force in rat diaphragm muscle fibers. J Appl Physiol, 2002 92(4): p. 1506–1514. [PubMed: 11896017]
222. Geiger PC, Cody MJ, Macken RL, Bayrd ME, and Sieck GC, Mechanisms underlying increased force generation by rat diaphragm muscle fibers during development. J Appl Physiol, 2001 90: p. 380–388. [PubMed: 11133931]
223. Geiger PC, Cody MJ, Macken RL, and Sieck GC, Maximum specific force depends on myosin heavy chain content in rat diaphragm muscle fibers. J Appl Physiol, 2000 89(2): p. 695–703. [PubMed: 10926656]
224. Geiger PC, Cody MJ, and Sieck GC, Force-calcium relationship depends on myosin heavy chain and troponin isoforms in rat diaphragm muscle fibers. J Appl Physiol, 1999 87(5): p. 1894–1900. [PubMed: 10562634]
225. Geiser M, Zimmermann B, Baumann M, and Cruz-Orive LM, Does lack of Cftr gene lead to developmental abnormalities in the lung? Exp Lung Res, 2000 26(7): p. 551–64. [PubMed: 11076312]
226. George JC and Shah RV, The Occurance Of A Striated Outer Muscular Sheath In The Lungs Of Lissemys punctata granosa. Shoepff. J. Anim. Morphol. Physiol, 1954 1: p. 13–16.
227. George L, Rehman SU, and Khan FA, Diaphragmatic rupture: A complication of violent cough. Chest, 2000 117(4): p. 1200–1. [PubMed: 10767262]
228. Gill PK and Kuno M, Excitatory and inhibitory actions on phrenic motoneurones. J Physiol, 1963 168: p. 274–289. [PubMed: 14062677]
229. Gillooly JF, Gomez JP, Mavrodiev EV, Rong Y, and McLamore ES, Body mass scaling of passive oxygen diffusion in endotherms and ectotherms. Proc Natl Acad Sci U S A, 2016 113(19): p. 5340–5. [PubMed: 27118837]
230. Gonella J, Bouvier M, and Blanquet F, Extrinsic nervous control of motility of small and large intestines and related sphincters. Physiol Rev, 1987 67(3): p. 902–61. [PubMed: 3299412]
231. Gonzalez-Crussi F and Boston RW, The absorptive function of the neonatal lung. Ultrastructural study of horseradish peroxidase uptake at the onset of ventilation. Lab Invest, 1972 26(1): p. 114–21. [PubMed: 5009211]
232. Gordon DC, Hammond CG, Fisher JT, and Richmond FJ, Muscle-fiber architecture, innervation, and histochemistry in the diaphragm of the cat. J Morphol, 1989 201(2): p. 131–143. [PubMed: 2474663]
233. Gosselin LE, Brice G, Carlson B, Prakash YS, and Sieck GC, Changes in satellite cell mitotic activity during acute period of unilateral diaphragm denervation. J. Appl. Physiol, 1994 77: p. 1128–1134. [PubMed: 7836114]
234. Gosselin LE, Martinez DA, Vailas AC, and Sieck GC, Passive length-force properties of senescent diaphragm: Relationship with collagen characteristics. J Appl Physiol, 1994 76: p. 2680–2685. [PubMed: 7928900]

235. Gosselin LE, Zhan WZ, and Sieck GC, Hypothyroid-mediated changes in adult rat diaphragm muscle contractile properties and MHC isoform expression. J Appl Physiol, 1996 80: p. 1934–1939. [PubMed: 8806897]
236. Gransee HM, Gonzalez Porras MA, Zhan WZ, Sieck GC, and Mantilla CB, Motoneuron glutamatergic receptor expression following recovery from cervical spinal hemisection. J Comp Neurol, 2017 525(5): p. 1192–1205. [PubMed: 27650492]
237. Gransee HM, Mantilla CB, and Sieck GC, Respiratory Muscle Plasticity. Compr Physiol, 2012 2(2): p. 1441–1462. [PubMed: 23798306]
238. Gransee HM, Zhan WZ, Sieck GC, and Mantilla CB, Adeno-associated viral delivery of TrkB receptor enhances functional recovery after cervical spinal hemisection FASEB J, 2012 26: p. LB822.
239. Gransee HM, Zhan WZ, Sieck GC, and Mantilla CB, Targeted Delivery of TrkB Receptor to Phrenic Motoneurons Enhances Functional Recovery of Rhythmic Phrenic Activity after Cervical Spinal Hemisection. PLoS One, 2013 8(5): p. e64755. [PubMed: 23724091]
240. Greer JJ, Control of breathing activity in the fetus and newborn. Compr Physiol, 2012 2(3): p. 1873–88. [PubMed: 23723027]
241. Greer JJ, Allan DW, Martin-Caraballo M, and Lemke RP, An overview of phrenic nerve and diaphragm muscle development in the perinatal rat. J Appl Physiol, 1999 86(3): p. 779–86. [PubMed: 10066685]
242. Greer JJ, Cote D, Allan DW, Zhang W, Babiuk RP, Ly L, Lemke RP, and Bagnall K, Structure of the primordial diaphragm and defects associated with nitrofen-induced CDH. J Appl Physiol, 2000 89(6): p. 2123–9. [PubMed: 11090558]
243. Greer JJ, Funk GD, and Ballanyi K, Preparing for the first breath: prenatal maturation of respiratory neural control. J Physiol, 2006 570(Pt 3): p. 437–44. [PubMed: 16284077]
244. Greer JJ, Smith JC, and Feldman JL, Respiratory and locomotor patterns generated in the fetal rat brain stem-spinal cord in vitro. J Neurophysiol, 1992 67(4): p. 996–9. [PubMed: 1588395]
245. Greising SM, Call JA, Lund TC, Blazar BR, Tolar J, and Lowe DA, Skeletal muscle contractile function and neuromuscular performance in Zmpste24 −/− mice, a murine model of human progeria. Age, 2012 34(4): p. 805–19. [PubMed: 21713376]
246. Greising SM, Mantilla CB, Gorman BA, Ermilov LG, and Sieck GC, Diaphragm muscle sarcopenia in aging mice. Exp Gerontol, 2013: p. [Epub ahead of print].
247. Greising SM, Mantilla CB, Medina-Martinez JS, Stowe JM, and Sieck GC, Functional Impact of Diaphragm Muscle Sarcopenia in both Male and Female Mice. Am J Physiol Lung Cell Mol Physiol, 2015 309(1): p. L46–52. [PubMed: 25934669]
248. Greising SM, Sieck DC, Sieck GC, and Mantilla CB, Novel method for transdiaphragmatic pressure measurements in mice. Respir Physiol Neurobiol, 2013 188(1): p. 56–59. [PubMed: 23632282]
249. Griffiths M, The Biology Of The Monotremes. 1978, New York: Academic Press.
250. Guenette JA, Witt JD, McKenzie DC, Road JD, and Sheel AW, Respiratory mechanics during exercise in endurance-trained men and women. J Physiol, 2007 581(Pt 3): p. 1309–22. [PubMed: 17412775]
251. Gunn HM and Davies AS, Histochemical characteristics of muscle fibres in the diaphragm. Biochem J, 1971 125(4): p. 108P–109P.
252. Guyton AC and Hall JE, eds. Textbook of Medical Physiology. 10th ed. 2000, W.B. Saunders Company.
253. Hackett DA and Chow CM, The Valsalva maneuver: its effect on intra-abdominal pressure and safety issues during resistance exercise. J Strength Cond Res, 2013 27(8): p. 2338–45. [PubMed: 23222073]
254. Haldane JS and Priestley JG, The regulation of the lung-ventilation. J Physiol, 1905 32(3–4): p. 225–66. [PubMed: 16992774]
255. Hamaji M, Burt BM, Ali SO, and Cohen DM, Spontaneous diaphragm rupture associated with vaginal delivery. Gen Thorac Cardiovasc Surg, 2013 61(8): p. 473–5. [PubMed: 22930128]

256. Hamm TM, Nemeth PM, Solanki L, Gordon DA, Reinking RM, and Stuart DG, Association between biochemical and physiological properties in single motor units. Muscle Nerve, 1988 11(3): p. 245–254. [PubMed: 3352659]

257. Hamoudi D, Bouderka MA, Benissa N, and Harti A, Diaphragmatic rupture during labor. Int J Obstet Anesth, 2004 13(4): p. 284–6. [PubMed: 15477063]

258. Hampton IF, Whittow GC, Szekerczes J, and Rutherford S, Heat transfer and body temperature in the Atlantic bottlenose dolphin, Tursiops truncatus. Int J Biometeorol, 1971 15(2): p. 247–53. [PubMed: 5146817]

259. Han YS, Geiger PC, Cody MJ, Macken RL, and Sieck GC, ATP consumption rate per cross bridge depends on myosin heavy chain isoform. J. Appl. Physiol, 2003 94(6): p. 2188–96. [PubMed: 12588786]

260. Han YS, Iyanoye A, Geiger PC, Cody MJ, and Sieck GC, Effects of denervation on mechanical and energetic properties of single fibers in rat diaphragm muscle. Biophysical J, 1999 76(1): p. A34.

261. Han YS, Proctor DN, Geiger PC, and Sieck GC, Reserve capacity of ATP consumption during isometric contraction in human skeletal muscle fibers. J Appl Physiol, 2001 90: p. 657–664. [PubMed: 11160066]

262. Harris AJ and McCaig CD, Motoneuron death and motor unit size during embryonic development of the rat. J Neurosci, 1984 4(1): p. 13–24. [PubMed: 6693936]

263. Hartzler LK, Munns SL, Bennett AF, and Hicks JW, Recovery from activity-induced metabolic acidosis in the American alligator, Alligator mississipiensis. Comp. Biochem. Physiol. A, 2006 143: p. 368–374.

264. Hartzler LK, Munns SL, and Hicks JW, Contribution of the hepatic piston to ventilation in the American alligator. FASEB J, 2004 18: p. A238.4.

265. Hasty P, Bradley A, Morris JH, Edmondson DG, Venuti JM, Olson EN, and Klein WH, Muscle deficiency and neonatal death in mice with a targeted mutation in the myogenin gene. Nature, 1993 364(6437): p. 501–506. [PubMed: 8393145]

266. Hawkes LA, Balachandran S, Batbayar N, Butler PJ, Frappell PB, Milsom WK, Tseveenmyadag N, Newman SH, Scott GR, Sathiyaselvam P, Takekawa JY, Wikelski M, and Bishop CM, The trans-Himalayan flights of bar-headed geese (Anser indicus). Proc Natl Acad Sci U S A, 2011 108(23): p. 9516–9. [PubMed: 21628594]

267. Hellyer NJ, Mantilla CB, Park EW, Zhan WZ, and Sieck GC, Neuregulin-dependent protein synthesis in C2C12 myotubes and rat diaphragm muscle. Am J Physiol Cell Physiol, 2006 291(5): p. C1056–61. [PubMed: 16790500]

268. Hemborg B, Moritz U, and Lowing H, Intra-abdominal pressure and trunk muscle activity during lifting. IV. The causal factors of the intra-abdominal pressure rise. Scand J Rehabil Med, 1985 17(1): p. 25–38. [PubMed: 3159082]

269. Herzog W and Ait-Haddou R, Considerations on muscle contraction. J Electromyogr Kinesiol, 2002 12(6): p. 425–33. [PubMed: 12435539]

270. Hicks JW and Farmer CG, Lung Ventilation and gas exchange in theropod dinosaurs. Science, 1998 281: p. 45–46. [PubMed: 9679017]

271. Higuchi T, Uchide K, Honda K, and Negoro H, Pelvic neurectomy abolishes the fetus-expulsion reflex and induces dystocia in the rat. Exp Neurol, 1987 96(2): p. 443–55. [PubMed: 3569466]

272. Hilaire G, Viemari JC, Coulon P, Simonneau M, and Bevengut M, Modulation of the respiratory rhythm generator by the pontine noradrenergic A5 and A6 groups in rodents. Respir Physiol Neurobiol, 2004 143(2–3): p. 187–97. [PubMed: 15519555]

273. Hilaire G, Voituron N, Menuet C, Ichiyama RM, Subramanian HH, and Dutschmann M, The role of serotonin in respiratory function and dysfunction. Respir Physiol Neurobiol, 2010 174(1–2): p. 76–88. [PubMed: 20801236]

274. Hill JR, The oxygen consumption of new-born and adult mammals. Its dependence on the oxygen tension in the inspired air and on the environmental temperature. J Physiol, 1959 149: p. 346–73. [PubMed: 13852377]

275. Hill R and Heller MB, Diaphragmatic rupture complicating labor. Ann Emerg Med, 1996 27(4): p. 522–4. [PubMed: 8604875]

276. Hindell MA, Slip DJ, Burton HR, and Bryden MM, Physiological implications of continuous, prolonged, and deep dives of the southern elephant seal (Mirounga leonina). Can J Zool, 1992 70: p. 370–379.

277. Hinds DS and Calder WA, Tracheal Dead Space in the Respiration of Birds. Evolution, 1971 25(2): p. 429–440. [PubMed: 28563117]

278. Hodge K, Powers SK, Coombes J, Fletcher L, Demirel HA, Dodd SL, and Martin D, Bioenergetic characteristics of the costal and crural diaphragm in mammals. Respir Physiol, 1997 109(2): p. 149–54. [PubMed: 9299646]

279. Hodges PW, Butler JE, McKenzie DK, and Gandevia SC, Contraction of the human diaphragm during rapid postural adjustments. J Physiol, 1997 505 (Pt 2): p. 539–48. [PubMed: 9423192]

280. Hodges PW and Gandevia SC, Activation of the human diaphragm during a repetitive postural task. J Physiol, 2000 522 Pt 1: p. 165–75. [PubMed: 10618161]

281. Hodges PW and Gandevia SC, Changes in intra-abdominal pressure during postural and respiratory activation of the human diaphragm. J Appl Physiol (1985), 2000 89(3): p. 967–76. [PubMed: 10956340]

282. Hodges PW, Moseley GL, Gabrielsson A, and Gandevia SC, Experimental muscle pain changes feedforward postural responses of the trunk muscles. Exp Brain Res, 2003 151(2): p. 262–71. [PubMed: 12783146]

283. Hodges PW, Sapsford R, and Pengel LH, Postural and respiratory functions of the pelvic floor muscles. Neurourol Urodyn, 2007 26(3): p. 362–71. [PubMed: 17304528]

284. Holstege G, Anatomical evidence for an ipsilateral rubrospinal pathway and for direct rubrospinal projections to motoneurons in the cat. Neurosci Lett, 1987 74(3): p. 269–74. [PubMed: 3561881]

285. Holstege G, Some anatomical observations on the projections from the hypothalamus to brainstem and spinal cord: an HRP and autoradiographic tracing study in the cat. J Comp Neurol, 1987 260(1): p. 98–126. [PubMed: 3496365]

286. Holstege G, The periaqueductal gray controls brainstem emotional motor systems including respiration. Prog Brain Res, 2014 209: p. 379–405. [PubMed: 24746059]

287. Holstege G, How the Emotional Motor System Controls the Pelvic Organs. Sex Med Rev, 2016 4(4): p. 303–328. [PubMed: 27872027]

288. Holstege G, Beers CM, and Subramanian HH, Preface. Breathing, emotion and evolution. Prog Brain Res, 2014 212: p. xi–xii. [PubMed: 25194207]

289. Holstege G and Kuypers HG, The anatomy of brain stem pathways to the spinal cord in cat. A labeled amino acid tracing study. Prog Brain Res, 1982 57: p. 145–75. [PubMed: 7156396]

290. Holstege G and Tan J, Supraspinal control of motoneurons innervating the striated muscles of the pelvic floor including urethral and anal sphincters in the cat. Brain, 1987 110 (Pt 5): p. 1323–44. [PubMed: 3676703]

291. Holstege G, van Neerven J, and Evertse F, Spinal cord location of the motoneurons innervating the abdominal, cutaneous maximus, latissimus dorsi and longissimus dorsi muscles in the cat. Exp Brain Res, 1987 67(1): p. 179–94. [PubMed: 2957225]

292. Hooper SB, Dickson KA, and Harding R, Lung liquid secretion, flow and volume in response to moderate asphyxia in fetal sheep. J Dev Physiol, 1988 10(5): p. 473–85. [PubMed: 3221062]

293. Hooper SB and Harding R, Effect of beta-adrenergic blockade on lung liquid secretion during fetal asphyxia. Am J Physiol, 1989 257(4 Pt 2): p. R705–10. [PubMed: 2508494]

294. Hooper SB and Harding R, Changes in lung liquid dynamics induced by prolonged fetal hypoxemia. J Appl Physiol (1985), 1990 69(1): p. 127–35. [PubMed: 2394642]

295. Hooper SB and Harding R, Fetal lung liquid: a major determinant of the growth and functional development of the fetal lung. Clin Exp Pharmacol Physiol, 1995 22(4): p. 235–47. [PubMed: 7671435]

296. Hoppeler H and Lindstedt SL, Malleability of skeletal muscle in overcoming limitations: Structural elements. J Exp Biol, 1985 115: p. 355–364. [PubMed: 4031775]

297. Hoppeler H, Mathieu O, Krauer R, Claassen H, Armstrong RB, and Weibel ER, Design of the mammalian respiratory system. VI. Distribution of mitochondria and capillaries in various muscles. Respir Physiol, 1981 44: p. 87–111. [PubMed: 7232888]

298. Hoppeler H, Mathieu O, Weibel ER, Krauer R, Lindstedt SL, and Taylor CR, Design of the mammalian respiratory system. VIII. capillaries in skeletal muscles*. Respir Physiol, 1981 44: p. 129–150. [PubMed: 7232883]

299. Hoppeler H and Weibel ER, Limits for oxygen and substrate transport in mammals. J Exp Biol, 1998 201(Pt 8): p. 1051–64. [PubMed: 9510519]

300. Horn CC, Why is the neurobiology of nausea and vomiting so important? Appetite, 2008 50(2–3): p. 430–4. [PubMed: 17996982]

301. Hornby PJ, Central neurocircuitry associated with emesis. Am J Med, 2001 111 Suppl 8A: p. 106S–112S. [PubMed: 11749934]

302. Hubmayr RD, Sprung J, and Nelson S, Determinants of transdiaphragmatic pressure in dogs. J Appl Physiol, 1990 69(6): p. 2050–2056. [PubMed: 2076999]

303. Hudson AL, Gandevia SC, and Butler JE, Control of human inspiratory motoneurones during voluntary and involuntary contractions. Respiratory physiology & neurobiology, 2011 179(1): p. 23–33. [PubMed: 21718808]

304. Hughes RL and Hall LS, Structural adaptations of the newborn marsupial, in The developing marsupial: Models for biomedical research, Tyndale-Biscoe CH and Jannsens PA, Editors. 1988, Springer: Berlin p. 9–27.

305. Hughes RL, Hall LS, Tyndale-Biscoe CH, and Hinds LA, Evolutionary implications of macropod organogenesis, in Kangaroos, Wallabies and Rat-Kangaroos, Grigg GC, Jarman P, and L. H, Editors. 1989, Surry Beatty and Sons: Chipping norton.

306. Hughes SM, Koishi K, Rudnicki M, and Maggs AM, MyoD protein is differentially accumulated in fast and slow skeletal muscle fibres and required for normal fibre type balance in rodents. Mech Dev, 1997 61(1–2): p. 151–63. [PubMed: 9076685]

307. Hull D, Oxygen Consumption and Body Temperature of New-Born Rabbits and Kittens Exposed to Cold. J Physiol, 1965 177: p. 192–202. [PubMed: 14301020]

308. Hull D, Lung expansion and ventilation during resuscitation of asphyxiated newborn infants. J Pediatr, 1969 75(1): p. 47–58. [PubMed: 4892794]

309. Humphreys PW and Strang LB, Effects of gestation and prenatal asphyxia on pulmonary surface properties of the foetal rabbit. J Physiol, 1967 192(1): p. 53–62. [PubMed: 6051807]

310. Husain AN and Hessel RG, Neonatal pulmonary hypoplasia: an autopsy study of 25 cases. Pediatr Pathol, 1993 13(4): p. 475–84. [PubMed: 8372032]

311. Hussain SN, Rabinovitch B, Macklem PT, and Pardy RL, Effects of separate rib cage and abdominal restriction on exercise performance in normal humans. J Appl Physiol (1985), 1985 58(6): p. 2020–6. [PubMed: 3159716]

312. Hutchison AA, McNicol KJ, and Loughlin GM, The effect of age on pulmonary epithelial permeability in unanesthetized lambs. Pediatr Pulmonol, 1985 1(1): p. 52–7. [PubMed: 3932948]

313. Huxley AF, Muscle structure and theories of contraction. Prog. Biophysics Biophys. Chem, 1957 7: p. 255–318.

314. Huynh HK, Willemsen AT, Lovick TA, and Holstege G, Pontine control of ejaculation and female orgasm. J Sex Med, 2013 10(12): p. 3038–48. [PubMed: 23981195]

315. Iqbal A, Haider M, Stadlhuber RJ, Karu A, Corkill S, and Filipi CJ, A study of intragastric and intravesicular pressure changes during rest, coughing, weight lifting, retching, and vomiting. Surg Endosc, 2008 22(12): p. 2571–5. [PubMed: 18810545]

316. Irving L, Scholander P, and Grinnell S, The respiration of the porpoise, Tursiops truncatus. J. Cell. Comp. Physiol, 1941 17: p. 145–168.

317. Iscoe S, Control of abdominal muscles. Prog Neurobiol, 1998 56(4): p. 433–506. [PubMed: 9775401]

318. Iscoe S, Dankoff J, Migicovsky R, and Polosa C, Recruitment and discharge frequency of phrenic motoneurones during inspiration. Respir Physiol, 1976 26(1): p. 113–128. [PubMed: 179122]

319. Ito H, Nishibayashi M, Kawabata K, Maeda S, Seki M, and Ebukuro S, Induction of Fos protein in neurons in the medulla oblongata after motion- and X-irradiation-induced emesis in musk shrews (Suncus murinus). Auton Neurosci, 2003 107(1): p. 1–8. [PubMed: 12927221]

320. Jakubowska AE, Billings K, Johns DP, Hooper SB, and Harding R, Respiratory function in lambs after prolonged oligohydramnios during late gestation. Pediatr Res, 1993 34(5): p. 611–7. [PubMed: 8284098]

321. Jammes Y, Arbogast S, and De Troyer A, Response of the rabbit diaphragm to tendon vibration. Neuroscience letters, 2000 290(2): p. 85–8. [PubMed: 10936683]

322. Janczewski WA and Feldman JL, Distinct rhythm generators for inspiration and expiration in the juvenile rat. J Physiol, 2006 570(Pt 2): p. 407–20. [PubMed: 16293645]

323. Jansen JKS and Fladby T, The perinatal organization of the innervation of skeletal muscle in mammals. Prog Neurobiol, 1990 34: p. 39–90. [PubMed: 2406795]

324. Jiang C and Lipski J, Extensive monosynaptic inhibition of ventral respiratory group neurons by augmenting neurons in the Botzinger complex in the cat. Exp Brain Res, 1990 81(3): p. 639–48. [PubMed: 2226695]

325. Jo SA, Zhu X, Marchionni MA, and Burden SJ, Neuregulins are concentrated at nerve-muscle synapses and activate ACh-receptor gene expression. Nature, 1995 373(6510): p. 158–61. [PubMed: 7816098]

326. Jodkowski JS, Viana F, Dick TE, and Berger AJ, Electrical properties of phrenic motoneurons in the cat: correlation with inspiratory drive. J Neurophysiol, 1987 58(1): p. 105–124. [PubMed: 3039077]

327. Johansen K and Burggren WW, Venous Return And Cardiac Filling In Varanid Lizards. J Exp Biol, 1984 113: p. 389–399.

328. Johnson BD, Saupe KW, and Dempsey JA, Mechanical constraints on exercise hyperpnea in endurance athletes. J Appl Physiol (1985), 1992 73(3): p. 874–86. [PubMed: 1400051]

329. Johnson BD and Sieck GC, Activation-induced reduction of SDH activity in diaphragm muscle fibers. J Appl Physiol, 1993 75: p. 2689–2695. [PubMed: 8125891]

330. Johnson BD and Sieck GC, Differential susceptibility of diaphragm muscle fibers to neuromuscular transmission failure. J Appl Physiol, 1993 75(1): p. 341–348. [PubMed: 8397179]

331. Johnson BD, Wilson LE, Zhan WZ, Watchko JF, Daood MJ, and Sieck GC, Contractile properties of the developing diaphragm correlate with myosin heavy chain phenotype. J Appl Physiol, 1994 77: p. 481–487. [PubMed: 7961272]

332. Jones FW, The Functional History of the Coelom and the Diaphragm. J Anat Physiol, 1913 47(Pt 3): p. 282–318. [PubMed: 17232958]

333. Jurgens KD, Etruscan shrew muscle: the consequences of being small. J Exp Biol, 2002 205(Pt 15): p. 2161–6. [PubMed: 12110649]

334. Jurgens KD, Bartels H, and Bartels R, Blood oxygen transport and organ weights of small bats and small non-flying mammals. Respir Physiol, 1981 45(3): p. 243–60. [PubMed: 7330485]

335. Kallay N, Crim L, Dunagan DP, Kavanagh PV, Meredith W, and Haponik EF, Massive left diaphragmatic separation and rupture due to coughing during an asthma exacerbation. South Med J, 2000 93(7): p. 729–31. [PubMed: 10923968]

336. Kanda K and Hashizume K, Factors causing difference in force output among motor units in the rat medial gastrocnemius muscle. J Physiol Lond, 1992 448: p. 677–695. [PubMed: 1593483]

337. Kanjhan R, Fogarty MJ, Noakes PG, and Bellingham MC, Developmental changes in the morphology of mouse hypoglossal motor neurons. Brain Struct Funct, 2016 221(7): p. 3755–86. [PubMed: 26476929]

338. Karlberg P, Adams FH, Geubelle F, and Wallgren G, Alteration of the infant's thorax during vaginal delivery. Acta Obstet Gynecol Scand, 1962 41: p. 223–9. [PubMed: 13962508]

339. Karlberg P, Cherry RB, Escardo FE, and Koch G, Respiratory Studies in Newborn Infants. II. Pulmonary Ventilation and the Mechanics od Breathing in the first Minutes of Life, Including the Onset of Respiration. Acta Paediatr, 1962 51: p. 121–136.

340. Karlberg P and Koch G, Respiratory studies in newborn infants. III. Development of mechanics of breathing during the first week of life. A longitudinal study. Acta Paediatr Suppl, 1962 135: p. 121–9. [PubMed: 14453970]

341. Katona PG, Frasz A, and Egbert J, Maturation of cardiac control in full-term and preterm infants during sleep. Early Hum Dev, 1980 4(2): p. 145–59. [PubMed: 7408745]

342. Katz B and Thesleff S, On the factors which determine the amplitude of the ‘miniature end-plate potential’. J Physiol, 1957 137(2): p. 267–278. [PubMed: 13449877]

343. Keith A, The Nature of the Mammalian Diaphragm and Pleural Cavities. J Anat Physiol, 1905 39(Pt 3): p. 243–84. [PubMed: 17232638]

344. Kelley MJ, Jawien W, Ortel TL, and Korczak JF, Mutation of MYH9, encoding non-muscle myosin heavy chain A, in May-Hegglin anomaly. Nat Genet, 2000 26(1): p. 106–8. [PubMed: 10973260]

345. Kernell D, The motoneurone and its muscle fibres. 2006, New York: Oxford University Press Inc.

346. Keswani NH and Hollinshead WH, The phrenic nucleus. III. Organization of the phrenic nucleus in the spinal cord of the cat and man. Proc Staff Meet Mayo Clin, 1955 30: p. 566–577. [PubMed: 13273519]

347. Khurram OU, Fogarty MJ, Sarrafian TL, Bhatt A, Mantilla CB, and Sieck GC, Impact of aging on diaphragm muscle function in male and female Fischer 344 rats. Physiol Rep, 2018 6(13): p. e13786. [PubMed: 29981218]

348. Kilarski W and Sjostrom M, Systematic distribution of muscle fibre types in the rat and rabbit diaphragm: a morphometric and ultrastructural analysis. J Anat, 1990 168: p. 13–30. [PubMed: 2139020]

349. Kim MJ, Druz WS, Danon J, Machnach W, and Sharp T, Mechanics of the canine diaphragm. J Appl Physiol, 1976 41: p. 369–382. [PubMed: 965306]

350. Kimura K, Takahashi Y, Iwamoto S, and Konishi M, Morphology of diaphragm in the crab-eating monkey (Macaca fascicularis). Primates, 1992 33(3): p. 359–370.

351. Kingsley JS, Comparative Anatomy of Vertebrates. 1912, York, PA: P Blakiston’s Son & Co.

352. Klaus M, Tooley WH, Weaver KH, and Clements JA, Lung volume in the newborn infant. Pediatrics, 1962 30: p. 111–6. [PubMed: 14456668]

353. Kleiber M, Body size and metabolism. Hilgardia, 1932 6: p. 315–351.

354. Kleiber M, Body size and metabolic rate. Physiol Rev, 1947 27(4): p. 511–41. [PubMed: 20267758]

355. Klein W, Abe AS, Andrade DV, and Perry SF, Structure of the posthepatic septum and its influence on visceral topology in the tegu lizard, Tupinambis merianae (Teiidae: Reptilia). J Morphol, 2003 258(2): p. 151–7. [PubMed: 14518009]

356. Klein W, Abe AS, and Perry SF, Static lung compliance and body pressures in Tupinambis merianae with and without post-hepatic septum. Respir Physiol Neurobiol, 2003 135(1): p. 73–86. [PubMed: 12706067]

357. Klein W, Andrade DV, Abe AS, and Perry SF, Role of the post-hepatic septum on breathing during locomotion in Tupinambis merianae (Reptilia: Teiidae). J Exp Biol, 2003 206(Pt 13): p. 2135–43. [PubMed: 12771163]

358. Klein W and Codd JR, Breathing and locomotion: comparative anatomy, morphology and function. Respir Physiol Neurobiol, 2010 173 Suppl: p. S26–32. [PubMed: 20417316]

359. Klein W and Owerkowicz T, Function of intracoelomic septa in lung ventilation of amniotes: lessons from lizards. Physiol Biochem Zool, 2006 79(6): p. 1019–32. [PubMed: 17041868]

360. Knox WF and Barson AJ, Pulmonary hypoplasia in a regional perinatal unit. Early Hum Dev, 1986 14(1): p. 33–42. [PubMed: 3732117]

361. Knudsen KA, Cell adhesion molecules in myogenesis. Curr Opin Cell Biol, 1990 2(5): p. 902–6. [PubMed: 2083089]

362. Kobayashi K, Lemke RP, and Greer JJ, Ultrasound measurements of fetal breathing movements in the rat. J Appl Physiol, 2001 91(1): p. 316–20. [PubMed: 11408446]

363. Koga T and Fukuda H, Neurons in the nucleus of the solitary tract mediating inputs from emetic vagal afferents and the area postrema to the pattern generator for the emetic act in dogs. Neurosci Res, 1992 14(3): p. 166–79. [PubMed: 1331921]

364. Koga T and Fukuda H, Bulbospinal augmenting inspiratory neurons may participate in contractions of the diaphragm during vomiting in decerebrate dogs. Neurosci Lett, 1994 180(2): p. 257–60. [PubMed: 7700590]

365. Koizumi H, Koshiya N, Chia JX, Cao F, Nugent J, Zhang R, and Smith JC, Structural-functional properties of identified excitatory and inhibitory interneurons within pre-Botzinger complex respiratory microcircuits. J Neurosci, 2013 33(7): p. 2994–3009. [PubMed: 23407957]

366. Komarek V and Lazar P, Body cavities in fishes. Folia Morphol (Praha), 1990 38(1): p. 55–62. [PubMed: 2341081]

367. Kong FJ and Berger AJ, Firing properties and hypercapnic responses of single phrenic motor axons in the rat. J. Appl. Physiol, 1986 61(6): p. 1999–2004. [PubMed: 3027021]

368. Kooyman G and Cornell L, Flow properties of expiration and inspiration in a trained bottle-nosed porpoise. Physiol. Zool, 1981 54(54): p. 55–61.

369. Kooyman GL, Wahrenbrock EA, Castellini MA, Davis RW, and Sinnett EE, Aerobic and anaerobic metabolism during voluntary diving in Weddell seals: evidence of preferred pathways from blood chemistry and behavior. J. Comp. Physiol, 1980 138B: p. 335–346.

370. Kotas RV and Avery ME, Accelerated appearance of pulmonary surfactant in the fetal rabbit. J Appl Physiol, 1971 30(3): p. 358–61. [PubMed: 5544115]

371. Krauss RS, Cole F, Gaio U, Takaesu G, Zhang W, and Kang JS, Close encounters: regulation of vertebrate skeletal myogenesis by cell-cell contact. J Cell Sci, 2005 118(Pt 11): p. 2355–62. [PubMed: 15923648]

372. Krnjevic K and Miledi R, Failure of neuromuscular propagation in rats. J Physiol, 1958 140: p. 440–461. [PubMed: 13514717]

373. Krnjevic K and Miledi R, Motor units in the rat diaphragm. J Physiol, 1958 140: p. 427–439. [PubMed: 13514716]

374. Krnjevic K and Miledi R, Presynaptic failure of neuromuscular propagation in rats. J Physiol (Lond), 1959 149: p. 1–22. [PubMed: 14412088]

375. Lachmann B, Grossmann G, Nilsson R, and Robertson B, Lung mechanics during spontaneous ventilation in premature and fullterm rabbit neonates. Respir Physiol, 1979 38(3): p. 283–302. [PubMed: 523846]

376. LaFramboise WA, Daood MJ, Guthrie RD, Butler-Browne GS, Whalen RG, and Ontell M, Myosin isoforms in neonatal rat extensor digitorum longus, diaphragm, and soleus muscles. Am J Physiol, 1990 259(2 Pt 1): p. L116–L122. [PubMed: 2382729]

377. LaFramboise WA, Daood MJ, Guthrie RD, Schiaffino S, Moretti P, Brozanski B, Ontell MP, Butler-Browne GS, Whalen RG, and Ontell M, Emergence of the mature myosin phenotype in the rat diaphragm muscle. Dev Biol, 1991 144: p. 1–15. [PubMed: 1995390]

378. Lahiri S and DeLaney RG, Relationship between carotid chemoreceptor activity and ventilation in the cat. Respir Physiol, 1975 24(3): p. 267–86. [PubMed: 242050]

379. Lahiri S and DeLaney RG, Stimulus interaction in the responses of carotid body chemoreceptor single afferent fibers. Respir Physiol, 1975 24(3): p. 249–66. [PubMed: 242049]

380. Lalley PM, Bischoff AM, and Richter DW, 5-HT-1A receptor-mediated modulation of medullary expiratory neurones in the cat. J Physiol, 1994 476(1): p. 117–30. [PubMed: 8046627]

381. Lalley PM, Bischoff AM, Schwarzacher SW, and Richter DW, 5-HT2 receptor-controlled modulation of medullary respiratory neurones in the cat. J Physiol, 1995 487(Pt 3): p. 653–61. [PubMed: 8544128]

382. Lance-Jones C, Motoneuron cell death in the developing lumbar spinal cord of the mouse. Dev Brain Res, 1982 4: p. 473–479.

383. Lane MA, Lee KZ, Fuller DD, and Reier PJ, Spinal circuitry and respiratory recovery following spinal cord injury. Respir Physiol Neurobiol, 2009 169(2): p. 123–32. [PubMed: 19698805]

384. Laporta D and Grassino A, Assessment of transdiaphragmatic pressure in humans. J Appl Physiol, 1985 58(5): p. 1469–1476. [PubMed: 3158636]

385. Larsen WJ, Human Embryology. Second ed 1997, Hong Kong: Churchill Livingstone Inc.

386. Laskowski MB, Norton AS, and Berger PK, Branching patterns of the rat phrenic nerve during development and reinnervation. Exp Neurol, 1991 113(2): p. 212–220. [PubMed: 1868904]

387. Laskowski MB and Sanes JR, Topographic mapping of motor pools onto skeletal muscles. J Neurosci, 1987 7(1): p. 252–260. [PubMed: 3543250]

388. Last RJ, Last's anatomy: regional and applied. Ninth ed 1994, Edinburgh: Churchill Livingstone Inc.

389. Le Double AF, Diaphragme, in Traité des Variations du Système Musculaire de l'homme et leur Signification au Point de Vue de l'Anthropologie Zoologique. 1897, Schleicher Frères: Paris p. 297–309.

390. Leduc D, Cappello M, Gevenois PA, and De Troyer A, Mechanics of the canine diaphragm in ascites: a CT study. J Appl Physiol (1985), 2008 104(2): p. 423–8. [PubMed: 18079259]

391. Lee HY, Yoo SM, Song IS, Yu H, Kim YS, Lee JB, and Shon DS, Spontaneous diaphragmatic rupture after vomiting: rapid diagnosis on multiplanar reformatted multidetector CT. J Thorac Imaging, 2006 21(1): p. 54–6. [PubMed: 16538159]

392. Leith DE, Comparative mammalian respiratory mechanics. Physiologist, 1976 19(4): p. 485–510. [PubMed: 996118]

393. Leith DE, Comparative mammalian respiratory mechanics. Am Rev Respir Dis, 1983 128(2 Pt 2): p. S77–82. [PubMed: 6881717]

394. Lemercier C, To RQ, Carrasco RA, and Konieczny SF, The basic helix-loop-helix transcription factor Mist1 functions as a transcriptional repressor of myoD. EMBO J, 1998 17(5): p. 1412–1422. [PubMed: 9482738]

395. Lewis MI and Sieck GC, Effect of acute nutritional deprivation on diaphragm structure and function. J Appl Physiol, 1990 68: p. 1938–1944. [PubMed: 2163377]

396. Li P, Janczewski WA, Yackle K, Kam K, Pagliardini S, Krasnow MA, and Feldman JL, The peptidergic control circuit for sighing. Nature, 2016 530(7590): p. 293–7. [PubMed: 26855425]

397. Liddell EGT and Sherrington CS, Recruitment and some other factors of reflex inhibition. Proc Roy Soc Lond (Biol), 1925 97: p. 488–518.

398. Lieber RL, Skeletal muscle structure, function, & plasticity: the physiological basis of rehabilitation. 2 ed 2002, Baltimore, MD: Lippincott Williams & Wilkins.

399. Liem KF, Form and Function of Lungs: the Evolution of Air Breathing Mechanisms. Am. Zool, 1988 28: p. 739–759.

400. Lillie MA, Vogl AW, Raverty S, Haulena M, McLellan WA, Stenson GB, and Shadwick RE, Controlling thoracic pressures in cetaceans during a breath-hold dive: importance of the diaphragm. J Exp Biol, 2017 220(Pt 19): p. 3464–3477. [PubMed: 28978638]

401. Lindsay AD and Feldman JL, Modulation of respiratory activity of neonatal rat phrenic motoneurones by serotonin. J Physiol, 1993 461: p. 213–33. [PubMed: 8350262]

402. Lindstedt SL, Hokanson JF, Wells DJ, Swain SD, Hoppeler H, and Navarro V, Running energetics in the pronghorn antelope. Nature, 1991 353(6346): p. 748–50. [PubMed: 1944533]

403. Lipski J, Zhang X, Kruszewska B, and Kanjhan R, Morphological study of long axonal projections of ventral medullary inspiratory neurons in the rat. Brain Res, 1994 640(1–2): p. 171–84. [PubMed: 8004446]

404. Lois JH, Rice CD, and Yates BJ, Neural circuits controlling diaphragm function in the cat revealed by transneuronal tracing. J Appl Physiol (1985), 2009 106(1): p. 138–52. [PubMed: 18974365]

405. Lowey S and Cohen C, Studies on the structure of myosin. J Mol Biol, 1962 4: p. 293–308. [PubMed: 14466961]

406. Ludbrook J, The musculovenous pumps of the human lower limb. Am Heart J, 1966 71(5): p. 635–41. [PubMed: 5935855]

407. Macefeild G and Gandevia SC, The cortical drive to human respiratory muscles in the awake state assessed by premotor cerebral potentials. J Physiol, 1991: p. 1–14.

408. MacFarlane PM and Frappell PB, Convection requirement is established by total metabolic rate in the newborn tammar wallaby. Respir Physiol, 2001 126(3): p. 221–31. [PubMed: 11403784]

409. Maggi CA, Giuliani S, Santicioli P, Patacchini R, and Meli A, Neural pathways and pharmacological modulation of defecation reflex in rats. Gen Pharmacol, 1988 19(4): p. 517–23. [PubMed: 2457537]

410. Mahdavi V, Chambers AP, and Nadal-Ginard B, Cardiac alpha- and beta-myosin heavy chain genes are organized in tandem. Proc Natl Acad Sci USA, 1984 81(9): p. 2626–2630. [PubMed: 6585819]

411. Maina JN, The morphology and morphometry of the adult normal baboon lung (Papio anubis). J Anat, 1987 150: p. 229–45. [PubMed: 3654336]

412. Maina JN, Comparative respiratory morphology: themes and principles in the design and construction of the gas exchangers. Anat Rec, 2000 261(1): p. 25–44. [PubMed: 10700733]

413. Maina JN, What it takes to fly: the structural and functional respiratory refinements in birds and bats. J Exp Biol, 2000 203(Pt 20): p. 3045–64. [PubMed: 11003817]

414. Maina JN, Fundamental structural aspects and features in the bioengineering of the gas exchangers: comparative perspectives. Adv Anat Embryol Cell Biol, 2002 163: p. III–XII, 1–108. [PubMed: 11892241]

415. Maina JN, Structure, function and evolution of the gas exchangers: comparative perspectives. J Anat, 2002 201(4): p. 281–304. [PubMed: 12430953]

416. Mantilla CB, Dow DE, and Sieck GC, Skeletal muscle changes in hypothyroidism, in Comprehensive Handbook of Iodine, Preedy VR, Burrow GN, and Watson RR, Editors. 2009, Academic Press: Oxford p. 1087–1101.

417. Mantilla CB, Fahim MA, Brandenburg JE, and Sieck GC, Functional Development of Respiratory Muscles, in Fetal and Neonatal Physiology, Polin R, et al., Editors. 2016, Elselvier: Philadelphia.

418. Mantilla CB, Gransee HM, Zhan WZ, and Sieck GC, Impact of glutamatergic and serotonergic neurotransmission on diaphragm muscle activity after cervical spinal hemisection. J Neurophysiol, 2017 118(3): p. 1732–1738. [PubMed: 28659464]

419. Mantilla CB, Greising SM, Stowe JM, Zhan WZ, and Sieck GC, TrkB Kinase Activity is Critical for Recovery of Respiratory Function after Cervical Spinal Cord Hemisection. Exp Neurol, 2014 261: p. 190–5. [PubMed: 24910201]

420. Mantilla CB, Greising SM, Zhan WZ, Seven YB, and Sieck GC, Prolonged C2 spinal hemisection-induced inactivity reduces diaphragm muscle specific force with modest, selective atrophy of type IIx and/or IIb fibers. J Appl Physiol, 2013 114(3): p. 380–386. [PubMed: 23195635]

421. Mantilla CB, Rowley KL, Fahim MA, Zhan WZ, and Sieck GC, Synaptic vesicle cycling at type-identified diaphragm neuromuscular junctions. Muscle Nerve, 2004 30(6): p. 774–83. [PubMed: 15478121]

422. Mantilla CB, Seven YB, and Sieck GC, Convergence of pattern generator outputs on a common mechanism of diaphragm motor unit recruitment. Prog Brain Res, 2014 209: p. 309–29. [PubMed: 24746055]

423. Mantilla CB, Seven YB, Zhan WZ, and Sieck GC, Diaphragm motor unit recruitment in rats. Respir Physiol Neurobiol, 2010 173(1): p. 101–6. [PubMed: 20620243]

424. Mantilla CB and Sieck GC, Invited Review: Mechanisms underlying motor unit plasticity in the respiratory system. J Appl Physiol, 2003 94(3): p. 1230–41. [PubMed: 12571144]

425. Mantilla CB and Sieck GC, Key aspects of phrenic motoneuron and diaphragm muscle development during the perinatal period. J Appl Physiol, 2008 104(6): p. 1818–27. [PubMed: 18403452]

426. Mantilla CB and Sieck GC, Trophic factor expression in phrenic motor neurons. Respir Physiol Neurobiol, 2008 164(1–2): p. 252–262. [PubMed: 18708170]

427. Mantilla CB and Sieck GC, Neuromuscular adaptations to respiratory muscle inactivity. Respir Physiol Neurobiol, 2009 169(2): p. 133–40. [PubMed: 19744580]

428. Mantilla CB and Sieck GC, Phrenic motor unit recruitment during ventilatory and non-ventilatory behaviors. Respir Physiol Neurobiol, 2011 179(1): p. 57–63. [PubMed: 21763470]

429. Mantilla CB and Sieck GC, The Diaphragm Muscle Does Not Atrophy as a Result of Inactivity. J Physiol, 2013.

430. Mantilla CB, Sill RV, Aravamudan B, Zhan WZ, and Sieck GC, Developmental effects on myonuclear domain size of rat diaphragm fibers. J Appl Physiol, 2008 104(3): p. 787–94. [PubMed: 18187618]

431. Mantilla CB, Zhan WZ, and Sieck GC, Retrograde labeling of phrenic motoneurons by intrapleural injection. J Neurosci Methods, 2009 182(2): p. 244–9. [PubMed: 19559048]
432. Martin-Caraballo M, Campagnaro PA, Gao Y, and Greer JJ, Contractile and fatigue properties of the rat diaphragm musculature during the perinatal period. J Appl Physiol, 2000 88(2): p. 573–80. [PubMed: 10658025]
433. Mathieu O, Krauer R, Hoppeler H, Gehr P, Lindstedt SL, Alexander RM, Taylor CR, and Weibel ER, Design of the mammalian respiratory system. VII. Scaling mitochondrial volume in skeletal muscle to body mass. Respir Physiol, 1981 44: p. 113–128. [PubMed: 7232882]
434. Matsevych OY, Blunt diaphragmatic rupture: four year's experience. Hernia, 2008 12(1): p. 73–8. [PubMed: 17891332]
435. McClaran SR, Wetter TJ, Pegelow DF, and Dempsey JA, Role of expiratory flow limitation in determining lung volumes and ventilation during exercise. J Appl Physiol (1985), 1999 86(4): p. 1357–66. [PubMed: 10194223]
436. McClellan AD, Higher order neurons in buccal ganglia of Pleurobranchaea elicit vomiting motor activity. J Neurophysiol, 1983 50(3): p. 658–70. [PubMed: 6619912]
437. McDermott WJ, Van Emmerik RE, and Hamill J, Running training and adaptive strategies of locomotor-respiratory coordination. Eur J Appl Physiol, 2003 89(5): p. 435–44. [PubMed: 12712351]
438. McKay LC, Janczewski WA, and Feldman JL, Sleep-disordered breathing after targeted ablation of preBotzinger complex neurons. Nat Neurosci, 2005 8(9): p. 1142–4. [PubMed: 16116455]
439. McLachlan AD and Karn J, Periodic charge distributions in the myosin rod amino acid sequence match cross-bridge spacings in muscle. Nature, 1982 299(5880): p. 226–31. [PubMed: 7202124]
440. McLachlan AD and Karn J, Periodic features in the amino acid sequence of nematode myosin rod. J Mol Biol, 1983 164(4): p. 605–26. [PubMed: 6341606]
441. McMahon T, Muscles, reflexes and locomotion. 1984, Princeton, NJ: Princeton Univ. Press.
442. Mendell LM, The size principle: a rule describing the recruitment of motoneurons. J Neurophysiol, 2005 93(6): p. 3024–6. [PubMed: 15914463]
443. Merendino KA, Johnson RJ, Skinner HH, and Maguire RX, The intradiaphragmatic distribution of the phrenic nerve with particular reference to the placement of diaphragmatic incisions and controlled segmental paralysis. Surgery, 1956 39(1): p. 189–98. [PubMed: 13298965]
444. Merrell AJ and Kardon G, Development of the diaphragm -- a skeletal muscle essential for mammalian respiration. FEBS J, 2013 280(17): p. 4026–35. [PubMed: 23586979]
445. Messina G, Biressi S, Monteverde S, Magli A, Cassano M, Perani L, Roncaglia E, Tagliafico E, Starnes L, Campbell CE, Grossi M, Goldhamer DJ, Gronostajski RM, and Cossu G, Nfix regulates fetal-specific transcription in developing skeletal muscle. Cell, 2010 140(4): p. 554–66. [PubMed: 20178747]
446. Michailova KN and Usunoff KG, Serosal membranes (pleura, pericardium, peritoneum). Normal structure, development and experimental pathology. Adv Anat Embryol Cell Biol, 2006 183: p. i–vii, 1–144, back cover. [PubMed: 16570866]
447. Milano S, Grelot L, Bianchi AL, and Iscoe S, Discharge patterns of phrenic motoneurons during fictive coughing and vomiting in decerebrate cats. J Appl Physiol, 1992 73(4): p. 1626–36. [PubMed: 1447114]
448. Miller AD, Respiratory muscle control during vomiting. Can J Physiol Pharmacol, 1990 68(2): p. 237–41. [PubMed: 2178748]
449. Miller AD, Nonaka S, and Jakus J, Brain areas essential or non-essential for emesis. Brain Res, 1994 647(2): p. 255–64. [PubMed: 7922502]
450. Miller AD and Ruggiero DA, Emetic reflex arc revealed by expression of the immediate-early gene c-fos in the cat. J Neurosci, 1994 14(2): p. 871–88. [PubMed: 8301366]
451. Miller K, Rosenmann M, and Morrison P, Oxygen uptake and temperature regulation of young harbor seals (Phoca vitulina richardi) in water. Comp Biochem Physiol A Comp Physiol, 1976 54(1): p. 105–7. [PubMed: 3329]
452. Milner AD and Sauders RA, Pressure and volume changes during the first breath of human neonates. Arch Dis Child, 1977 52(12): p. 918–24. [PubMed: 606168]

453. Mitchelle A and Watson C, The organization of spinal motor neurons in a monotreme is consistent with a six-region schema of the mammalian spinal cord. J Anat, 2016 229(3): p. 394–405. [PubMed: 27173752]

454. Miyata H, Zhan WZ, Prakash YS, and Sieck GC, Influence of inactivity on contribution of neuromuscular transmission failure to diaphragm fatigue. Med Sci Sports Exerc, 1994 26: p. S167.

455. Miyata H, Zhan WZ, Prakash YS, and Sieck GC, Myoneural interactions affect diaphragm muscle adaptations to inactivity. J Appl Physiol, 1995 79: p. 1640–1649. [PubMed: 8594024]

456. Moessinger AC, Santiago A, Paneth NS, Rey HR, Blanc WA, and Driscoll JM Jr., Time-trends in necropsy prevalence and birth prevalence of lung hypoplasia. Paediatr Perinat Epidemiol, 1989 3(4): p. 421–31. [PubMed: 2587409]

457. Morgan FG, The Australian Taipan Oxyuranus s. scutellatus (Peters), in Venoms, Buckley EE and Porges N, Editors. 1956, American Association for the Advancement of Science: Washington.

458. Morin D, Monteau R, and Hilaire G, Compared effects of serotonin on cervical and hypoglossal inspiratory activities: an in vitro study in the newborn rat. J Physiol, 1992 451: p. 605–29. [PubMed: 1403827]

459. Mortola JP, Dynamics of breathing in newborn mammals. Physiol Rev, 1987 67(1): p. 187–243. [PubMed: 3543976]

460. Mortola JP, Fisher JT, Smith B, Fox G, and Weeks S, Dynamics of breathing in infants. J Appl Physiol Respir Environ Exerc Physiol, 1982 52(5): p. 1209–15. [PubMed: 7096145]

461. Mortola JP, Fisher JT, Smith JB, Fox GS, Weeks S, and Willis D, Onset of respiration in infants delivered by cesarean section. J Appl Physiol Respir Environ Exerc Physiol, 1982 52(3): p. 716–24. [PubMed: 7068487]

462. Mortola JP, Frappell PB, and Woolley PA, Breathing through skin in a newborn mammal. Nature, 1999 397(6721): p. 660. [PubMed: 10067890]

463. Mortola JP and Lanthier C, Scaling the amplitudes of the circadian pattern of resting oxygen consumption, body temperature and heart rate in mammals. Comp Biochem Physiol A Mol Integr Physiol, 2004 139(1): p. 83–95. [PubMed: 15471685]

464. Mount LE and Rowell JG, Body-weight and age in relation to the metabolic-rate of the young pig. Nature, 1960 186: p. 1054–5. [PubMed: 14424735]

465. Mount LE and Rowell JG, Body size, body temperature and age in relation to the metabolic rate of the pig in the first five weeks after birth. J Physiol, 1960 154: p. 408–16. [PubMed: 13773261]

466. Muller Botha GS, The anatomy of phrenic nerve termination and the motor innervation of the diaphragm. Thorax, 1957 12(1): p. 50–6. [PubMed: 13422397]

467. Munn AJ and Dawson TJ, Energy requirements of the red kangaroo (Macropus rufus): impacts of age, growth and body size in a large desert-dwelling herbivore. J Comp Physiol B, 2003 173(7): p. 575–82. [PubMed: 12879349]

468. Munn AJ, Dawson TJ, and Maloney SK, Ventilation patterns in red kangaroos (Macropus rufus Desmarest): juveniles work harder than adults at thermal extremes, but extract more oxygen per breath at thermoneutrality. J Exp Biol, 2007 210(Pt 15): p. 2723–9. [PubMed: 17644687]

469. Munns SL, Owerkowicz T, Andrewartha SJ, and Frappell PB, The accessory role of the diaphragmaticus muscle in lung ventilation in the estuarine crocodile Crocodylus porosus. J. Exp. Biol, 2012 215: p. 845–852. [PubMed: 22323207]

470. Muraskas JK, Husain A, Myers TF, Anderson CL, and Black PR, An association of pulmonary hypoplasia with unilateral agenesis of the diaphragm. J Pediatr Surg, 1993 28(8): p. 999–1002. [PubMed: 8229607]

471. Nabeshima Y, Hanaoka K, Hayasaka M, Esumi E, Li S, Nonaka I, and Nabeshima Y, Myogenin gene disruption results in perinatal lethality because of severe muscle defect. Nature, 1993 364(6437): p. 532–535. [PubMed: 8393146]

472. Nadelhaft I and Booth AM, The location and morphology of preganglionic neurons and the distribution of visceral afferents from the rat pelvic nerve: a horseradish peroxidase study. J Comp Neurol, 1984 226(2): p. 238–45. [PubMed: 6736301]

473. Nalfeh KH, Huggins SE, and Hoff HE, The nature of the ventilatory period in crocodilian respiration. Respir. Physiol, 1970 10: p. 339–348.

474. Narula M, McGovern AE, Yang SK, Farrell MJ, and Mazzone SB, Afferent neural pathways mediating cough in animals and humans. J Thorac Dis, 2014 6(Suppl 7): p. S712–9. [PubMed: 25383205]

475. Nattie E and Li A, Central chemoreception is a complex system function that involves multiple brain stem sites. J Appl Physiol (1985), 2009 106(4): p. 1464–6. [PubMed: 18467549]

476. Nava S, Zanotti E, Ambrosino N, Fracchia C, Scarabelli C, and Rampulla C, Evidence of acute diaphragmatic fatigue in a “natural” condition. The diaphragm during labor. Am Rev Respir Dis, 1992 146(5 Pt 1): p. 1226–30. [PubMed: 1443875]

477. Nemeth PM, Hamm TM, Gordon DA, Reinking RM, and Stuart DG, Application of cross-sectional single-fiber microchemistry to the study of motor-unit fatigability, in Motor Control, Gantchev GN, Dimitrov B, and Gatev P, Editors. 1986, Plenum: New York.

478. Nemeth PM, Solanki L, Gordon DA, Hamm TM, Reinking RM, and Stuart DG, Uniformity of metabolic enzymes within individual motor units. J Neurosci, 1986 6(3): p. 892–898. [PubMed: 3958798]

479. Ngo ST, Balke C, Phillips WD, and Noakes PG, Neuregulin potentiates agrin-induced acetylcholine receptor clustering in myotubes. Neuroreport, 2004 15(16): p. 2501–5. [PubMed: 15538183]

480. Ngo ST, Cole RN, Sunn N, Phillips WD, and Noakes PG, Neuregulin-1 potentiates agrin-induced acetylcholine receptor clustering through muscle-specific kinase phosphorylation. J Cell Sci, 2012 125(Pt 6): p. 1531–43. [PubMed: 22328506]

481. Noren SR and Williams TM, Body size and skeletal muscle myoglobin of cetaceans: adaptations for maximizing dive duration. Comp Biochem Physiol A Mol Integr Physiol, 2000 126(2): p. 181–91. [PubMed: 10936758]

482. Normand IC, Olver RE, Reynolds EO, and Strang LB, Permeability of lung capillaries and alveoli to non-electrolytes in the foetal lamb. J Physiol, 1971 219(2): p. 303–30. [PubMed: 5158386]

483. Oliver TK Jr., Demis JA, and Bates GD, Serial blood-gas tensions and acid-base balance during the first hour of life in human infants. Acta Paediatr, 1961 50: p. 346–60. [PubMed: 13730823]

484. Olson EN, Signal transduction pathways that regulate skeletal muscle gene expression. Mol Endocrinol, 1993 7(11): p. 1369–1378. [PubMed: 8114752]

485. Olver RE and Strang LB, Ion fluxes across the pulmonary epithelium and the secretion of lung liquid in the foetal lamb. J Physiol, 1974 241(2): p. 327–57. [PubMed: 4443921]

486. Onishi T, Mori T, Yanagihara M, Furukawa N, and Fukuda H, Similarities of the neuronal circuit for the induction of fictive vomiting between ferrets and dogs. Auton Neurosci, 2007 136(1–2): p. 20–30. [PubMed: 17478125]

487. Oppenheim RW, The neurotrophic theory and naturally occurring motoneuron death. Trends in Neurosciences, 1989 12(7): p. 252–5. [PubMed: 2475935]

488. Oppenheim RW, Neurotrophic survival molecules for motoneurons: an embarrassment of riches. Neuron, 1996 17(2): p. 195–7. [PubMed: 8780643]

489. Oppenheim RW, Haverkamp LJ, Prevette D, McManaman JL, and Appel SH, Reduction of naturally occurring motoneuron death in vivo by a target-derived neurotrophic factor. Science, 1988 240(4854): p. 919–22. [PubMed: 3363373]

490. Oppenheim RW, Houenou LJ, Parsadanian AS, Prevette D, Snider WD, and Shen L, Glial cell line-derived neurotrophic factor and developing mammalian motoneurons: regulation of programmed cell death among motoneuron subtypes. J Neurosci, 2000 20(13): p. 5001–11. [PubMed: 10864958]

491. Oppenheim RW, Prevette D, Qin-Wei Y, Collins F, and MacDonald J, Control of embryonic motoneuron survival in vivo by ciliary neurotrophic factor. Science, 1991 251: p. 1616–1618. [PubMed: 2011743]

492. Oppenheim RW, Wiese S, Prevette D, Armanini M, Wang S, Houenou LJ, Holtmann B, Gotz R, Pennica D, and Sendtner M, Cardiotrophin-1, a muscle-derived cytokine, is required for the survival of subpopulations of developing motoneurons. J Neurosci, 2001 21(4): p. 1283–91. [PubMed: 11160399]

493. Otake K, Sasaki H, Ezure K, and Manabe M, Axonal projections from Botzinger expiratory neurons to contralateral ventral and dorsal respiratory groups in the cat. Exp Brain Res, 1988 72(1): p. 167–77. [PubMed: 3169184]

494. Owerkowicz T, Farmer C, Hicks JW, and Brainerd EL, Contribution of gular pumping to lung ventilation in monitor lizards. Science, 1999 284: p. 1661–1663. [PubMed: 10356394]

495. Pabst DA, Intramuscular morphology and tendon geometry of the epaxial swimming muscles of dolphins. J. Zool. Lond, 1993 230: p. 159–176.

496. Pansky B, Review of Medical Embryology. 1982, Alameda, CA: Embryome Sciences, Inc.

497. Pappenheimer JR, Fencl V, Heisey SR, and Held D, Role of Cerebral Fluids in Control of Respiration as Studied in Unanesthetized Goats. Am J Physiol, 1965 208: p. 436–50. [PubMed: 14264731]

498. Perks AM and Cassin S, The effects of arginine vasopressin and epinephrine on lung liquid production in fetal goats. Can J Physiol Pharmacol, 1989 67(5): p. 491–8. [PubMed: 2766095]

499. Perks AM, Kindler PM, Marshall J, Woods B, Craddock M, and Vonder Muhll I, Lung liquid production by in vitro lungs from fetal guinea pigs: effects of arginine vasopressin and arginine vasotocin. J Dev Physiol, 1993 19(5): p. 203–12. [PubMed: 8083497]

500. Perry SF and Carrier DR, The coupled evolution of breathing and locomotion as a game of leapfrog. Physiol Biochem Zool, 2006 79(6): p. 997–9. [PubMed: 17041865]

501. Perry SF, Christian A, Breuer T, Pajor N, and Codd JR, Implications of an avian-style respiratory system for gigantism in sauropod dinosaurs. J Exp Zool A Ecol Genet Physiol, 2009 311(8): p. 600–10. [PubMed: 19189317]

502. Perry SF and Duncker HR, Lung architecture volume and static mechanics in five species of lizards. Respir Physiol, 1978 34(1): p. 61–81. [PubMed: 705077]

503. Perry SF, Similowski T, Klein W, and Codd JR, The evolutionary origin of the mammalian diaphragm. Respir Physiol Neurobiol, 2010 171(1): p. 1–16. [PubMed: 20080210]

504. Personius KE and Balice-Gordon RJ, Activity-dependent editing of neuromuscular synaptic connections. Brain Res Bull, 2000 53(5): p. 513–22. [PubMed: 11165786]

505. Pierce SE, Clack JA, and Hutchinson JR, Comparative axial morphology in pinnipeds and its correlation with aquatic locomotory behaviour. J Anat, 2011 219(4): p. 502–14. [PubMed: 21668895]

506. Pierce SL, Kutschke W, Cabeza R, and England SK, In vivo measurement of intrauterine pressure by telemetry: a new approach for studying parturition in mouse models. Physiol Genomics, 2010 42(2): p. 310–6. [PubMed: 20460604]

507. Plowman S and Smith D, Exercise physiology for health, fitness, and performance. 1997, Boston, Mass: Allyn & Bacon.

508. Polkey MI, Harris ML, Hughes PD, Hamnegard CH, Lyons D, Green M, and Moxham J, The contractile properties of the elderly human diaphragm. Am J Respir Crit Care Med, 1997 155(5): p. 1560–4. [PubMed: 9154857]

509. Poole DC and Erickson HH, Highly athletic terrestrial mammals: horses and dogs. Compr Physiol, 2011 1(1): p. 1–37. [PubMed: 23737162]

510. Poole DC, Petrisko RN, Anderson L, Fedde MR, and Erickson HH, Structural and oxidative enzyme characteristics of the diaphragm. Equine Vet J Suppl, 2002(34): p. 459–63. [PubMed: 12405734]

511. Poole DC, Sexton WL, Farkas GA, Powers SK, and Reid MB, Diaphragm structure and function in health and disease. Med Sci Sports Exerc, 1997 29(6): p. 738–54. [PubMed: 9219201]

512. Prakash YS, Fournier M, and Sieck GC, Effects of prenatal undernutrition on developing rat diaphragm. J Appl Physiol, 1993 75: p. 1044–1052. [PubMed: 8226510]

513. Prakash YS, Mantilla CB, Zhan WZ, Smithson KG, and Sieck GC, Phrenic motoneuron morphology during rapid diaphragm muscle growth. J Appl Physiol, 2000 89(2): p. 563–72. [PubMed: 10926639]

514. Prakash YS, Miller SM, Huang M, and Sieck GC, Morphology of diaphragm neuromuscular junctions on different fibre types. J Neurocytol, 1996 25(2): p. 88–100. [PubMed: 8699198]

515. Prakash YS and Sieck GC. Morphometric analysis of phrenic motoneuron pools using confocal microscopy. in Kemp Station Symposium on Regulation of Respiration 1992.
516. Prakash YS and Sieck GC, Age-related remodeling of neuromuscular junctions on type-identified diaphragm fibers. Muscle Nerve, 1998 21(7): p. 887–895. [PubMed: 9626248]
517. Prakash YS, Smithson KG, and Sieck GC, Growth-related alterations in motor endplates of type-identified diaphragm muscle fibres. J Neurocytol, 1995 24: p. 225–235. [PubMed: 7798115]
518. Prodhom LS, Levison H, Cherry RB, Drorbaugh JE, Hubbell JP Jr., and Smith CA, Adjustment of Ventilation, Intrapulmonary Gas Exchange, and Acid-Base Balance during the First Day of Life. Normal Values in Well Infants of Diabetic Mothers. Pediatrics, 1964 33: p. 682–93. [PubMed: 14159662]
519. Proske U and Gandevia SC, The proprioceptive senses: their roles in signaling body shape, body position and movement, and muscle force. Physiological reviews, 2012 92(4): p. 1651–97. [PubMed: 23073629]
520. Qiu K, Lane MA, Lee KZ, Reier PJ, and Fuller DD, The phrenic motor nucleus in the adult mouse. Exp Neurol, 2010 226(1): p. 254–8. [PubMed: 20816820]
521. Rada CC, Pierce SL, Grotegut CA, and England SK, Intrauterine telemetry to measure mouse contractile pressure in vivo. J Vis Exp, 2015(98): p. e52541. [PubMed: 25867820]
522. Rana S, Sieck GC, and Mantilla CB, Diaphragm electromyographic activity following unilateral midcervical contusion injury in rats. J Neurophysiol, 2017 117(2): p. 545–555. [PubMed: 27832610]
523. Randell SH, Mercer RR, and Young SL, Neonatal hyperoxia alters the pulmonary alveolar and capillary structure of 40-day-old rats. Am J Pathol, 1990 136(6): p. 1259–66. [PubMed: 2356858]
524. Rassler B and Kohl J, Coordination-related changes in the rhythms of breathing and walking in humans. Eur J Appl Physiol, 2000 82(4): p. 280–8. [PubMed: 10958370]
525. Ray AP, Chebolu S, and Darmani NA, Receptor-selective agonists induce emesis and Fos expression in the brain and enteric nervous system of the least shrew (Cryptotis parva). Pharmacol Biochem Behav, 2009 94(1): p. 211–8. [PubMed: 19699757]
526. Redfern P, Neuromuscular transmission in new-born rats. J. Physiol, 1970 209: p. 701–709. [PubMed: 5499804]
527. Reid MB, Ericson GC, Feldman HA, and Johnson RLJ, Fiber types and fiber diameters in canine respiratory muscles. J Appl Physiol, 1987 62: p. 1705–1712. [PubMed: 3597242]
528. Reid WD, Wiggs BR, Pare PD, and Pardy RL, Fiber type and regional differences in oxidative capacity and glycogen content in the hamster diaphragm. Am Rev Respir Dis, 1992 146(5 Pt 1): p. 1266–1271. [PubMed: 1443883]
529. Remmers JE, Inhibition of inspiratory activity by intercostal muscle afferents. Respir Physiol, 1970 10(3): p. 358–83. [PubMed: 4248924]
530. Remmers JE, Extra-segmental reflexes derived from intercostal afferents: phrenic and laryngeal responses. J Physiol, 1973 233(1): p. 45–62. [PubMed: 4759121]
531. Remmers JE, Torgerson C, Harris M, Perry SF, Vasilakos K, and Wilson RJ, Evolution of central respiratory chemoreception: a new twist on an old story. Respir Physiol, 2001 129(1–2): p. 211–7. [PubMed: 11738655]
532. Ren J and Greer JJ, Ontogeny of rhythmic motor patterns generated in the embryonic rat spinal cord. J Neurophysiol, 2003 89(3): p. 1187–95. [PubMed: 12626606]
533. Reynolds DJ, Barber NA, Grahame-Smith DG, and Leslie RA, Cisplatin-evoked induction of c-fos protein in the brainstem of the ferret: the effect of cervical vagotomy and the anti-emetic 5-HT3 receptor antagonist granisetron (BRL 43694). Brain Res, 1991 565(2): p. 231–6. [PubMed: 1668810]
534. Rhodes SJ and Konieczny SF, Identification of MRF4: a new member of the muscle regulatory factor gene family. Genes Dev, 1989 3(12b): p. 2050–2061. [PubMed: 2560751]
535. Richardson RS, Poole DC, Knight DR, Kurdak SS, Hogan MC, Grassi B, Johnson EC, Kendrick KF, Erickson BK, and Wagner PD, High muscle blood flow in man: is maximal O2 extraction compromised? J Appl Physiol (1985), 1993 75(4): p. 1911–6. [PubMed: 8282650]

536. Richter DW, Generation and maintenance of the respiratory rhythm. J Exp Biol, 1982 100: p. 93–107. [PubMed: 6757372]

537. Richter DW, Jordan D, Ballantyne D, Meesmann M, and Spyer KM, Presynaptic depolarization in myelinated vagal afferent fibres terminating in the nucleus of the tractus solitarius in the cat. Pflugers Arch, 1986 406(1): p. 12–9. [PubMed: 3951964]

538. Richter DW and Smith JC, Respiratory rhythm generation in vivo. Physiology (Bethesda), 2014 29(1): p. 58–71. [PubMed: 24382872]

539. Ridgway SH, Scronce BL, and Kanwisher J, Respiration and deep diving in the bottlenose porpoise. Science, 1969 166(3913): p. 1651–4. [PubMed: 5360592]

540. Rogers FB, Leavitt BJ, and Jensen PE, Traumatic transdiaphragmatic intercostal hernia secondary to coughing: case report and review of the literature. J Trauma, 1996 41(5): p. 902–3. [PubMed: 8913225]

541. Rommel S and Reynolds JE 3rd, Diaphragm structure and function in the Florida manatee (Trichechus manatus latirostris). Anat Rec, 2000 259(1): p. 41–51. [PubMed: 10760742]

542. Ross DB and Stiles GE, Spontaneous rupture of the diaphragm in labour: a case report. Can J Surg, 1989 32(3): p. 212–3. [PubMed: 2713776]

543. Rowley KL, Mantilla CB, and Sieck GC, Respiratory muscle plasticity. Respir Physiol Neurobiol, 2005 147(2–3): p. 235–51. [PubMed: 15871925]

544. Roy CH, Barnes RJ, Heath MF, and Sensky PL, A modified helium dilution technique for measuring small lung gas volumes. J Dev Physiol, 1992 17(2): p. 87–92. [PubMed: 1500637]

545. Ruano R, Aubry MC, Dumez Y, Zugaib M, and Benachi A, Predicting neonatal deaths and pulmonary hypoplasia in isolated congenital diaphragmatic hernia using the sonographic fetal lung volume-body weight ratio. AJR Am J Roentgenol, 2008 190(5): p. 1216–9. [PubMed: 18430834]

546. Ruano R, Peiro JL, da Silva MM, Campos JA, Carreras E, Tannuri U, and Zugaib M, Early fetoscopic tracheal occlusion for extremely severe pulmonary hypoplasia in isolated congenital diaphragmatic hernia: preliminary results. Ultrasound Obstet Gynecol, 2013 42(1): p. 70–6. [PubMed: 23349059]

547. Ruben JA, Dal Sasso C, Geist NR, Hillenius WJ, Jones TD, and Signore M, Pulmonary function and metabolic physiology of theropod dinosaurs. Science, 1999 283(5401): p. 514–6. [PubMed: 9915693]

548. Ruben JA, Jones TD, and Geist NR, Respiratory and reproductive paleophysiology of dinosaurs and early birds. Physiol Biochem Zool, 2003 76(2): p. 141–64. [PubMed: 12794669]

549. Ruben JA, Jones TD, Geist NR, and Hillenius WJ, Lung structure and ventilation in theropod dinosaurs. Science, 1997 278: p. 1267–1270.

550. Rubin S, Sandu S, Durand E, and Baehrel B, Diaphragmatic rupture during labour, two years after an intra-oesophageal rupture of a bronchogenic cyst treated by an omental wrapping. Interact Cardiovasc Thorac Surg, 2009 9(2): p. 374–6. [PubMed: 19423509]

551. Rubner M, Über den einfluss der körpergrösse auf stoff- und kraftwechsel. Zeit. Biol, 1883 19(536–562).

552. Rudnicki MA, Braun T, Hinuma S, and Jaenisch R, Inactivation of MyoD in mice leads to up-regulation of the myogenic HLH gene Myf-5 and results in apparently normal muscle development. Cell, 1992 71: p. 383–390. [PubMed: 1330322]

553. Rudnicki MA, Schnegelsberg PN, Stead RH, Braun T, Arnold HH, and Jaenisch R, MyoD or Myf-5 is required for the formation of skeletal muscle. Cell, 1993 75(7): p. 1351–9. [PubMed: 8269513]

554. Rybak IA, O'Connor R, Ross A, Shevtsova NA, Nuding SC, Segers LS, Shannon R, Dick TE, Dunin-Barkowski WL, Orem JM, Solomon IC, Morris KF, and Lindsey BG, Reconfiguration of the pontomedullary respiratory network: a computational modeling study with coordinated in vivo experiments. J Neurophysiol, 2008 100(4): p. 1770–99. [PubMed: 18650310]

555. Sabourin LA and Rudnicki MA, The molecular regulation of myogenesis. Clin Genet, 2000 57(1): p. 16–25. [PubMed: 10733231]

556. Saez LJ, Gianola KM, McNally E, Feghali R, Eddy R, Shows T, and Leinwand LA, Human cardiac myosin heavy chain genes and their linkage in the genome. Nucleic Acids Res, 1987 15: p. 5443–5459. [PubMed: 3037493]
557. Saji M and Miura M, Evidence that glutamate is the transmitter mediating respiratory drive from medullary premotor neurons to phrenic motoneurons: a double labeling study in the rat. Neurosci Lett, 1990 115(2–3): p. 177–82. [PubMed: 1978263]
558. Sanchez J, Medrano G, Debesse B, Riquet M, and Derenne JP, Muscle fibre types in costal and crural diaphragm in normal men and in patients with moderate chronic respiratory disease. Bull Eur Physiopathol Respir, 1985 21(4): p. 351–6. [PubMed: 4041660]
559. Sander PM, An evolutionary cascade model for sauropod dinosaur gigantism--overview, update and tests. PLoS One, 2013 8(10): p. e78573. [PubMed: 24205267]
560. Sander PM, Christian A, Clauss M, Fechner R, Gee CT, Griebeler EM, Gunga HC, Hummel J, Mallison H, Perry SF, Preuschoft H, Rauhut OW, Remes K, Tutken T, Wings O, and Witzel U, Biology of the sauropod dinosaurs: the evolution of gigantism. Biol Rev Camb Philos Soc, 2011 86(1): p. 117–55. [PubMed: 21251189]
561. Sander PM and Clauss M, Paleontology. Sauropod gigantism. Science, 2008 322(5899): p. 200–1. [PubMed: 18845734]
562. Sandhu MS, Dougherty BJ, Lane MA, Bolser DC, Kirkwood PA, Reier PJ, and Fuller DD, Respiratory neuroplasticity following high cervical hemisection. Respir Physiol Neurobiol, 2009.
563. Sandrock AW Jr., Dryer SE, Rosen KM, Gozani SN, Kramer R, Theill LE, and Fischbach GD, Maintenance of acetylcholine receptor number by neuregulins at the neuromuscular junction in vivo. Science, 1997 276(5312): p. 599–603. [PubMed: 9110980]
564. Sanes JR and Lichtman JW, Development of the vertebrate neuromuscular junction. Annual Review of Neuroscience, 1999 22: p. 389–442.
565. Sanes JR and Lichtman JW, Induction, assembly, maturation and maintenance of a postsynaptic apparatus. Nat Rev Neurosci, 2001 2(11): p. 791–805. [PubMed: 11715056]
566. Sant'Ambrogio G, Tsubone H, and Sant'Ambrogio FB, Sensory information from the upper airway: role in the control of breathing. Respir Physiol, 1995 102(1): p. 1–16. [PubMed: 8610203]
567. Saunders RA and Milner AD, Pulmonary pressure/volume relationships during the last phase of delivery and the first postnatal breaths in human subjects. J Pediatr, 1978 93(4): p. 667–73. [PubMed: 702249]
568. Savage VM, Improved approximations to scaling relationships for species, populations, and ecosystems across latitudinal and elevational gradients. J Theor Biol, 2004 227(4): p. 525–34. [PubMed: 15038987]
569. Scarpelli EM, Clutario BC, and Traver D, Failure of immature lungs to produce foam and retain air at birth. Pediatr Res, 1979 13(11): p. 1285–9. [PubMed: 259986]
570. Scarpelli EM, Kumar A, Doyle C, and Clutario BC, Functional anatomy and volume-pressure characteristics of immature lungs. Respir Physiol, 1981 45(1): p. 25–41. [PubMed: 6895116]
571. Schachner ER, Clen RL, Butler JP, and Farmer CG, Unidirectional pulmonary airflow in the savannah monitor lizard. Nature, 2014 506(7488): p. 367–370. [PubMed: 24336209]
572. Schachner ER, Hutchinson JR, and Farmer C, Pulmonary anatomy in the Nile crocodile and the evolution of unidirectional airflow in Archosauria. PeerJ, 2013 1: p. e60. [PubMed: 23638399]
573. Schmidt-Nielsen K, Energy metabolism, body size, and problems of scaling. Fed Proc, 1970 29(4): p. 1524–32. [PubMed: 5459901]
574. Schmidt-Nielsen K and Pennycuik P, Capillary density in mammals in relation to body size and oxygen consumption. Am J Physiol, 1961 200: p. 746–50. [PubMed: 13748094]
575. Schorr GS, Falcone EA, Moretti DJ, and Andrews RD, First Long-Term Behavioral Records from Cuvier's Beaked Whales (Ziphius cavirostris) Reveal Record-Breaking Dives. PLoS One, 2014 9(3): p. e92633. [PubMed: 24670984]
576. Scott GR, Hawkes LA, Frappell PB, Butler PJ, Bishop CM, and Milsom WK, How bar-headed geese fly over the Himalayas. Physiology (Bethesda), 2015 30(2): p. 107–15. [PubMed: 25729056]

577. Scott GR and Milsom WK, Control of breathing and adaptation to high altitude in the bar-headed goose. Am J Physiol Regul Integr Comp Physiol, 2007 293(1): p. R379–91. [PubMed: 17491113]
578. Scott R, Innervation of the Diaphragm and Its Practical Aspects in Surgery. Thorax, 1965 20: p. 357–61. [PubMed: 14321725]
579. Seebacher F, Grigg GC, and Beard LA, Crocodiles as dinosaurs: behavioural thermoregulation in very large ectotherms leads to high and stable body temperatures. J Exp Biol, 1999 202(1): p. 77–86. [PubMed: 9841897]
580. Servais EL, Stiles BM, Finnerty BM, and Paul S, Ruptured diaphragmatic eventration: a rare cause of acute postpartum dyspnea. Ann Thorac Surg, 2012 93(6): p. e143–4. [PubMed: 22632531]
581. Seven YB, Mantilla CB, and Sieck GC, Recruitment of Rat Diaphragm Motor Units Across Motor Behaviors with Different Levels of Diaphragm Activation. J Appl Physiol, 2014 117(11): p. 1308–16. [PubMed: 25257864]
582. Seven YB, Mantilla CB, Zhan WZ, and Sieck GC, Non-stationarity and power spectral shifts in EMG activity reflect motor unit recruitment in rat diaphragm muscle. Respir Physiol Neurobiol, 2013 185(2): p. 400–9. [PubMed: 22986086]
583. Sexton WL and Poole DC, Costal diaphragm blood flow heterogeneity at rest and during exercise. Respir Physiol, 1995 101(2): p. 171–82. [PubMed: 8570919]
584. Seymour RS, Bennett-Stamper CL, Johnston SD, Carrier DR, and Grigg GC, Evidence for endothermic ancestors of crocodiles at the stem of archosaur evolution. Physiol Biochem Zool, 2004 77(6): p. 1051–67. [PubMed: 15674775]
585. Shafik A, Dilatation and closing anal reflexes. Description and clinical significance of new reflexes: preliminary report. Acta Anat (Basel), 1991 142(4): p. 293–8. [PubMed: 1801520]
586. Shafik A, Straining puborectalis reflex: description and significance of a “new” reflex. Anat Rec, 1991 229(2): p. 281–4. [PubMed: 2012316]
587. Shafik A, Straining urethral reflex: description of a reflex and its clinical significance. Preliminary report. Acta Anat (Basel), 1991 140(2): p. 104–7. [PubMed: 1867048]
588. Shafik A and Moneim KA, Dynamic study of the rectal detrusor activity at defecation. Digestion, 1991 49(3): p. 167–74. [PubMed: 1769432]
589. Shannon R, Bolser DC, and Lindsey BG, Medullary expiratory activity: influence of intercostal tendon organs and muscle spindle endings. J Appl Physiol (1985), 1987 62(3): p. 1057–62. [PubMed: 3571062]
590. Sharratt MT, Henke KG, Aaron EA, Pegelow DF, and Dempsey JA, Exercise-induced changes in functional residual capacity. Respir Physiol, 1987 70(3): p. 313–26. [PubMed: 3685654]
591. Shaw JM, Hamad NM, Coleman TJ, Egger MJ, Hsu Y, Hitchcock R, and Nygaard IE, Intra-abdominal pressures during activity in women using an intra-vaginal pressure transducer. J Sports Sci, 2014 32(12): p. 1176–85. [PubMed: 24575741]
592. Shea SA, Behavioural and arousal-related influences on breathing in humans. Exp Physiol, 1996 81(1): p. 1–26. [PubMed: 8869137]
593. Sherrington CS, Flexion-reflex of the limb, crossed extension-reflex, and reflex stepping and standing. J Physiol, 1910 40(1–2): p. 28–121. [PubMed: 16993027]
594. Sherrington CS, Remarks on some aspects of reflex inhibition. Proc R Soc Lond (Biol), 1925 97(686): p. 519–545.
595. Shirley D, Hodges PW, Eriksson AE, and Gandevia SC, Spinal stiffness changes throughout the respiratory cycle. J Appl Physiol (1985), 2003 95(4): p. 1467–75. [PubMed: 12970374]
596. Shrager JB, Desjardins PR, Burkman JM, Konig SK, Stewart SK, Su L, Shah MC, Bricklin E, Tewari M, Hoffman R, Rickels MR, Jullian EH, Rubinstein NA, and Stedman HH, Human skeletal myosin heavy chain genes are tightly linked in the order embryonic-IIa-IId/x-ILb-perinatal-extraocular. J Muscle Res Cell Motil, 2000 21(4): p. 345–55. [PubMed: 11032345]
597. Sieck DC, Zhan WZ, Fang YH, Ermilov LG, Sieck GC, and Mantilla CB, Structure-activity relationships in rodent diaphragm muscle fibers vs. neuromuscular junctions. Respir Physiol Neurobiol, 2012 180(1): p. 88–96. [PubMed: 22063925]
598. Sieck GC, Diaphragm muscle: structural and functional organization. Clin Chest Med, 1988 9(2): p. 195–210. [PubMed: 3292123]

599. Sieck GC, Recruitment and frequency coding of diaphragm motor units during ventilatory and non-ventilatory behaviors, in Respiratory Control, Swanson GD, Grodins FS, and Hughson RL, Editors. 1989, Plenum Press: New York p. 441–450.

600. Sieck GC, Conceptual model of ventilatory muscle recruitment and diaphragmatic fatigue, in Modeling and Parameter Estimation in Respiratory Control, Khoo MCK, Editor. 1990, Plenum Press: New York p. 113–123.

601. Sieck GC, Diaphragm motor units and their response to altered use. Sem Respir Med, 1991 12: p. 258–269.

602. Sieck GC, Neural control of the inspiratory pump. NIPS, 1991 6: p. 260–264.

603. Sieck GC, Physiological effects of diaphragm muscle denervation and disuse. Clin Chest Med, 1994 15(4): p. 641–59. [PubMed: 7867280]

604. Sieck GC, Organization and recruitment of diaphragm motor units, in The Thorax, Roussos C, Editor. 1995, Marcel Dekker: New York, NY p. 783–820.

605. Sieck GC, Recruitment of diaphragm motor units during ventilatory and non-ventilatory behaviors, in Motor Control VII. Proceedings of the VIIth International Symposium on Motor Control, Borovets, Bulgaria, Stuart DG, et al., Editors. 1996, Motor Control Press: Tucson, AZ p. 39–42.

606. Sieck GC and Blanco CE, Postnatal changes in the distribution of succinate dehydrogenase activities among diaphragm muscle fibers. Pediatr Res, 1991 29(6): p. 586–593. [PubMed: 1830959]

607. Sieck GC, Cheung TS, and Blanco CE, Diaphragm capillarity and oxidative capacity during postnatal development. J Appl Physiol, 1991 70: p. 103–111. [PubMed: 1826289]

608. Sieck GC, Ferreira LF, Reid MB, and Mantilla CB, Mechanical properties of respiratory muscles. Comprehensive Physiology, 2013 3(4): p. 1553–67. [PubMed: 24265238]

609. Sieck GC and Fournier M, Contractile and fatigue properties of diaphragm motor units, in Respiratory Muscles and Their Neuromotor Control, Sieck GC, Gandevia SC, and Cameron WE, Editors. 1987, Alan R. Liss, Inc.: New York p. 227–237.

610. Sieck GC and Fournier M, Diaphragm motor unit recruitment during ventilatory and nonventilatory behaviors. J Appl Physiol, 1989 66(6): p. 2539–2545. [PubMed: 2745316]

611. Sieck GC and Fournier M, Changes in diaphragm motor unit EMG during fatigue. J Appl Physiol, 1990 68(5): p. 1917–1926. [PubMed: 2163376]

612. Sieck GC, Fournier M, and Belman MJ, Physiological properties of motor units in the diaphragm, in Neurogenesis of Central Respiratory Rhythm, Bianchi AL and Denavit-Saubie M, Editors. 1985, MTP: Hingham, MA p. 227–229.

613. Sieck GC, Fournier M, and Enad JG, Fiber type composition of muscle units in the cat diaphragm. Neurosci Letters, 1989 97(1–2): p. 29–34.

614. Sieck GC, Fournier M, Prakash YS, and Blanco CE, Myosin phenotype and SDH enzyme variability among motor unit fibers. J Appl Physiol, 1996 80(6): p. 2179–2189. [PubMed: 8806928]

615. Sieck GC and Gransee HM, Respiratory Muscles: Structure, Function & Regulation Colloquium Series on Integrated Systems Physiology: From Molecule to Function to Disease, ed. Granger DN and Granger JP. 2012: Morgan & Claypool Life Sciences.

616. Sieck GC, Han YS, Prakash YS, and Jones KA, Cross-bridge cycling kinetics, actomyosin ATPase activity and myosin heavy chain isoforms in skeletal and smooth respiratory muscles. Comp Biochem Physiol, 1998 119(3): p. 435–450.

617. Sieck GC, Lewis MI, and Blanco CE, Effects of undernutrition on diaphragm fiber size, SDH activity, and fatigue resistance. J Appl Physiol, 1989 66: p. 2196–2205. [PubMed: 2745285]

618. Sieck GC and Prakash YS, Fatigue at the neuromuscular junction. Branch point vs. presynaptic vs. postsynaptic mechanisms. Adv Exp Med Biol, 1995 384: p. 83–100. [PubMed: 8585479]

619. Sieck GC and Prakash YS, Cross bridge kinetics in respiratory muscles. Eur. Respir. J, 1997 10(9): p. 2147–2158. [PubMed: 9311518]

620. Sieck GC and Prakash YS, The diaphragm muscle, in Neural Control of the Respitatory Muscles, Miller AD, Bianchi AL, and Bishop BP, Editors. 1997, CRC Press: Boca Raton, FL p. 7–20.

621. Sieck GC, Prakash YS, Han YS, Fang YH, Geiger PC, and Zhan WZ, Changes in actomyosin ATP consumption rate in rat diaphragm muscle fibers during postnatal development. J. Appl. Physiol, 2003 94: p. 1896–1902. [PubMed: 12562672]

622. Sieck GC, Roy RR, Powell P, Blanco C, Edgerton VR, and Harper RM, Muscle fiber type distribution and architecture of the cat diaphragm. J Appl Physiol, 1983 55(5): p. 1386–1392. [PubMed: 6643176]

623. Sieck GC, Sacks RD, and Blanco CE, Absence of regional differences in the size and oxidative capacity of diaphragm muscle fibers. J Appl Physiol, 1987 63(3): p. 1076–1082. [PubMed: 3654455]

624. Sieck GC, Trelease RB, and Harper RM, Sleep influences on diaphragmatic motor unit discharge. Exp Neurol, 1984 85(2): p. 316–335. [PubMed: 6745377]

625. Sieck GC, Zhan WZ, Prakash YS, Daood MJ, and Watchko JF, SDH and actomyosin ATPase activities of different fiber types in rat diaphragm muscle. J Appl Physiol, 1995 79(5): p. 1629–1639. [PubMed: 8594023]

626. Sierra E, Fernandez A, Espinosa de los Monteros A, Diaz-Delgado J, Bernaldo de Quiros Y, Garcia-Alvarez N, Arbelo M, and Herraez P, Comparative histology of muscle in free ranging cetaceans: shallow versus deep diving species. Sci Rep, 2015 5: p. 15909. [PubMed: 26514564]

627. Simpson SJ, Flecknoe SJ, Clugston RD, Greer JJ, Hooper SB, and Frappell PB, Structural and functional development of the respiratory system in a newborn marsupial with cutaneous gas exchange. Physiol Biochem Zool, 2011 84(6): p. 634–49. [PubMed: 22030856]

628. Simpson SJ, Fong AY, Cummings KJ, and Frappell PB, The ventilatory response to hypoxia and hypercapnia is absent in the neonatal fat-tailed dunnart. J Exp Biol, 2012 215(Pt 24): p. 4242–7. [PubMed: 22972898]

629. Sinervo B and Licht P, Proximate constraints on the evolution of egg size, number, and total clutch mass in lizards. Science, 1991 252(5010): p. 1300–2. [PubMed: 17842955]

630. Singh J, Prasad B, Kumar R, Kohli RN, and Rathor SS, Treatment of diaphragmatic hernia in buffaloes. Aust Vet J, 1977 53(10): p. 473–5. [PubMed: 612319]

631. Skatrud JB and Dempsey JA, Interaction of sleep state and chemical stimuli in sustaining rhythmic ventilation. J Appl Physiol Respir Environ Exerc Physiol, 1983 55(3): p. 813–22. [PubMed: 6415011]

632. Slijper EJ, Die Cetaceen vergleichend anatomisch und systematisch. Capita. Zool, 1936 6–7: p. 1–590.

633. Slijper EJ, Whales/Translated by A. J. Pomerans. 1962, New York: Basic Books.

634. Smith EN, Behavioral and physiological thermoregulation of crocodilians. Amer. Zool, 1979 19: p. 239–247.

635. Smith JC, Ellenberger HH, Ballanyi K, Richter DW, and Feldman JL, Pre-Botzinger complex: a brainstem region that may generate respiratory rhythm in mammals. Science, 1991 254(5032): p. 726–9. [PubMed: 1683005]

636. Snyder GK, Respiratory adaptations in diving mammals. Respir Physiol, 1983 54(3): p. 269–94. [PubMed: 6369460]

637. Song A, Ashwell KW, and Tracey DJ, Development of the rat phrenic nucleus and its connections with brainstem respiratory nuclei. Anat Embryol (Berl), 2000 202(2): p. 159–77. [PubMed: 10985434]

638. Spicer DB, Rhee J, Cheung WL, and Lassar AB, Inhibition of myogenic bHLH and MEF2 transcription factors by the bHLH protein Twist. Science, 1996 272 (5267): p. 1476–1480. [PubMed: 8633239]

639. Spletter ML and Schnorrer F, Transcriptional regulation and alternative splicing cooperate in muscle fiber-type specification in flies and mammals. Experimental Cell Research, 2014 321(1): p. 90–8. [PubMed: 24145055]

640. Steyn FJ, Lee K, Fogarty MJ, Veldhuis JD, McCombe PA, Bellingham MC, Ngo ST, and Chen C, Growth hormone secretion is correlated with neuromuscular innervation rather than motor neuron number in early-symptomatic male amyotrophic lateral sclerosis mice. Endocrinology, 2013 154(12): p. 4695–706. [PubMed: 24108071]

641. Stowe CM and Good AL, Estimation of cardiac output by the direct Fick technique in domestic animals, with observations on a case of traumatic pericarditis. Am J Vet Res, 1961 22: p. 1093–6. [PubMed: 13917574]

642. Straus C, Vasilakos K, Wilson RJ, Oshima T, Zelter M, Derenne JP, Similowski T, and Whitelaw WA, A phylogenetic hypothesis for the origin of hiccough. Bioessays, 2003 25(2): p. 182–8. [PubMed: 12539245]

643. Symonds MR and Elgar MA, Phylogeny affects estimation of metabolic scaling in mammals. Evolution, 2002 56(11): p. 2330–3. [PubMed: 12487362]

644. Sypert GW and Munson JB, Basis of segmental motor control: Motoneuron size or motor unit type? Neurosurg, 1981 8(5): p. 608–621.

645. Tafti AK, Diaphragmatic hernia in a goat. Aust Vet J, 1998 76(3): p. 166. [PubMed: 9578749]

646. Tan NH, Ponnudurai G, and Mirtschin PJ, A comparative study of the biological properties of venoms from juvenile and adult inland taipan (Oxyuranus microlepidotus) snake venoms. Toxicon, 1993 31(3): p. 363–7. [PubMed: 8470140]

647. Tanaka H, Furuya T, Kameda N, Kobayashi T, and Mizusawa H, Triad proteins and intracellular Ca2+ transients during development of human skeletal muscle cells in aneural and innervated cultures. J Muscle Res Cell Motil, 2000 21(6): p. 507–26. [PubMed: 11206130]

648. Taylor CR, Structural and functional limits to oxidative metabolism: insights from scaling. Annu Rev Physiol, 1987 49: p. 135–46. [PubMed: 3551793]

649. Taylor CR, Karas RH, Weibel ER, and Hoppeler H, Adaptive variation in the mammalian respiratory system in relation to energetic demand: II. Reaching the limits to oxygen flow. Respir Physiol, 1987 69: p. 7–26.

650. Taylor CR, Longworth KE, and Hoppeler H, Matching O2 delivery to O2 demand in muscle: II. Allometric variation in energy demand. Adv Exp Med Biol, 1988 227: p. 171–81. [PubMed: 3289315]

651. Taylor CR, Maloiy GM, Weibel ER, Langman VA, Kamau JM, Seeherman HJ, and Heglund NC, Design of the mammalian respiratory system. III Scaling maximum aerobic capacity to body mass: wild and domestic mammals. Respir Physiol, 1981 44(1): p. 25–37. [PubMed: 7232885]

652. Taylor CR and Weibel ER, Design of the mammalian respiratory system. I. Problem and strategy. Respir Physiol, 1981 44: p. 1–10.

653. Taylor CR, Weibel ER, Weber JM, Vock R, Hoppeler H, Roberts TJ, and Brichon G, Design of the oxygen and substrate pathways. I. Model and strategy to test symmorphosis in a network structure. J Exp Biol, 1996 199(Pt 8): p. 1643–9. [PubMed: 8708571]

654. Taylor MP and Wedel MJ, Why sauropods had long necks; and why giraffes have short necks. PeerJ, 2013 1: p. e36. [PubMed: 23638372]

655. Taylor PM, Oxygen consumption in new-born rats. J Physiol, 1960 154: p. 153–68. [PubMed: 13775641]

656. Tenney SM and Remmers JE, Comparative quantitative morphology of the mammalian lung: diffusing area. Nature, 1963 197: p. 54–6. [PubMed: 13980583]

657. Tolep K, Higgins N, Muza S, Criner G, and Kelsen SG, Comparison of diaphragm strength between healthy adult elderly and young men. Am J Respir Crit Care Med, 1995 152(2): p. 677–82. [PubMed: 7633725]

658. Townsley MI, Structure and composition of pulmonary arteries, capillaries, and veins. Compr Physiol, 2012 2(1): p. 675–709. [PubMed: 23606929]

659. Trinidad JC, Fischbach GD, and Cohen JB, The Agrin/MuSK signaling pathway is spatially segregated from the neuregulin/ErbB receptor signaling pathway at the neuromuscular junction. J Neurosci, 2000 20(23): p. 8762–70. [PubMed: 11102484]

660. Truitt WA and Coolen LM, Identification of a potential ejaculation generator in the spinal cord. Science, 2002 297(5586): p. 1566–9. [PubMed: 12202834]

661. Tryba AK, Pena F, Lieske SP, Viemari JC, Thoby-Brisson M, and Ramirez JM, Differential modulation of neural network and pacemaker activity underlying eupnea and sigh-breathing activities. J Neurophysiol, 2008 99(5): p. 2114–25. [PubMed: 18287547]

662. Tyndale-Biscoe CH and Renfree MB, Reproductive Physiology of Marsupials. 1987, Cambridge: Cambridge University Press.

663. Ullah M, Localization of the phrenic nucleus in the spinal cord of the rabbit. J Anat, 1978 125: p. 377–386. [PubMed: 624684]

664. Uriona TJ and Farmer CG, Recruitment of the diaphragmaticus, ischiopubis and other respiratory muscles to control pitch and roll in the American alligator (Alligator mississippiensis). J Exp Biol, 2008 211(Pt 7): p. 1141–7. [PubMed: 18344489]

665. Vasilakos K, Kimura N, Wilson RJ, and Remmers JE, Lung and buccal ventilation in the frog: uncoupling coupled oscillators. Physiol Biochem Zool, 2006 79(6): p. 1010–8. [PubMed: 17041867]

666. Vasilakos K, Wilson RJ, Kimura N, and Remmers JE, Ancient gill and lung oscillators may generate the respiratory rhythm of frogs and rats. J Neurobiol, 2005 62(3): p. 369–85. [PubMed: 15551345]

667. Velten BP, Dillaman RM, Kinsey ST, McLellan WA, and Pabst DA, Novel locomotor muscle design in extreme deep-diving whales. J Exp Biol, 2013 216(Pt 10): p. 1862–71. [PubMed: 23393275]

668. Verheul AJ, Mantilla CB, Zhan WZ, Bernal M, Dekhuijzen PN, and Sieck GC, Influence of corticosteroids on myonuclear domain size in the rat diaphragm muscle. J Appl Physiol, 2004 97(5): p. 1715–22. [PubMed: 15234958]

669. Viemari JC and Hilaire G, Monoamine oxidase A-deficiency and noradrenergic respiratory regulations in neonatal mice. Neurosci Lett, 2003 340(3): p. 221–4. [PubMed: 12672546]

670. Viemari JC and Ramirez JM, Norepinephrine differentially modulates different types of respiratory pacemaker and nonpacemaker neurons. J Neurophysiol, 2006 95(4): p. 2070–82. [PubMed: 16394066]

671. Vizek M, Pickett CK, and Weil JV, Increased carotid body hypoxic sensitivity during acclimatization to hypobaric hypoxia. J Appl Physiol (1985), 1987 63(6): p. 2403–10. [PubMed: 3436874]

672. Vizzard MA, Brisson M, and de Groat WC, Transneuronal labeling of neurons in the adult rat central nervous system following inoculation of pseudorabies virus into the colon. Cell Tissue Res, 2000 299(1): p. 9–26. [PubMed: 10654066]

673. Vyas H, Milner AD, and Hopkins IE, Intrathoracic pressure and volume changes during the spontaneous onset of respiration in babies born by cesarean section and by vaginal delivery. J Pediatr, 1981 99(5): p. 787–91. [PubMed: 7299559]

674. Wagner PD, Symmorphosis or Dysmorphosis, in Oxygen Transport to Tissue XVI, Hogan MC, et al., Editors. 1994, Springer: Boston.

675. Wagner PD, Why doesn't exercise grow the lungs when other factors do? Exerc Sport Sci Rev, 2005 33(1): p. 3–8. [PubMed: 15640714]

676. Wait JL, Staworn D, and Poole DC, Diaphragm thickness heterogeneity at functional residual capacity and total lung capacity. J Appl Physiol (1985), 1995 78(3): p. 1030–6. [PubMed: 7775295]

677. Wallace MJ, Hooper SB, and Harding R, Regulation of lung liquid secretion by arginine vasopressin in fetal sheep. Am J Physiol, 1990 258(1 Pt 2): p. R104–11. [PubMed: 2301621]

678. Walters DV and Olver RE, The role of catecholamines in lung liquid absorption at birth. Pediatr Res, 1978 12(3): p. 239–42. [PubMed: 205826]

679. Wang NS, Anatomy of the pleura. Clin Chest Med, 1998 19(2): p. 229–40. [PubMed: 9646978]

680. Watchko JF, Daood MJ, and Sieck GC, Myosin heavy chain transitions during development. Functional implications for the respiratory musculature. Comp Biochem Physiol, 1998 119(3): p. 459–470.

681. Watchko JF, Daood MJ, Vazquez RL, Brozanski BS, LaFramboise WA, Guthrie RD, and Sieck GC, Postnatal expression of myosin isoforms in an expiratory muscle--external abdominal oblique. J Appl Physiol, 1992 73(5): p. 1860–1866. [PubMed: 1474062]

682. Webber CL, Wurster RD, and Chung JM, Cat phrenic nucleus architecture as revealed by horseradish peroxidase mapping. Exp Brain Res, 1979 35: p. 395–406. [PubMed: 456448]

683. Wedel MJ, Origin of postcranial skeletal pneumaticity in dinosaurs. Integr Zool, 2006 1(2): p. 80–5. [PubMed: 21395998]

684. Wedel MJ, Evidence for bird-like air sacs in saurischian dinosaurs. J Exp Zool A Ecol Genet Physiol, 2009 311(8): p. 611–28. [PubMed: 19204909]

685. Wedel MJ and Taylor MP, Caudal pneumaticity and pneumatic hiatuses in the sauropod dinosaurs Giraffatitan and Apatosaurus. PLoS One, 2013 8(10): p. e78213. [PubMed: 24205162]

686. Weibel ER, Morphometry of the Human Lung. 1963, New York: Academic.

687. Weibel ER, Physiology: the pitfalls of power laws. Nature, 2002 417(6885): p. 131–2. [PubMed: 12000943]

688. Weibel ER, Hsia CC, and Ochs M, How much is there really? Why stereology is essential in lung morphometry. J Appl Physiol, 2007 102(1): p. 459–67. [PubMed: 16973815]

689. Weibel ER, Taylor CR, and Hoppeler H, The concept of symmorphosis: a testable hypothesis of structure-function relationship. Proc Natl Acad Sci U S A, 1991 88(22): p. 10357–61. [PubMed: 1946456]

690. Weibel ER, Taylor CR, and Hoppeler H, Variations in function and design: testing symmorphosis in the respiratory system. Respir Physiol, 1992 87(3): p. 325–48. [PubMed: 1604056]

691. Weiss A, McDonough D, Wertman B, Acakpo-Satchivi L, Montgomery K, Kucherlapati R, Leinwand L, and Krauter K, Organization of human and mouse skeletal myosin heavy chain gene clusters is highly conserved. Proc Natl Acad Sci U S A, 1999 96(6): p. 2958–63. [PubMed: 10077619]

692. Weiss A, Schiaffino S, and Leinwand LA, Comparative sequence analysis of the complete human sarcomeric myosin heavy chain family: implications for functional diversity. J Mol Biol, 1999 290(1): p. 61–75. [PubMed: 10388558]

693. West GB, Brown JH, and Enquist BJ, A general model for the origin of allometric scaling laws in biology. Science, 1997 276(5309): p. 122–6. [PubMed: 9082983]

694. West JB, Why doesn't the elephant have a pleural space? News Physiol Sci, 2002 17: p. 47–50. [PubMed: 11909991]

695. White CR, Phillips NF, and Seymour RS, The scaling and temperature dependence of vertebrate metabolism. Biol Lett, 2006 2(1): p. 125–7. [PubMed: 17148344]

696. White J, Elapsid snakes: Aspects of envenomation, in Toxic Plants & Animals: a guide for Australia, Covacevich J, Davie P, and Pearn J, Editors. 1987, Queensland Museum: Brisbane.

697. Wilson RJ, Vasilakos K, and Remmers JE, Phylogeny of vertebrate respiratory rhythm generators: the Oscillator Homology Hypothesis. Respir Physiol Neurobiol, 2006 154(1–2): p. 47–60. [PubMed: 16750658]

698. Wilson TA and De Troyer A, Diagrammatic analysis of the respiratory action of the diaphragm. J Appl Physiol (1985), 2010 108(2): p. 251–5. [PubMed: 19940094]

699. Wilson TA, Legrand A, Gevenois PA, and De Troyer A, Respiratory effects of the external and internal intercostal muscles in humans. J Physiol, 2001 530(Pt 2): p. 319–30. [PubMed: 11208979]

700. Witton MP and Habib MB, On the size and flight diversity of giant pterosaurs, the use of birds as pterosaur analogues and comments on pterosaur flightlessness. PLoS One, 2010 5(11): p. e13982. [PubMed: 21085624]

701. Woods BA, Doe S, and Perks AM, Effects of epinephrine on lung liquid production by in vitro lungs from fetal guinea pigs. Can J Physiol Pharmacol, 1997 75(7): p. 772–80. [PubMed: 9315343]

702. Yokota S, Oka T, Tsumori T, Nakamura S, and Yasui Y, Glutamatergic neurons in the Kolliker-Fuse nucleus project to the rostral ventral respiratory group and phrenic nucleus: a combined retrograde tracing and in situ hybridization study in the rat. Neurosci Res, 2007 59(3): p. 341–6. [PubMed: 17888537]

703. Young IS, Alexander R, Woakes AJ, Butler PJ, and Anderson L, The synchronization of ventilation and locomotion in horses (Equus caballus). J Exp Biol, 1992 166: p. 19–31. [PubMed: 1602274]

704. Zajac FE and Faden JS, Relationship among recruitment order, axonal conduction velocity, and muscle-unit properties of type-identified motor units in cat plantaris muscle. J Neurophysiol, 1985 53(5): p. 1303–1322. [PubMed: 2987433]

705. Zamora IJ, Olutoye OO, Cass DL, Fallon SC, Lazar DA, Cassady CI, Mehollin-Ray AR, Welty SE, Ruano R, Belfort MA, and Lee TC, Prenatal MRI fetal lung volumes and percent liver herniation predict pulmonary morbidity in congenital diaphragmatic hernia (CDH). J Pediatr Surg, 2014 49(5): p. 688–93. [PubMed: 24851749]

706. Zengel JE, Reid SA, Sypert GW, and Munson JB, Membrane electrical properties and prediction of motor-unit type of medial gastrocnemius motoneurons in the cat. J Neurophysiol, 1985 53(5): p. 1323–1344. [PubMed: 3839011]

707. Zhan WZ, Farkas GA, Schroeder MA, Gosselin LE, and Sieck GC, Regional adaptations of rabbit diaphragm muscle fibers to unilateral denervation. J. Appl. Physiol, 1995 79: p. 941–950. [PubMed: 8567538]

708. Zhan WZ, Miyata H, Prakash YS, and Sieck GC, Metabolic and phenotypic adaptations of diaphragm muscle fibers with inactivation. J Appl Physiol, 1997 82(4): p. 1145–53. [PubMed: 9104851]

709. Zhang W, Behringer RR, and Olson EN, Inactivation of the myogenic bHLH gene MRF4 results in up-regulation of myogenin and rib anomalies. Genes Dev, 1995 9: p. 1388–1399. [PubMed: 7797078]

710. Zhang W, Carreno FR, Cunningham JT, and Mifflin SW, Chronic sustained hypoxia enhances both evoked EPSCs and norepinephrine inhibition of glutamatergic afferent inputs in the nucleus of the solitary tract. J Neurosci, 2009 29(10): p. 3093–102. [PubMed: 19279246]

711. Zholudeva LV, Karliner JS, Dougherty KJ, and Lane MA, Anatomical Recruitment of Spinal V2a Interneurons into Phrenic Motor Circuitry after High Cervical Spinal Cord Injury. J Neurotrauma, 2017 34(21): p. 3058–3065. [PubMed: 28548606]

712. Zhu X, Lai C, Thomas S, and Burden SJ, Neuregulin receptors, erbB3 and erbB4, are localized at neuromuscular synapses. EMBO J, 1995 14(23): p. 5842–8. [PubMed: 8846777]

713. Zimmermann T, [An unusual trauma in labor: diaphragmatic rupture]. Zentralbl Gynakol, 1999 121(2): p. 92–4. [PubMed: 10096176]

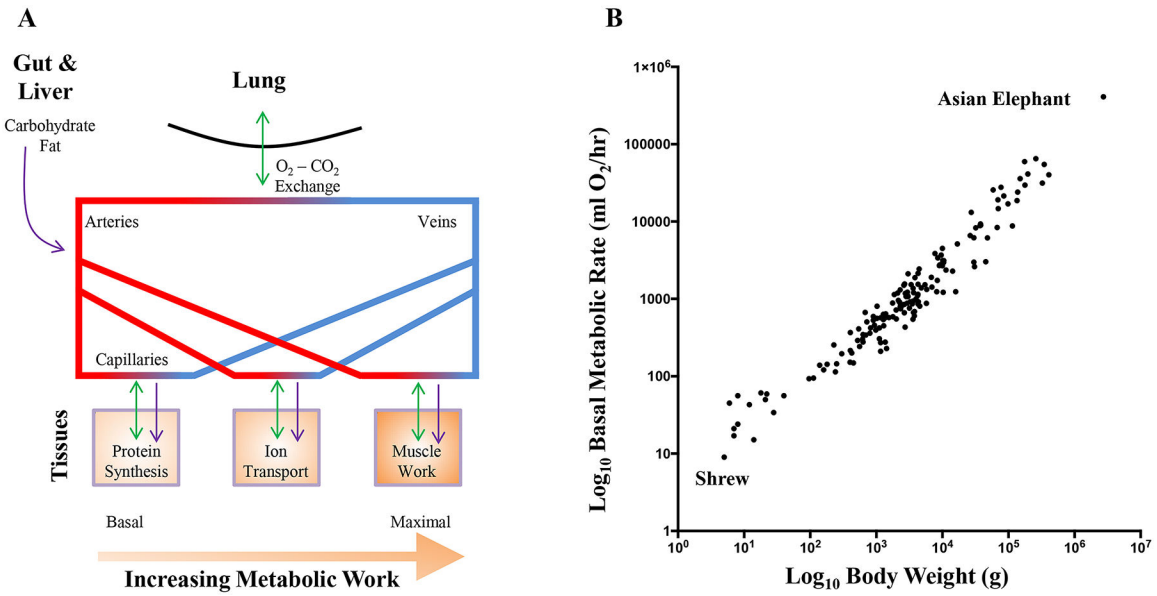

Figure 1:

Cells require energy substrates to function, even at basal levels of low metabolic work (**A**). The major energy substrate for ATP production is oxygen (O_2), supplies by gaseous exchange within the lung. Other major energy substrates include carbohydrates and fats, delivered via the arterial circulation from sources within the gastrointestinal tract and liver. At the level of the capillaries, cells uptake these energy substrates and excrete waste products of ATP generation, including carbon dioxide (CO_2), which is returned to the atmosphere during gaseous exchange. Metabolic work increases the requirement for ATP, and during muscle activity, gaseous exchange must be increased in order to cope with the increased demand for O_2 and removal of CO_2. **B** shows the allometric relationship of basal metabolic rate against body weight. Adapted from data within refs 105, 159, 229, 258, 451, 463, 568, 643 and 693.

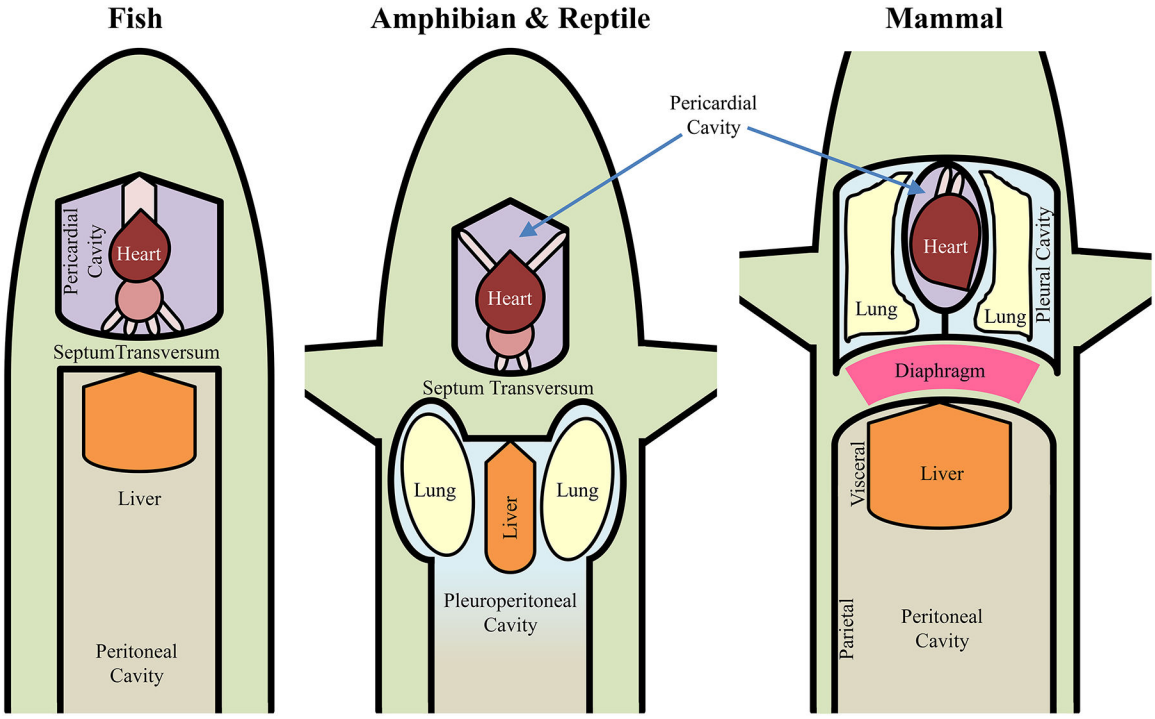

Figure 2:

The septum transversum is found in all vertebrates, and serves as a partition to separate the heart and pericardium from the peritoneum of the abdominal cavity. It forms in relation to the pericardium and folds caudally in association with the liver. In fish, the septum transversum divides the pericardial and peritoneal cavities. In amphibians and reptiles, it divides the pericardial cavity and the common pleuroperitoneal cavity, which contains the lungs, urogenital and visceral abdominal organs. In the mammals, the septum transversum, now muscularized in the form of the diaphragm muscle, extends the entire span of the body cavity, forming a separation between the collection of the pericardial and pleural (containing the lung) cavities and the peritoneal cavity (i.e. a thoracic cavity and an abdominal cavity). By partitioning separate abdominal and thoracic cavities, smaller relative abdominal and thoracic spaces are created, which improves the efficiency of P_{ab} and P_{th} generation. Note that in fish, amphibians and most reptiles, this partition is incomplete and less efficient. In advanced reptiles and all mammals, a complete separation of the thoracic and abdominal cavities is achieved, with this separation being muscularized in the case of mammals, the diaphragm muscle. After Kingsley [351].

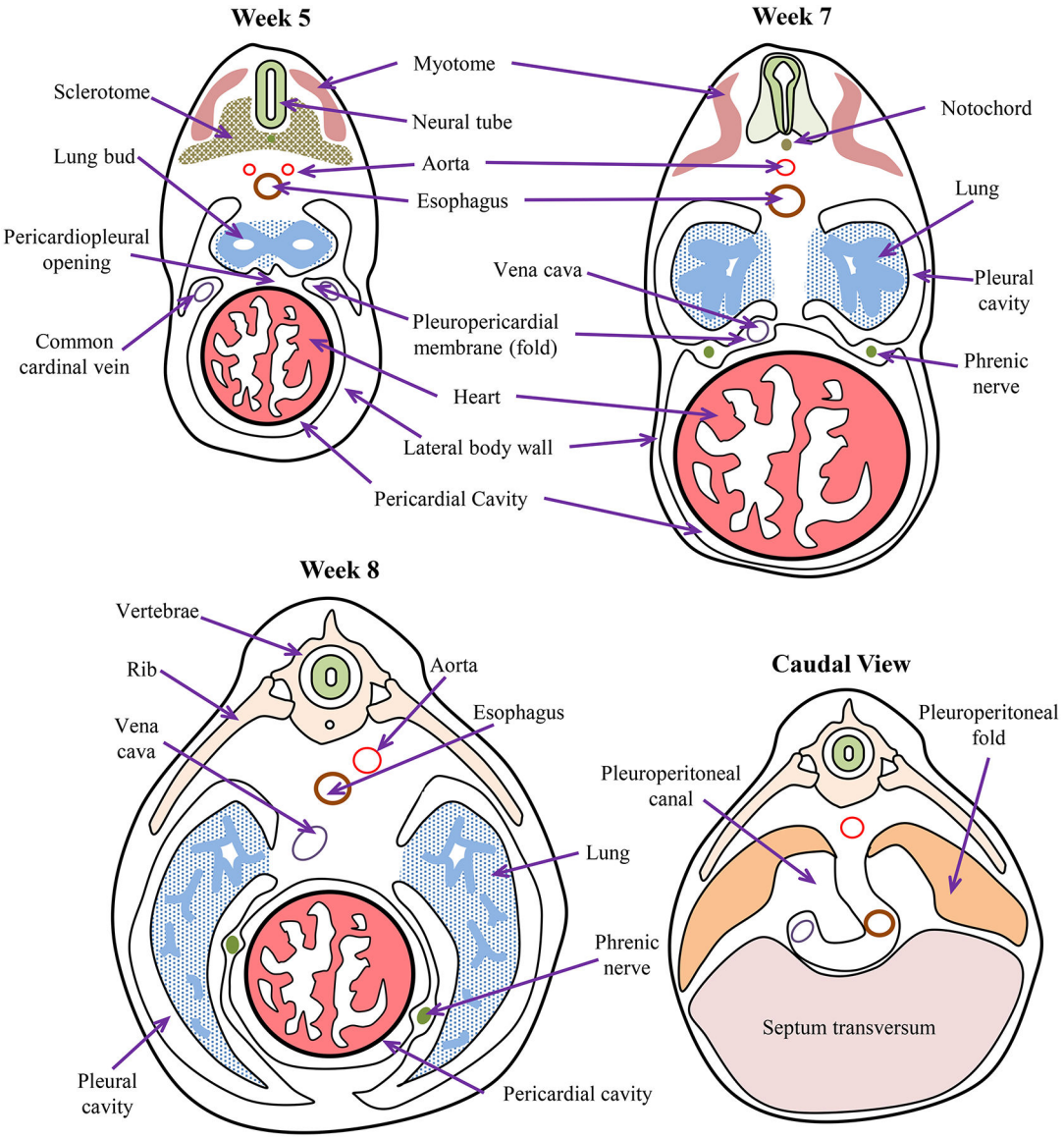

Figure 3:

Embryonic timeline of body cavity formation in humans. By week 5, pleuroperitoneal membranes are a pair of membranes which gradually separate the pleural and peritoneal cavities, produced as the pleural cavities expand by invading the body wall. The pleuropericardial membranes separate the developing heart from the developing lung buds. Pleuropericardial membranes initially appear as small folds or ridges projecting into the primitive undivided thoracic cavity. The folds contain the common cardinal veins which drain the primitive venous system into the sinus venosus of the primitive heart. During week 6, the edges of these membranous folds have fused with the dorsal mesentery of the esophagus and with the septum transversum to separate the pleural and pericardial cavities. As the heart descends and the pleural cavities expand, the membranes are drawn out in a mesentery like fold that extends from the lateral wall. By week 7, these membranes fuse with the mesoderm ventral to the esophagus, forming a single pericardial cavity and left and

right pleural cavities. During week 8, the lung buds grow into the medial walls of the nascent pleural cavities; and the pleural cavities expand around the heart into the body wall. After Pansky [496].

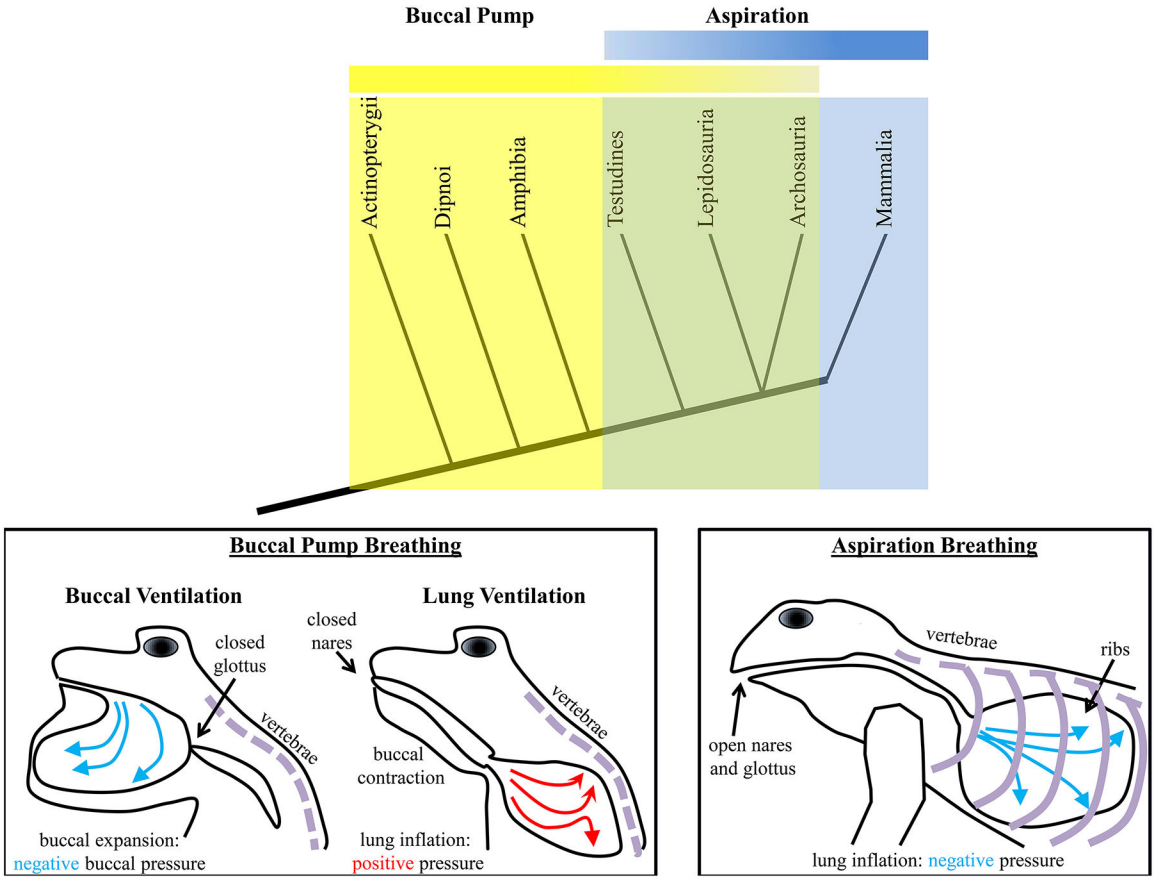

Figure 4:

The evolution of air breathing occurred before the evolution of aspiration breathing. The simplified clade diagram shows that ray-finned fishes (actinoptarygii) employed buccal pump ventilation of the gills. Air breathing lungfish (dipnoi) and amphibians also employed this mechanism of ventilation, which involved buccal expansion to draw air into the oral cavity under negative pressure, followed by buccal compression, with a closed mouth and nares to inflate lungs under positive pressure. Turtles (testudines), scaled reptiles (lepidosauria), crocodiles (archosauria – also includes birds) and mammals all breathe using an aspiration mechanism, whereby the lungs are inflated with a negative intra-thoracic pressure. Importantly, aspiration breathing requires ribs being attached to the vertrebrae. The ribs serve to stabilize the coelomic cavity for walking and act as a bellows for aspiration. The evolution of aspiration breathing occurred some point between emergence of amphibians and reptiles, though in some reptiles, buccal breathing mechanisms are employed intermittently.

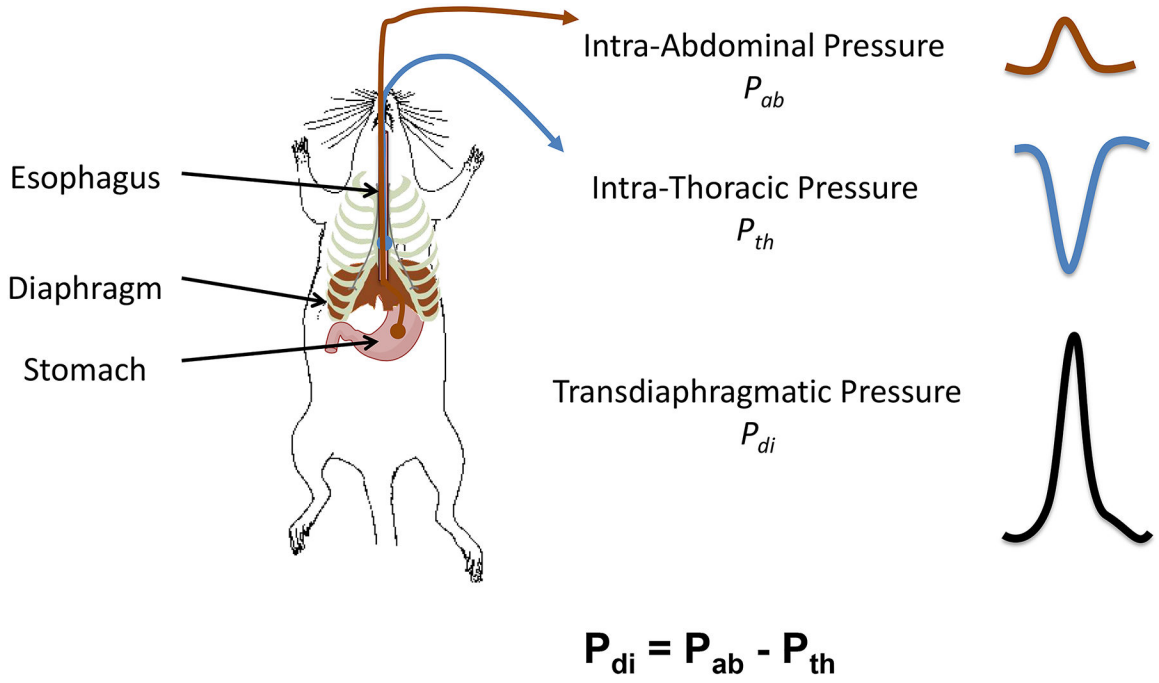

Figure 5:

Anatomical schematic showing placement of the solid-state pressure catheters for measurement of esophageal intra-thoracic (P_{th}) and gastric intra-abdominal (P_{ab}) pressures in rodents. As the DIAm contracts it moves caudally, creating a negative P_{th} and inspiratory airflow and a positive P_{ab}. The resulting transdiaphragmatic pressure ($P_{di} = P_{ab} – P_{th}$) reflects DIAm force generation.

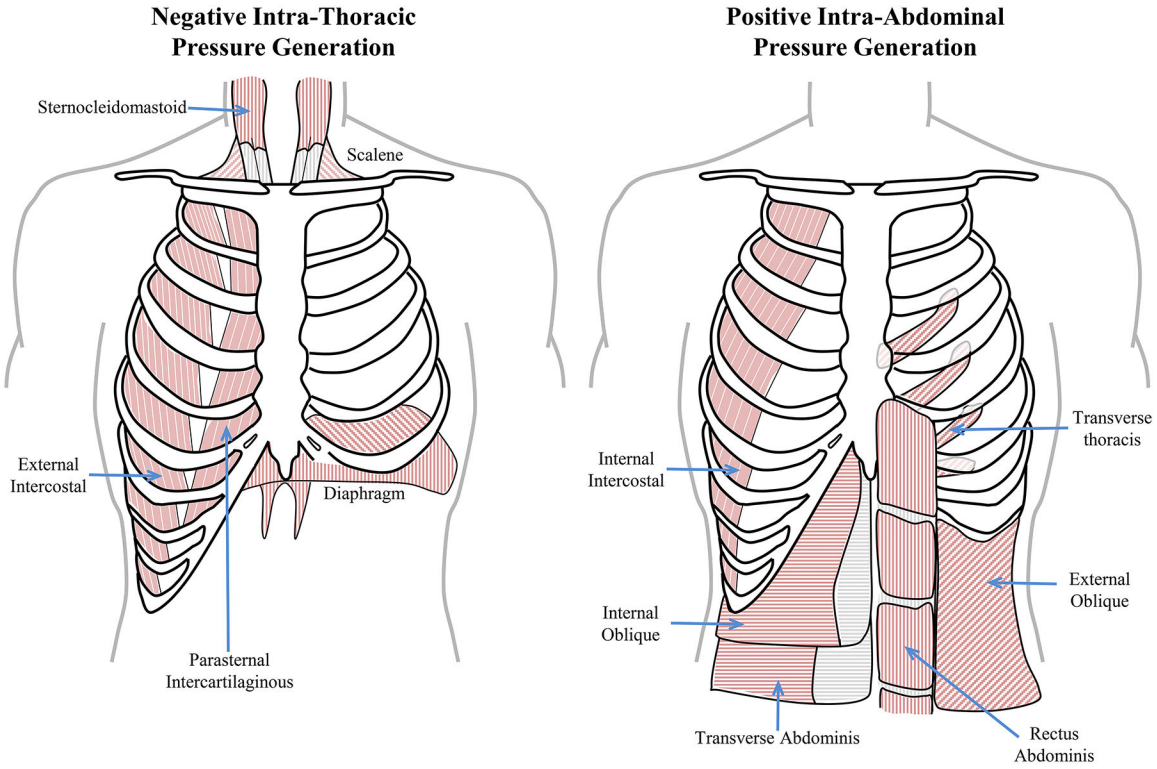

Figure 6:

The muscles of the thoracic wall provide for radial expansion of the chest wall (the external intercostal muscles), cranial expansion of the ribcage (parasternals, sternocleidomastoid and scalene) and caudal expansion of the thoracic cavity (the diaphragm muscle). In concert these provide for the generation of negative intra-thoracic pressures. The muscles of the abdominal walls include the lateral (internal intercostal, internal oblique, external oblique and transverse abdominal muscles) and ventral walls (the rectus abdominis and transverse thoracis), that serve to increase intra-abdominal pressured by compressing the abdomen. The cranial wall of the abdominal cavity is provided by the diaphragm muscle, which when activated reduces the cranial extent of the abdominal cavity, thus increasing intra-abdominal pressures.

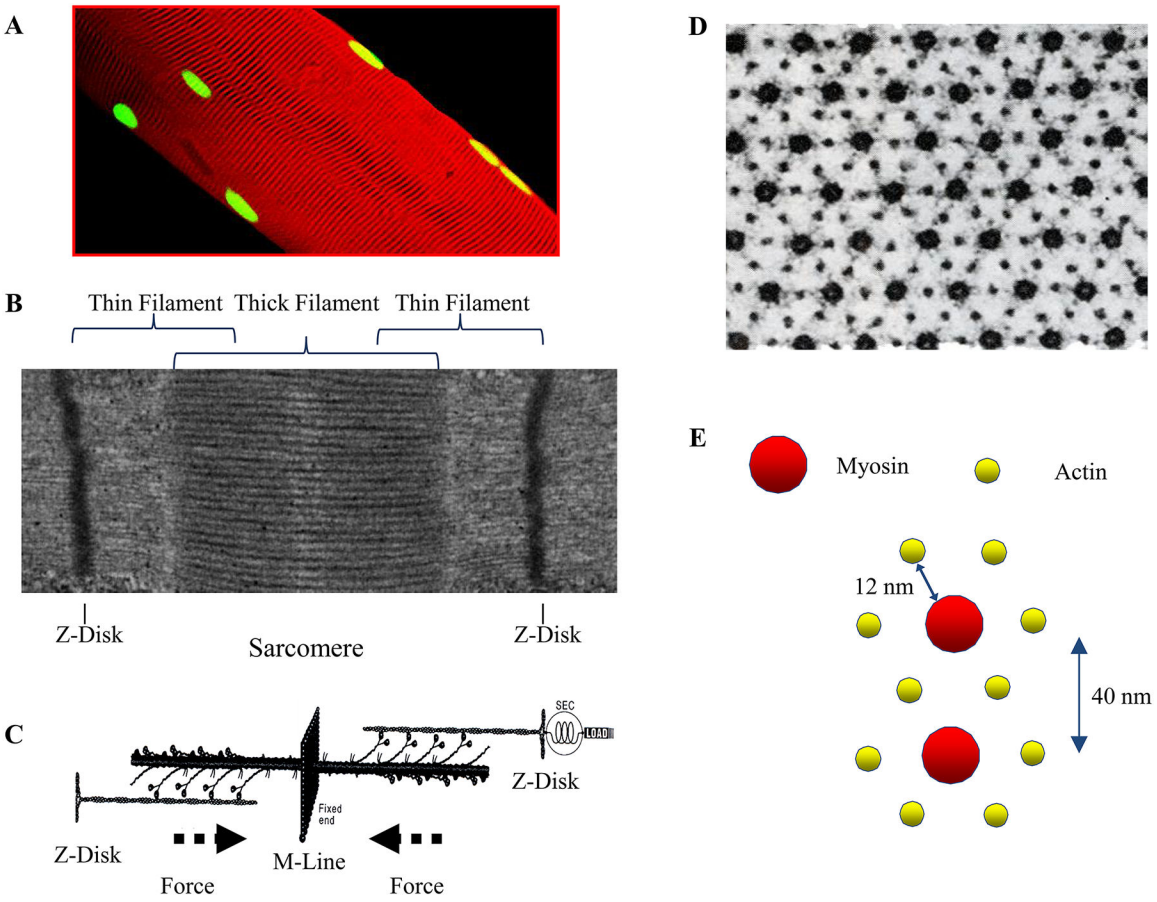

Figure 7:

Single multinucleated (green, propidium iodide myonuclear stain) diaphragm muscle fibers (**A**) exhibit striated sarcomeric structures (membrane stained with RH414, red). These striations comprise of the thin (actin) and thick filaments (myosin) seen in transmission electron micrographs (**B**). In response to Ca^{2+}, overlapping filaments undego cross-bridge formation, driving the production of force. The mechanical cycling of cross bridges causes a force vector from the Z-disc towards the midline of the sarcomere (**C**). The electron micrograph of a skeletal muscle cross-section (**D**) shows the classical myofilament lattice spacing. The larger structures are the myosin filaments, each surrounded by six smaller actin filaments (**E**). Each actin filament is surrounded by three myosin filaments, and two actin filaments are shared by any given myosin filament. Thus arrangement allows for the doubled hexagonal crystalline array of the myofilament lattice, the distance between the center of the myosin filament and the center of an adjacent actin filament is 12 nm. The distance between the centers of adjacent myosin filaments is 40 nm. Adapted from elements within ref 608 and 615.

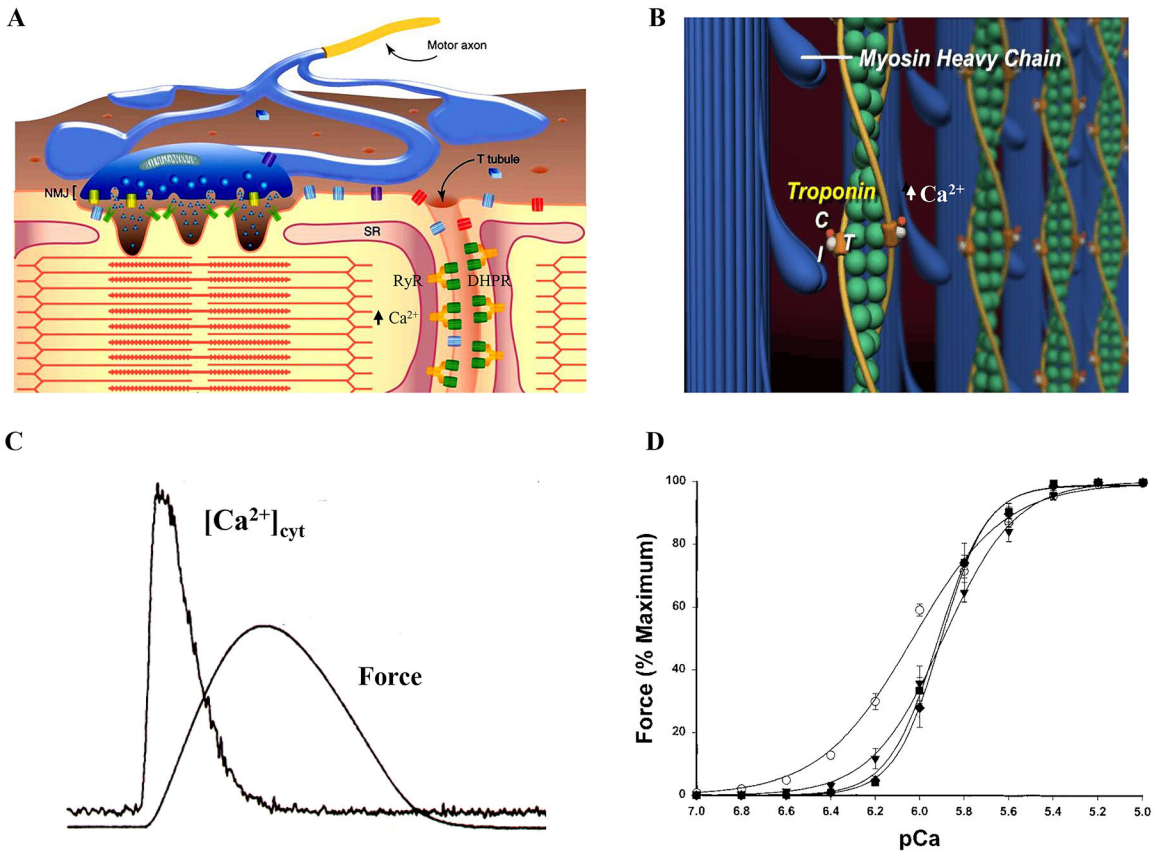

Figure 8:

Excitation-contraction coupling is mediated by the sarcoplasmic reticulum, which acts as a store for Ca^{2+} (**A**). Within the T-tubules, depolarization waves activate dihydropyridine receptors (DHPRs; voltage sensitive L-type Ca2+ channels), which in turn induces an initial ryanodine receptor (RyR) mediated Ca^{2+} release. A positive feedback process induces further Ca^{2+}-induced Ca^{2+} release. This process rapidly floods the cytosolic space surrounding contractile proteins with free Ca^{2+}, eventually binding to troponin C, removing the steric hindrance and allowing for cross-bridge formation (**B**). This regulation of myosin attachment to actin also involves troponin T (TnT), which binds the troponin complex to the tropomyosin molecule and troponin I (TnI) that actually blocks the actin binding site. Release of Ca^{2+} to the cytosol is followed by the development of muscle fiber force (**C**). The Ca^{2+} binding of troponin complexes regulate the attachment of myosin heads to actin and thus regulate force generation, as reflected by a sigmoidal force-Ca^{2+} relationship. Adapted from elements within refs 224, 608 and 615.

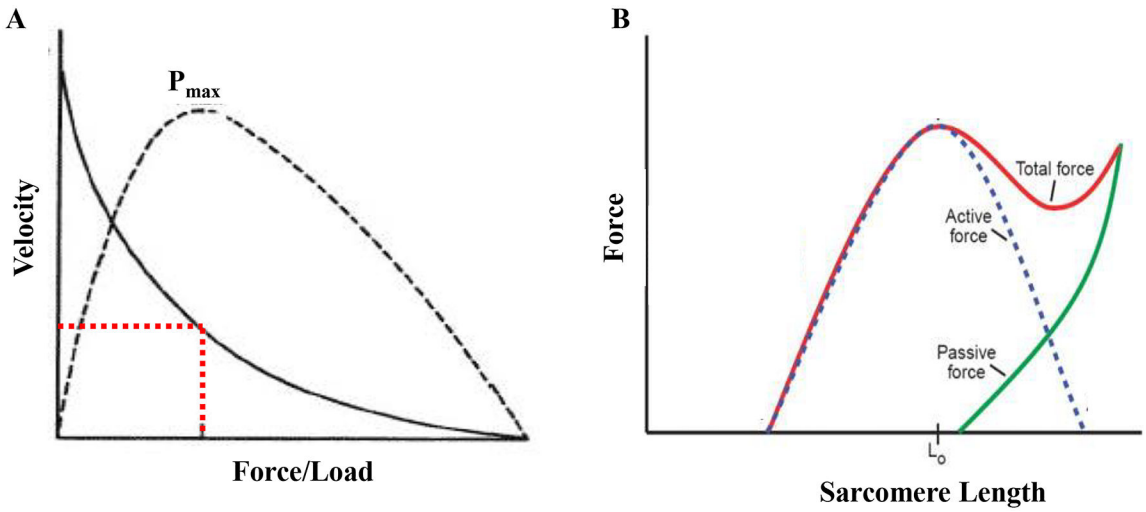

Figure 9:

In the DIAm, maximal power output is achieved at ~30% of maximal shortening velocity and ~30% of maximal force generation/load (**A**). The force a muscle fiber generates is related to its length (B). At sub-optimal lengths, not all actin and myosin elements are able to form cross-links, thus force is limited. At optimal length (L_o), maximal actin and myosin cross bridge formation is possible, thus force generation is maximal. Beyond this length, passive tension (stretch) causes reduction in the possible number of cross-bridges able to be formed and active force generation is reduced. Adapted from elements within refs 615, 619 and 620.

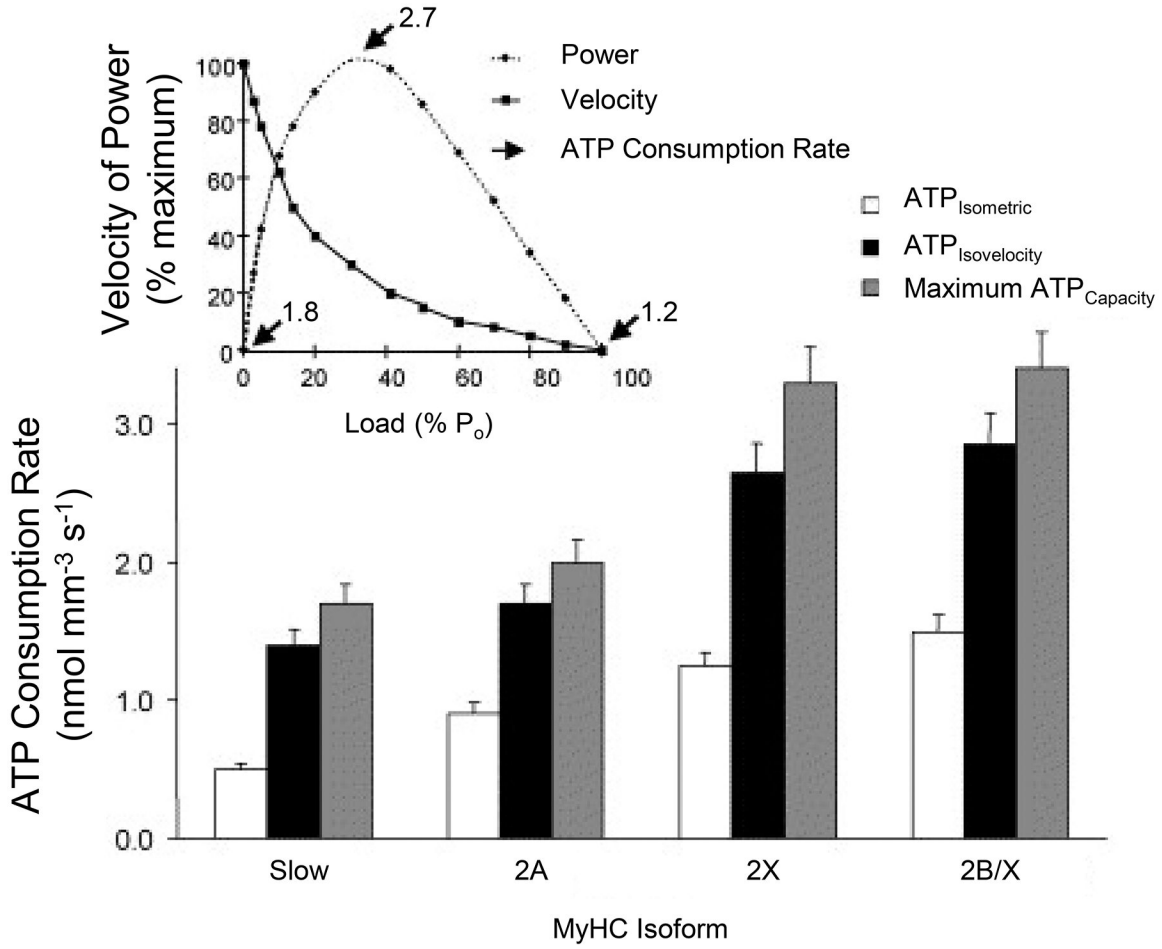

Figure 10:

Peak ATP consumption rates (2.7 nmol mm^{-3} s^{-1}) occur at peak power output for diaphragm muscle (top graph). Within different diaphragm muscle fiber types, ATP consumption varies according to MyHC concentration (increasing with increased MyHC) and the apparent rate of cross-bridge detachment (lower graph). Adapted from ref 543.

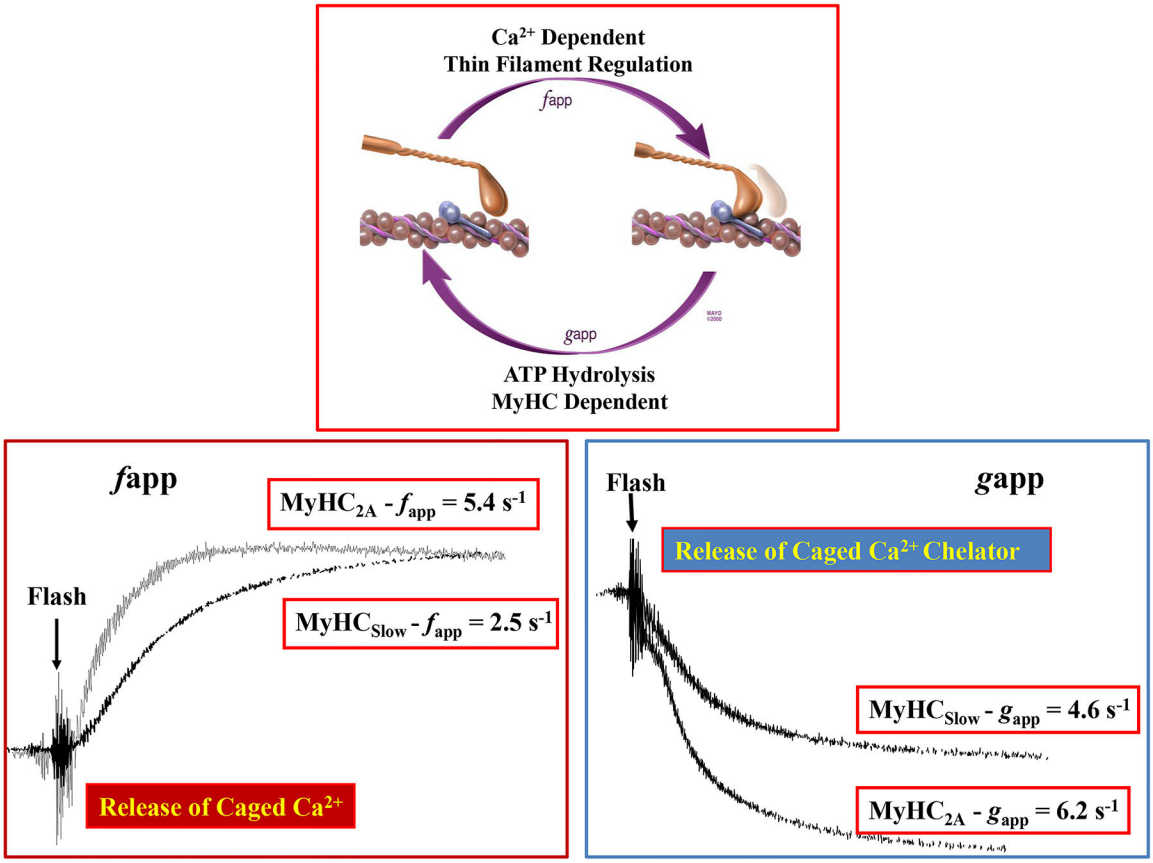

Figure 11:

Cross-bridges cycle between a strongly bound and an unbound state during force generation and contraction. Cross-bridge cycling determines rates of cross-bridge attachment (f_{app}) and detachment (g_{app}). The rate of force development (f_{app}) and cross-bridge cycling (g_{app}) in $MyHC_{2A}$-expressing fibers is greater than that of $MyHC_{SLOW}$- expressing fibers. Adapted from ref 608.

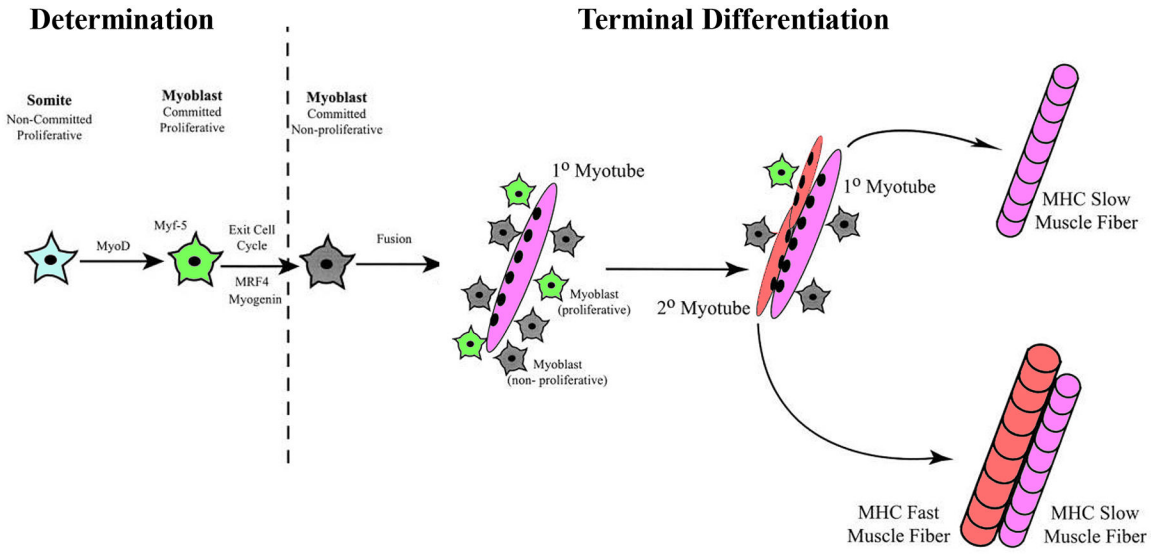

Figure 12:

During the determination phase of myogenesis, stem cells divide and are committed to myoblasts, a process requiring expression of the regulatory factors MyoD and Myf-5. Subsequently, myoblast that are non-proliferative fuse to form primary myotubes, which eventually become muscle fibers that express $MyHC_{SLOW}$. Primary myotubes that have further fusion of non-proliferative myoblasts become secondary myotubes. These myotubes develop into muscle fibers capable of expressing $MyHC_{SLOW}$ or any of the fast MyHC isoforms.

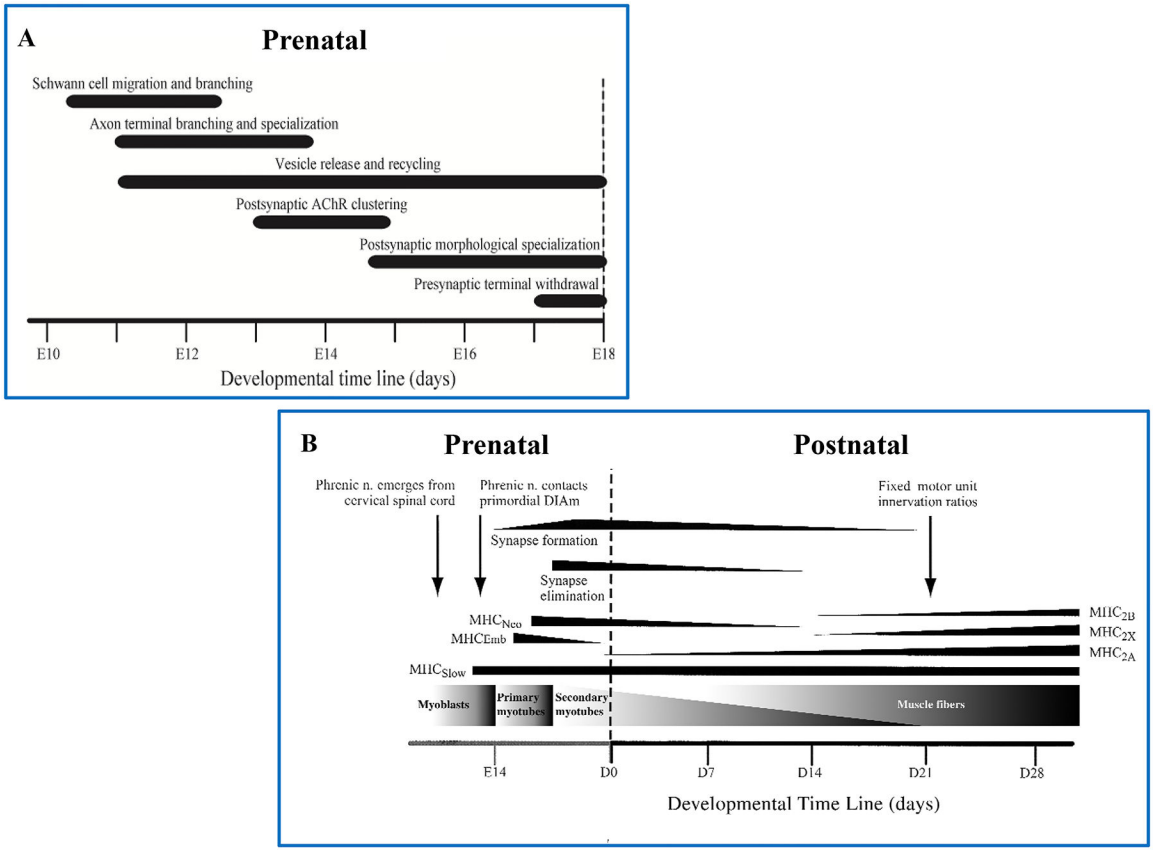

Figure 13:

The prenatal determination of phrenic nerve emergence, axon terminal vesicular release and neuromuscular junction specialization is independent of muscle cells until embryonic (E) day 13, where it contacts the primordial DIAm (**A**). Muscle development and synaptic formations then enter into a state of co-dependence with nerve (**B**), with the establishment of adult muscle fiber types, innervation ratios and the lack of polyneuronal innervation (synapse elimination) occurring postnatally (**B**). Adapted from ref 425.

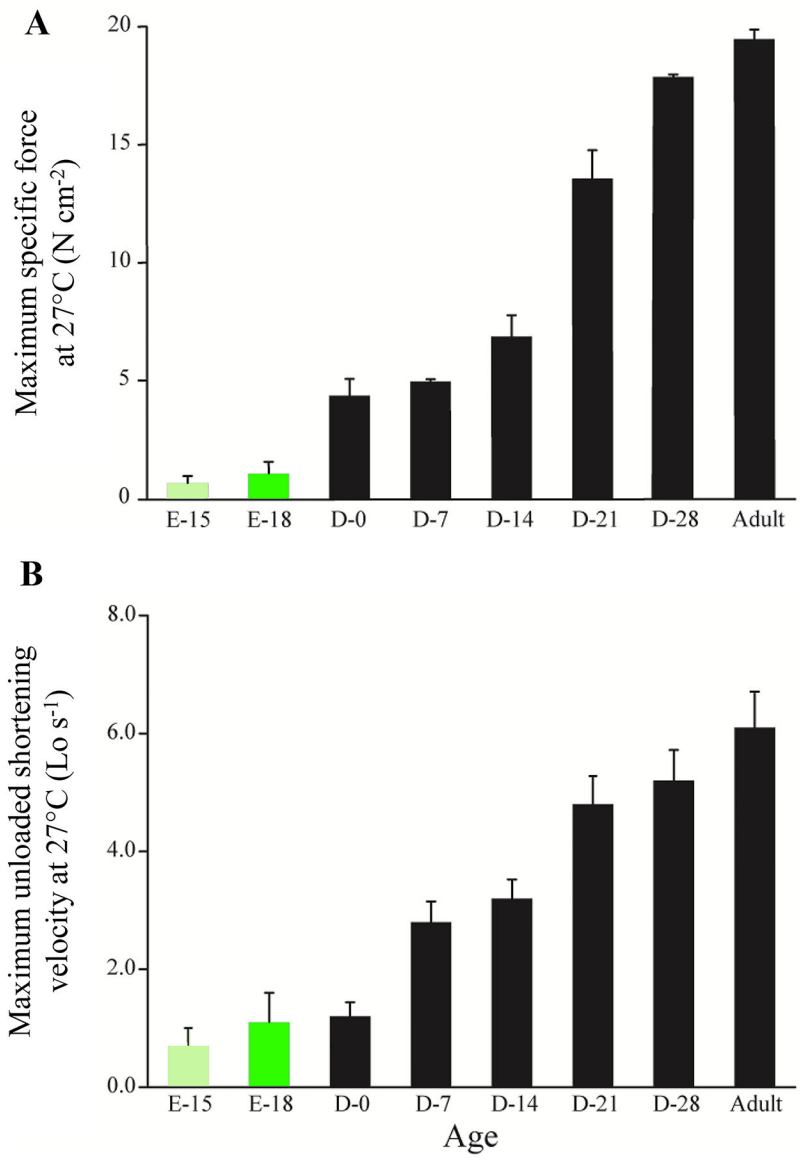

Figure 14:

Pre- and postnatal developmental changes in maximum DIAm specific force (normalized to muscle cross-sectional area) show a ~20-fold increase from embryonic to adult (**A**). The maximum velocity of DIAm shortening increases ~5-fold in the same timespan (**B**). Adapted from refs 222 and 219.

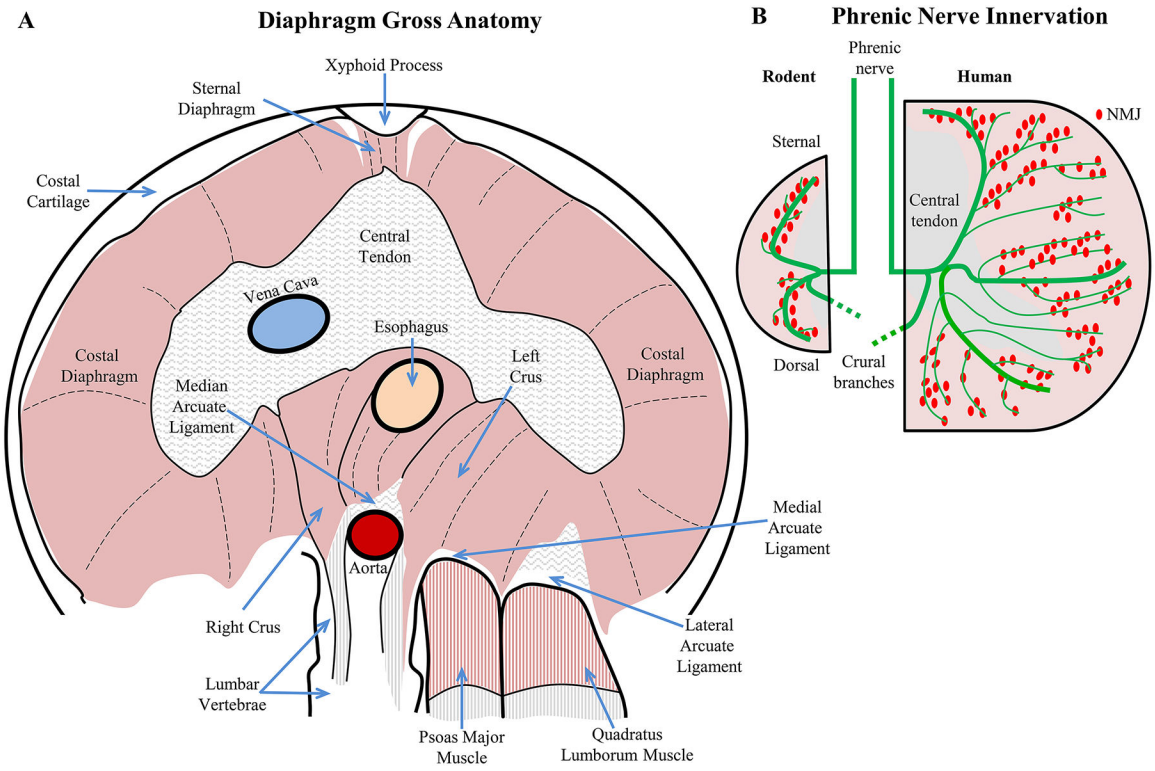

Figure 15:

The abdominal view of the DIAm (**A**) clearly shows the vena cava and aortic vessels passing through the central tendon and aortic hiatus, respectively. The esophagus passes through the left and right crus of the DIAm, forming the esophageal sphincter. The crus inset on the lumbar vertebrae caudal to the thoracic vertebrae where the ribs articulate, helping to create the domed structure of the DIAm. After Downey [152]. There is a marked difference in phrenic nerve branching and neuromuscular junction (NMJ) innervation of the diaphragm in small and large species, such as rats and humans (**B**). In rats, the NMJ innervation is very linear. In humans and other larger species, there is less linearity to the NMJ innervations and more numerous and elaborate secondary phrenic nerve branching.

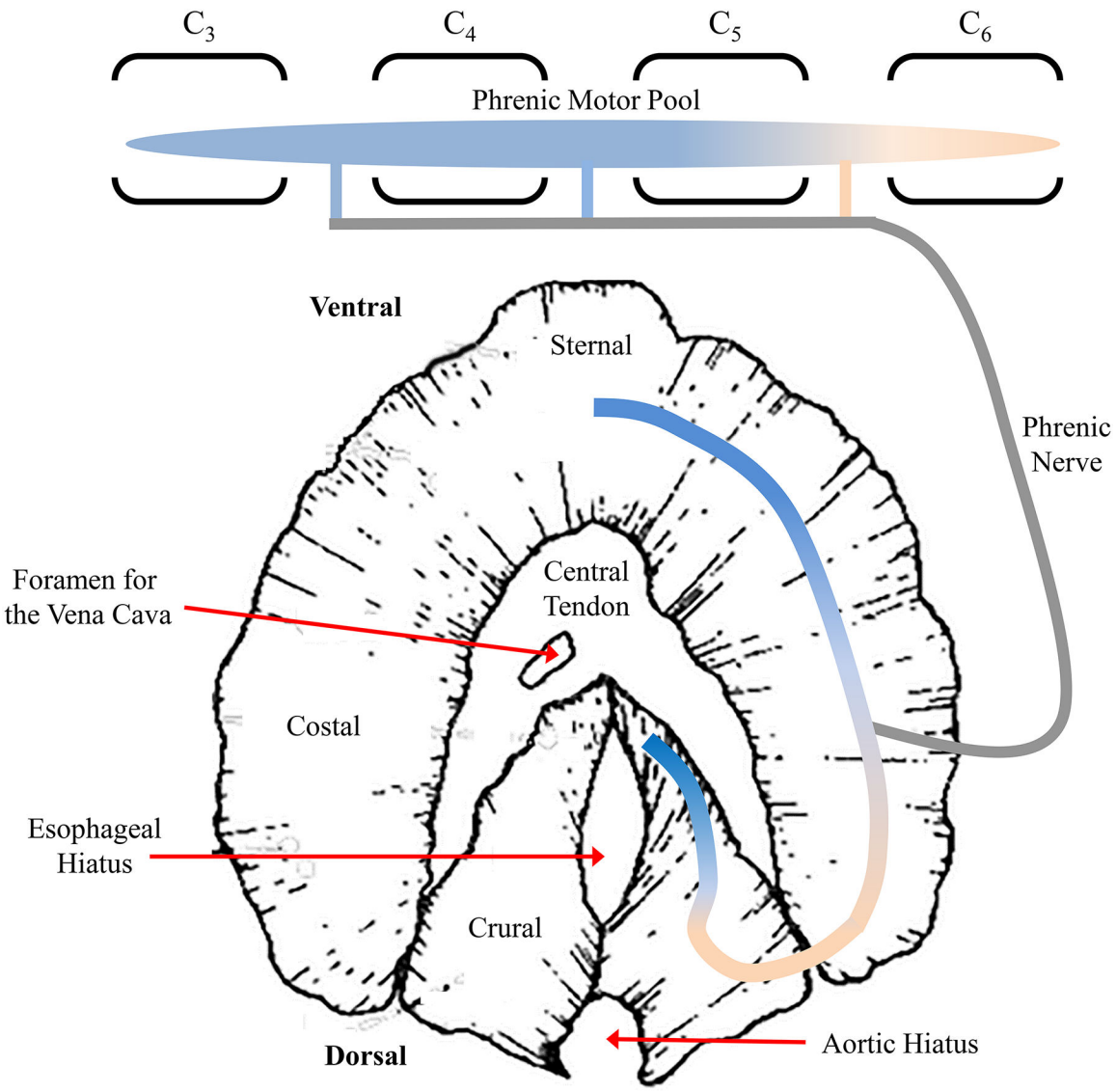

Figure 16:

The DIAm consists of four major anatomical divisions, the sternal, costal and crural muscular regions and the central tendon. The DIAm is innervated via the phrenic nerve, emanating from C_3-C_6. Innervation of the DIAm exhibits somatotopy, where phrenic motor neurons from the cranial regions of the phrenic motor pool innervate the more ventral sternal and ventral costal regions. Phrenic motor neurons from the more caudal portion of the phrenic motor neuron pool innervate the dorsal costal and dorsal crural regions of the DIAm. This figure has been amended from ref 608.

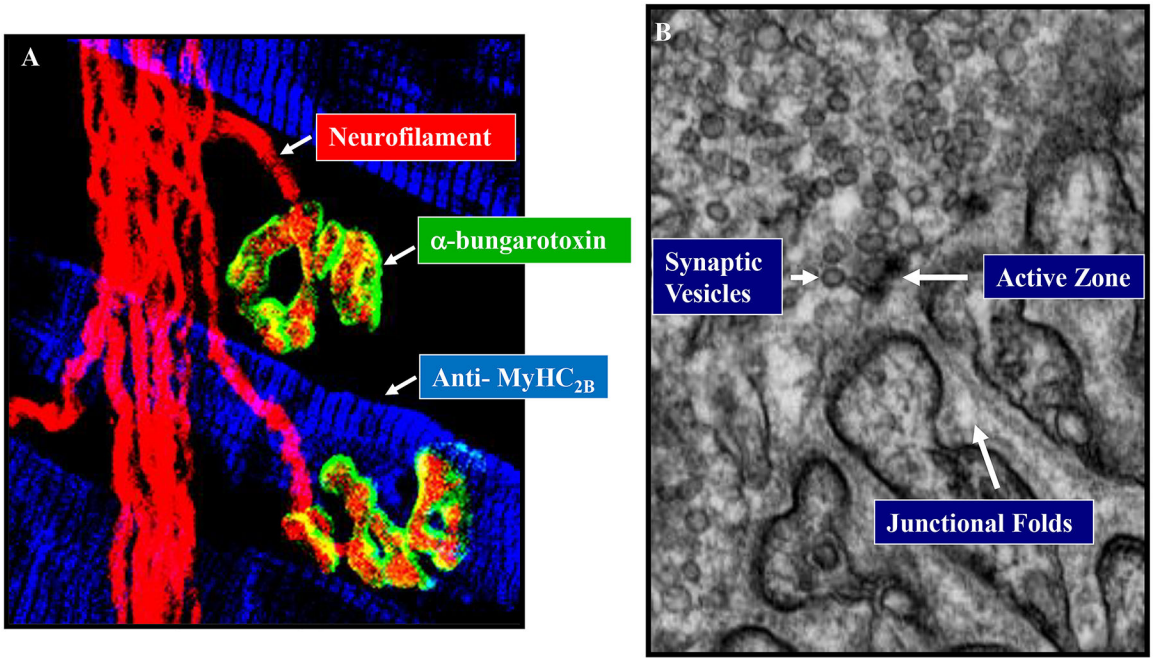

Figure 17:

Signaling between the phrenic nerve and the DIAm occurs across the neuromuscular junction. Neurofilament (red), labels phrenic nerve axons (presynaptic), with α-bungarotoxin labeling the postsynaptic acetylcholine receptors (green) on muscle fibers (with $MyHC_{2B}$ expressing fibers labeled in blue) (**A**). The ultrastucture of the neuromuscular junction is illustrated using electron microscopy, with synaptic vesicles (acetylcholine) released at active zones via exocytosis into the junctional fold (**B**). Adapted from ref 425.

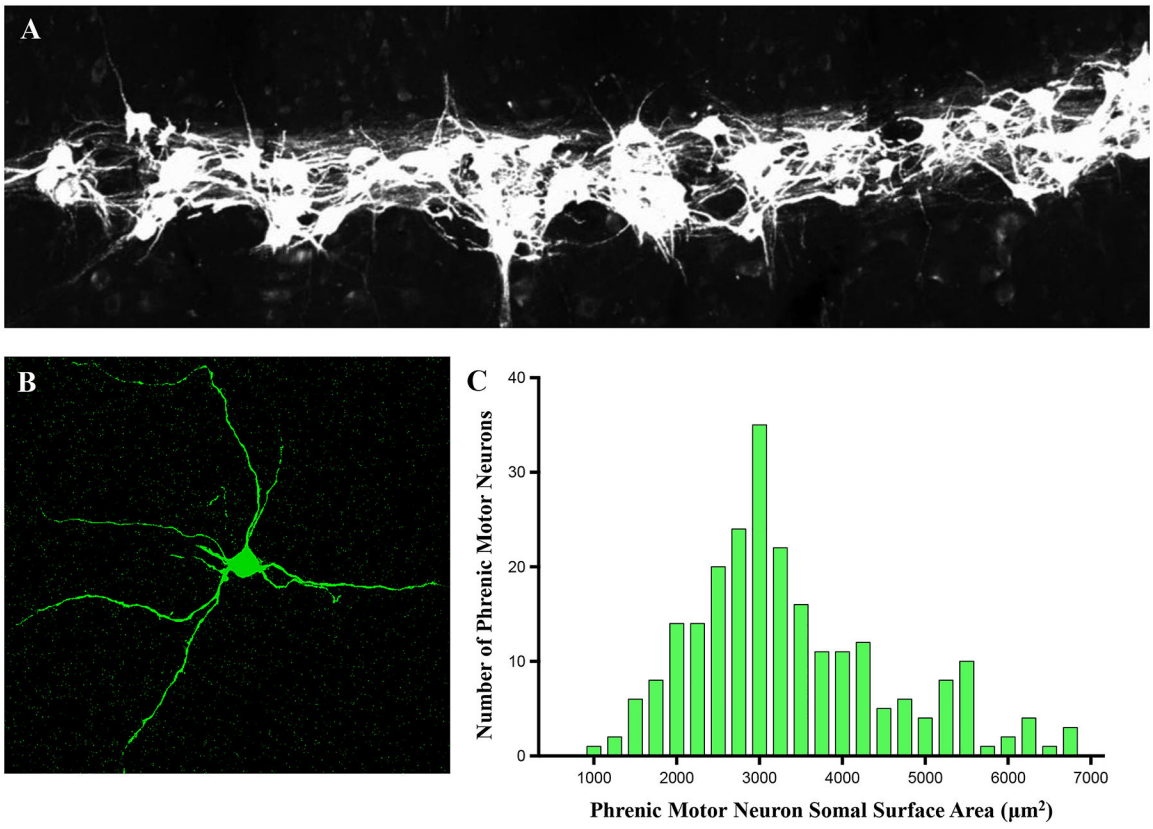

Figure 18:

Phrenic motor neurons exist bilaterally in the cervical spinal cord (~C_{3-6}) and are readily labeled by intrapleural injection of fluorescently-conjugated cholera-toxin subunit B (**A**). Phrenic motor neurons have extensive dendritic arborisations (**B**) and exhibit a large heterogeneity in somatic surface areas (**C**), passive electrical properties which largely determine motor unit recruitment order.

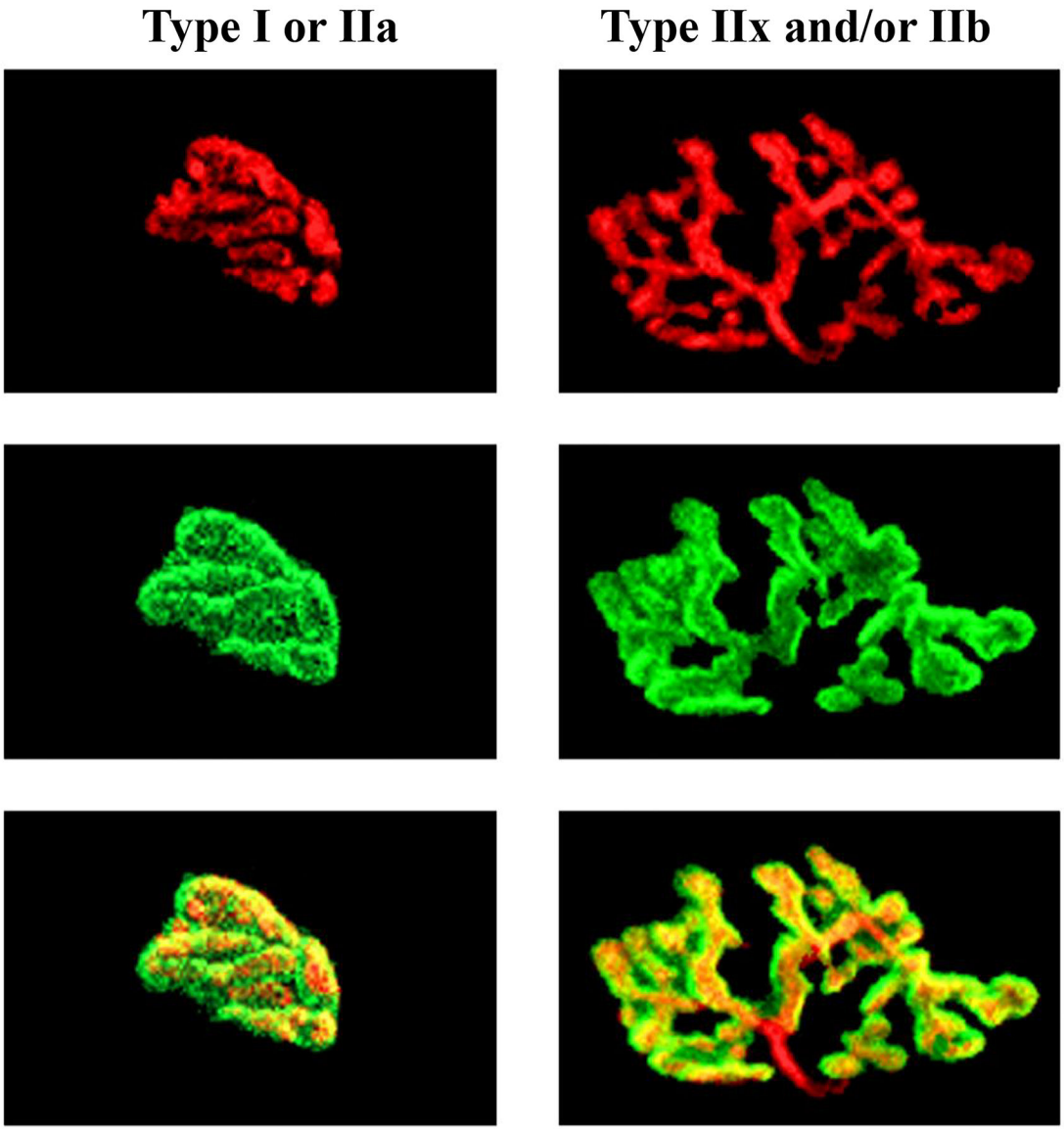

Figure 19:

Different motor unit types exhibit different size and complexity of presynaptic axon terminal (red) and postsynaptic acetylcholine receptor (green) structures. Note that neuromuscular junctions of type IIx and/or IIb muscle fibers are markedly larger and more complex compared to neuromuscular junctions of type I or IIa muscle fibers.

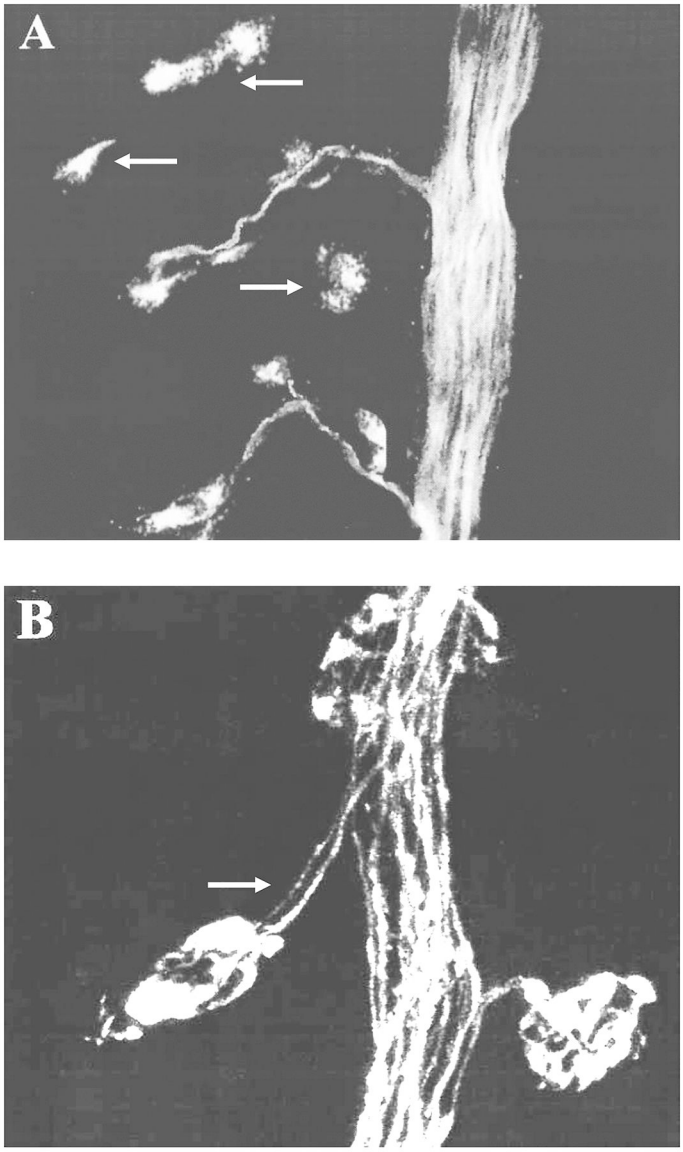

Figure 20:

At E16, many postsynaptic acetylcholine receptor clusters are not innervated yet by axons (arrows in **A**). At birth, polyneuronal innervation of one acetylcholine receptor cluster by two motor axons is clearly shown (arrow in **B**).

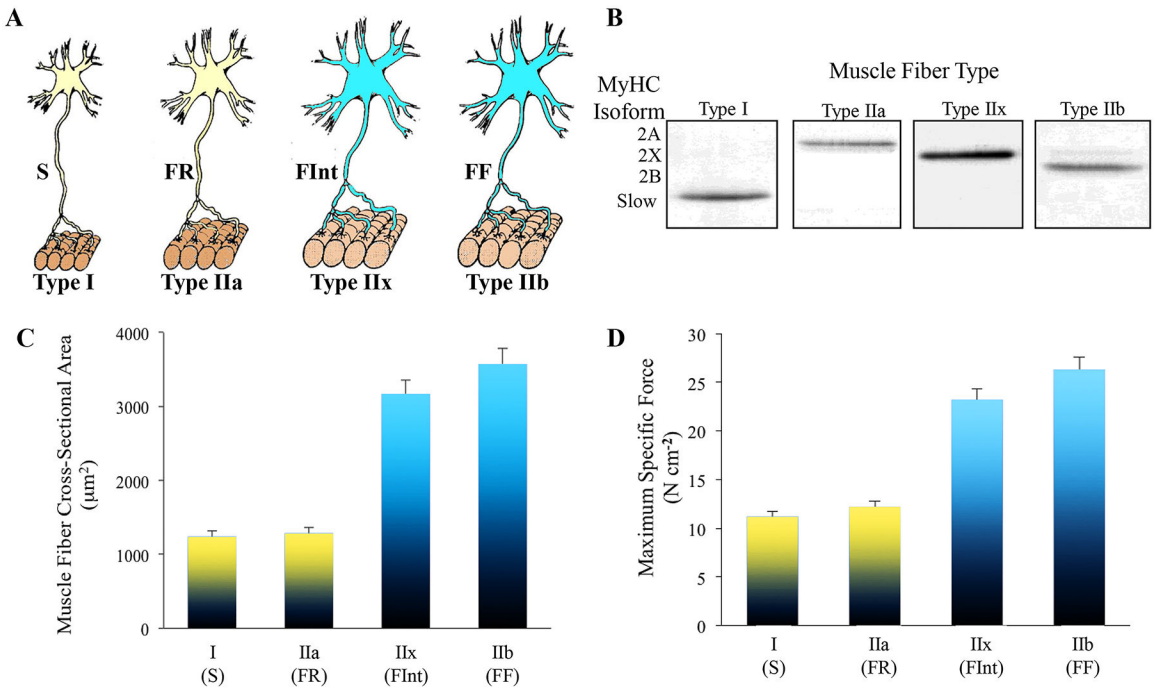

Figure 21:

Different DIAm motor unit types are distinguished by their intrinsic, mechanical and fatigue properties and are classified as type S, FR, FInt and FF (**A**). Within a particular motor unit, all muscle fibers are homogeneous, as evidenced by myosin heavy chain (MyHC) expression (**B**). In the DIAm of most species, type I and IIa diaphragm muscle fibers have smaller cross-sectional areas than those of type IIx and IIb fibers (**C**). Differences in specific force between different fiber types is related to the different MyHC content per half sarcomere and differing unitary forces produced by different MyHC isoforms (**D**). Adapted from elements within refs 186 and 223.

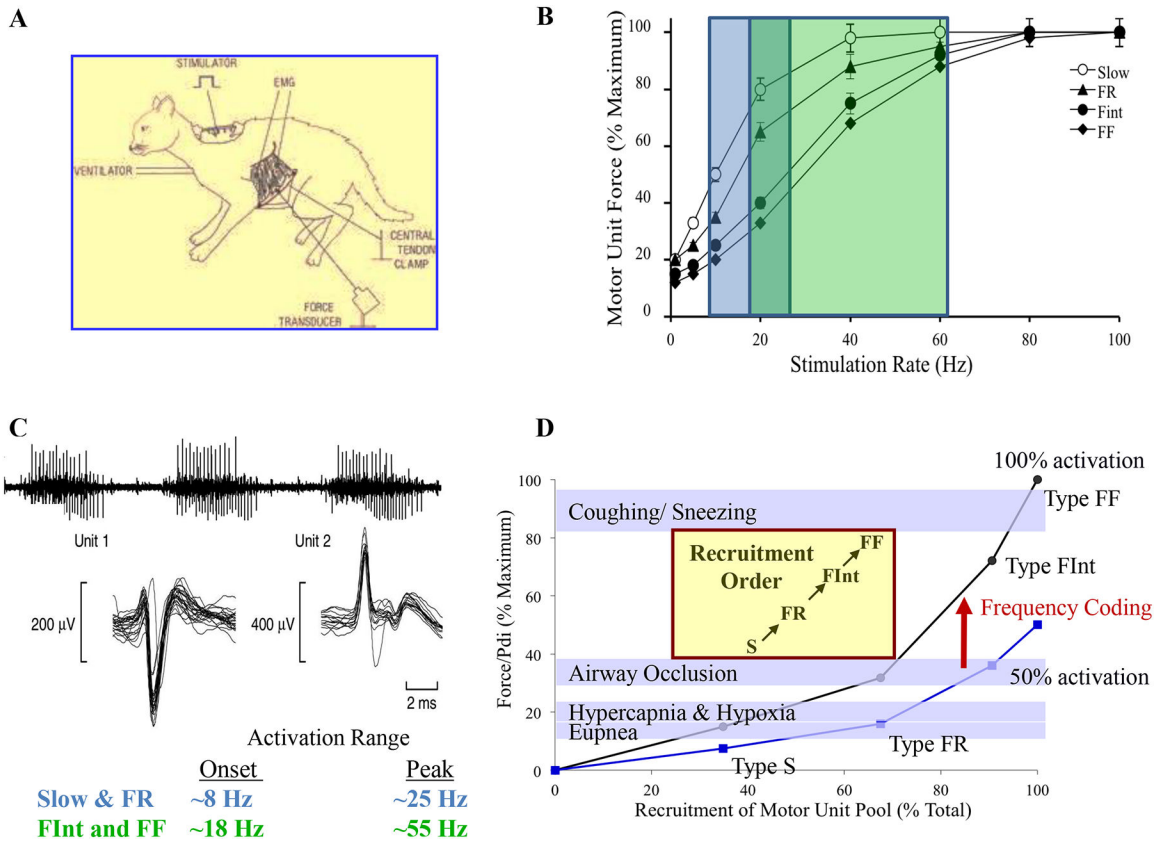

Figure 22:

The initial model for force-frequency coding and DIAm motor unit recruitment was based on direct measurements performed in cats (**A**). Onset activation frequency for type S and FR motor units is ~8 Hz and maximal activation range is ~25 Hz (blue portion). For type FInt and FF motor units, onset is ~12 Hz and maximal activation ~60 Hz (green portion). The steepest portion of the force-frequency curve occurs between 10 and 30 Hz for all types of motor units in the diaphragm muscle (**B**). Individual motor unit recordings show that motor units with larger discharges are recruited after those with smaller discharges (**C**). Motor units are recruited in an orderly fashion with type S > FR > FInt > FF (**D**). Recruitment of type S and FR motor units is sufficient to accomplish ventilatory behaviors, including eupnea, response to hypoxia/hypercapnea and breathing against an occluded airway. To accomplish higher force expulsive/straining behaviors, such as coughing, sneezing, vomiting and defecation, recruitment of higher-force generating type FInt and FF motor units is necessitated. In general, diaphragm motor units operate in the steep portion of the frequency-coding curve (i.e., between 50–100% activation). Adapted from elements within refs 186.

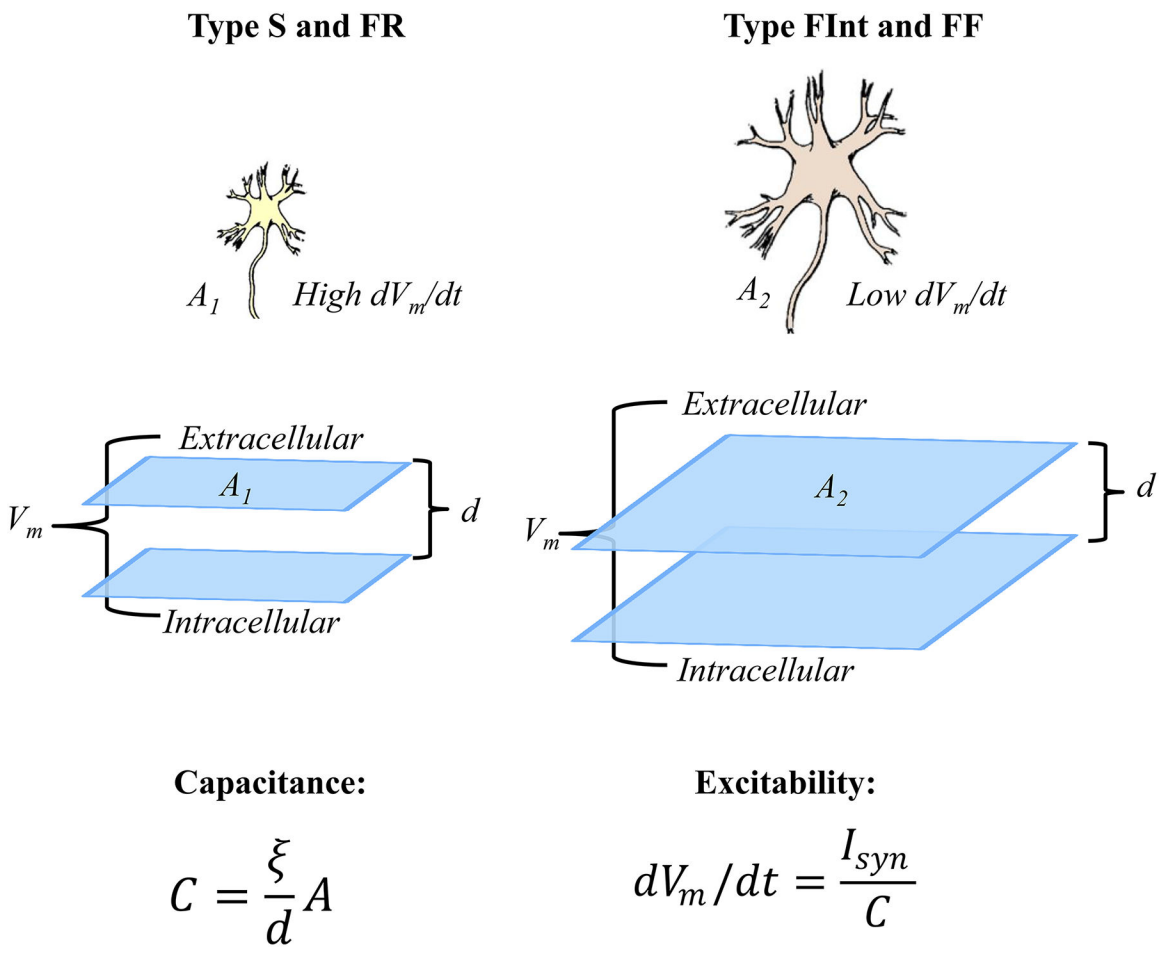

Figure 23:

The order of motor unit recruitment is related to the intrinsic properties of motor neurons. Of these the most important is motor neuron surface area, the size principle. Neuronal membrane acts as a capacitor, with total membrane capacitance (C) primarily determined by membrane surface area (A) and distance between the membrane lipid bilayer (d). As membrane bilayers are unchanged, a larger neuronal surface area ($A_2 > A_1$) will increase capacitance. For a given synaptic input (I_{syn}), the excitability of the membrane (dV_m/dt) is inversely related to neuronal capacitance. Thus, smaller motor neurons (type S and FR) with low capacitance are more excitable and recruited before larger motor neurons (type FInt and FF).

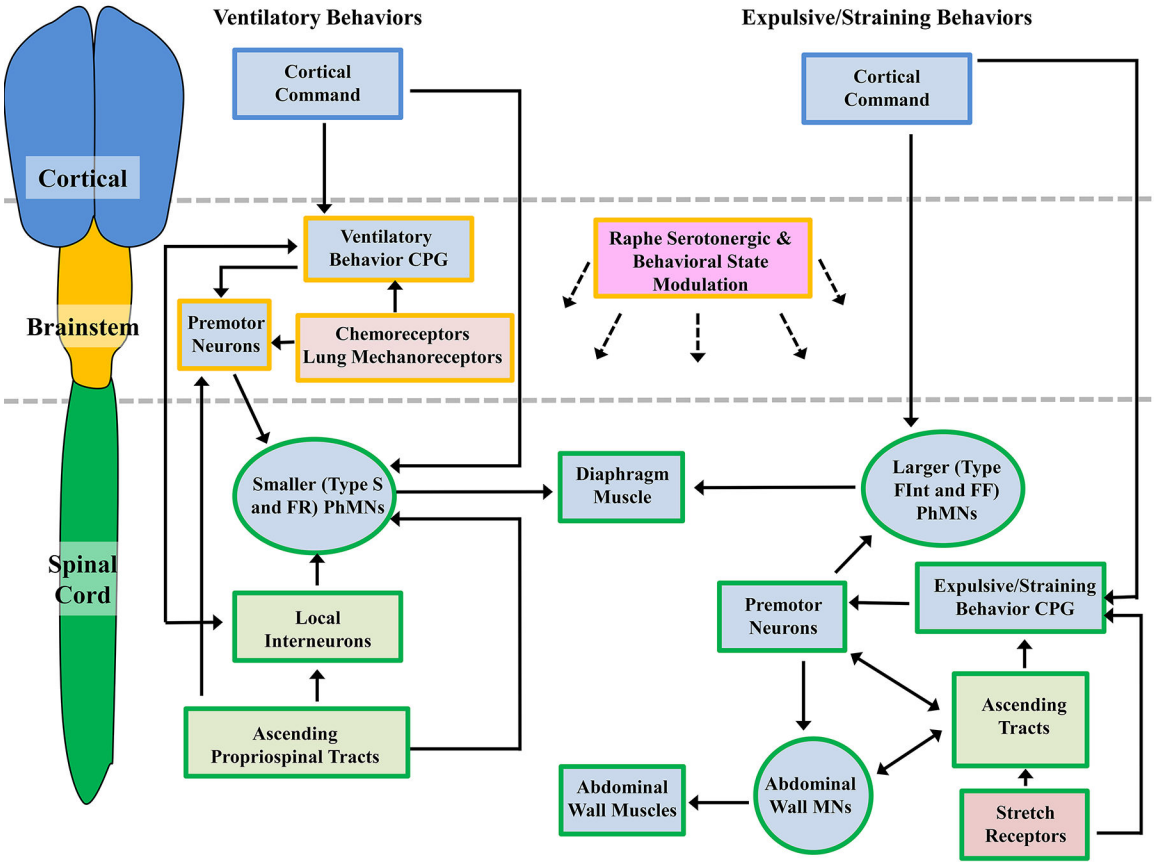

Figure 24:

Neuromotor control of DIAm ventilatory and expulsive/straining behaviors requires cortical, brainstem and spinal cord centers. Ventilatory behaviors are the most-well characterized of these systems and require the recruitment of predominantly type S and FR motor units. Cortical pathways are able to modulate the eupnic rhythm by interactions with the ventilatory central pattern generator (CPG) or directly via synapses onto phrenic motor neurons (PhMNs). The ventilatory CPG activates brainstem premotor neurons that in turn innervate the PhMNs. Activity of PhMNs during ventilation is also modulated (directly and indirectly) by spinal cord ascending tracts and interneurons. Brainstem chemoreceptors and lung mechanoreceptors regulate the activity of premotor neurons, and act to increase premotor neuron discharge (and thus PhMN activity) during hypoxia/hypercapnia. In the case of expulsive/straining behaviors, the majority of control centers are located within the spinal cord, and recruitment of type FInt and FF motor units (higher-force producing units) is necessitated. Some cortical control of the PhMNs and spinal expulsive/straining CPG may be evident, but rectal and vaginal stretch receptors also elicit strong P_{ab} generation. There may be shared spinal premotor neurons within the spinal cord for PhMNs and abdominal muscle MNs, and a variety of ascending projections may facilitate the coordinated activity of all MNs involved in expulsive/straining maneuvers. Overall, expulsive behaviors result in near maximal co-contractions of the DIAm and abdominal wall muscles.